

**INTEGRATION OF EDDY COVARIANCE FLUXES, TREE RING
RECORDS AND STABLE ISOTOPE COMPOSITIONS TO STUDY
ENVIRONMENTAL CONTROLS ON GROWTH IN DIFFERENT-AGE
PINE PLANTATION FORESTS**

INTEGRATION OF EDDY COVARIANCE FLUXES, TREE RING RECORDS
AND STABLE ISOTOPE COMPOSITIONS TO STUDY ENVIRONMENTAL
CONTROLS ON GROWTH IN DIFFERENT-AGE PINE PLANTATION
FORESTS.

By SHAWN MICHAEL MCKENZIE, B.Sc. *Honours*, M.Sc. M.Ed.

A Thesis Submitted to the School of Graduate Studies in Partial Fulfillment of the
Requirements for the Degree Doctor of Philosophy

(Library and Archives Canada page)

DOCTOR OF PHILOSOPHY (2018) McMaster University
(Department of Geography and Environmental Sciences) Hamilton, Ontario

TITLE: Integration of Eddy Covariance Fluxes, Tree Ring
Records and Stable Isotope Compositions to Study
Environmental Controls on Growth in Different-
Age Pine Plantation Forests.

SHORT TITLE: Environmental Controls on Growth in Different-
Age Pine Plantation Forests.

AUTHOR: Shawn Michael McKenzie
Bachelor of Geology *Honours* (University of Mary
Washington, 2005)
Master of Education (University of Mary
Washington, 2014)
Master of Geology (University of Saskatchewan,
2011)

SUPERVISOR: Dr. M. Altaf Arain
School of Geography and Earth Sciences

NUMBER OF PAGES: xv, 155

ABSTRACT

Global warming and extreme weather events have impacted the ability of Earth's forest ecosystems to sequester atmospheric carbon dioxide. The full effects of these events on forest productivity, vulnerability, and the carbon cycle have not yet been fully assessed. One potentially fruitful approach is to explore past climate and forest growth patterns through tree ring records. These records may be used to explore how past environmental events may have impacted tree growth and provide insight into the functioning of forest ecosystems in the future. The stable isotope ratios (e.g. ^{13}C to ^{12}C) of tree ring material also provide additional information about tree growth trajectories and environmental stressors that may not be recognized in radial growth. In this study, tree ring and stable isotope records were measured and constructed to explore the dynamics of growth over the lifespan of plantation pine stands in southern Ontario.

Tree ring growth records were used to determine the effects of climate and other environmental changes on radial growth. These records were constructed from two white pine (*Pinus strobus* L.) plantations established in 1939 (TP39) and 1974 (TP74) and one red pine plantation established in 1931 (TP31). Air temperature, precipitation, and drought indices were analyzed at monthly combinations to determine controls on growth. Temperature was consistently negatively correlated to growth, while precipitation and Palmer Drought Severity Index (PDSI) were consistently positively correlated to growth. The effectiveness of each climate variable to control ring growth differed between sites which may be related to stand age, stand density, and management factors.

In both white pine plantations, inter-annual eddy-flux quantifications of gross ecosystem productivity (GEP) was found to be significantly related to tree ring growth over the overlapping period from 2003 to 2017. These relationships enabled an inter-annual estimate of GEP to be constructed for both growth chronologies over the period 1942 to 2017 for TP39 and 1981 to 2017 for TP74). Additionally, growth rings from three specimens in two different-age (14- and 77-year old) white pine plantation forests were analyzed for stable carbon isotope ratios to identify both short- and long-term variations in the physiological response to changing environmental conditions. Variations in $\delta^{13}\text{C}$ time series from whole wood samples provided a potential record of intrinsic water use efficiency (iWUE) for these three trees. These iWUE records were compared to climate records and inter-annual eddy-flux quantifications of GEP and evapotranspiration (ET). Long-term iWUE was found to increase by 50 μmol

$\text{mol}^{-1} \text{ yr}^{-1}$, with nearly all of the increase occurring as the tree shifted into active homeostasis of stomatal control in the late 1960s. Changes in time series of internal and external concentration of CO_2 (ratio) also displayed a significant shift from first increasing and then decreasing trend. In the three wood samples, air temperature, ET, and GEP were found to be significantly, but inconsistently related to iWUE.

The work of this thesis shows that tree ring properties are strongly related to key environmental variables such as temperature and drought stress in pine plantation forests in southern Ontario, Canada. Results also suggest that dendrochronology and isotope tracers are useful tools to be used to evaluate historical environmental impacts on growth in these different-age plantation stands. The background knowledge of climate drivers acting on tree ring growth and ring isotopic compositions over the forests' history may be used to make informed management decisions to promote tree productivity in a changing climate in Eastern North America.

ACKNOWLEDGEMENTS

This work would not have been possible without the guidance of Professor Altaf Arain, whose knowledge and experience were critical in bringing this thesis to fruition. I am extremely grateful for the opportunities and experiences that have come from being a part of his group under his supervision.

A portion of this work was completed at Brock University Paleoecology Laboratory. I am sincerely grateful to Professor Michael F.J. Pisaric for use of his facility for tree ring analysis and his insightful discussion and contribution to this thesis and manuscripts.

I am also deeply appreciative of extremely valuable discussions and collaboration with Dr. Greg F. Slater over the course of this project to produce meaningful results and conclusive analyses of data used for my research.

I am thankful for the thorough examination of this work by Dr. Sean Thomas of the University of Toronto. I am indebted for his time spent in careful review of both the earlier and current submission of this document and for his notable contributions and suggestions.

Professor Sang-Tae Kim's and Martin Knyf's assistance with stable isotope analysis and use of the McMaster Research Group for Stable Isotopologues facility was also instrumental in completing this project.

I would also like to thank the McMaster Faculty of Science for their financial support in awarding International Excellence Awards for each year of my

enrollment, as well as the School of Geography and Environmental Science for four years of Research Scholarships.

My fellow graduate students deserve their own share of acknowledgement. Every time you answered a question, helped me understand a problem, or assisted me in any number of ways, you earned my gratitude. So, thank you Eric Beamesderfer, Alanna Bodo, Brandon Burns, Oliver Champagne, Felix Chan, Katey Daly, Myroslava Khomik, Jung K. Lee, Stéfan Sauer, Rachel Skubel, Robin Thorne, and Bing Xu. I would like to thank Frank Bahula and Bruce Whitside and their families for providing access to their private forests to conduct this research.

A very special thank you is given to the late Dr. Neil Tibert (d. 20 December 2015) whose passion for paleoclimate and paleoproxies inspired me as an undergraduate to pursue an academic career. I am thankful for his support during the first two years of my Ph.D. program.

I also thank Pastor Loretta and Kimber'el Eventide for their spiritual teachings over the past four years. I also wish to thank the support of my dear friend Tarja Paabo. A final thank you goes to my parents, Michael and Linda, for their unending patience as I completed 14 years of post-secondary education in four degree programs.

PREFACE

This dissertation consists of five chapters: an introduction, three research papers and conclusion. The three research papers were written as manuscripts with the intention of their submission to peer-reviewed journals for publication. The focus of first paper is to identify environmental effects on growth in two different-age (78- and 43-year old) white pine (*Pinus strobus* L.) plantation forests in southern Ontario, Canada using dendrochronological analysis. The second paper focuses on evaluating tree ring chronologies to identify impact of environmental stresses on growth in a >80-year old red pine (*Pinus resinosa*) plantation forest in the same area. The third paper assesses carbon isotope chronologies extracted from tree rings of different-age white pine stands to identify environmental factors affecting their growth and water use efficiency.

Titles of all three manuscripts that underpin this dissertation are given below.

Chapter 2: Climate sensitivities and productivity derived from tree ring records from two white pine (*Pinus strobus*) plantation forests in southern Ontario.

Chapter 3: Tree ring growth records track drought and heat stress in an afforested red pine (*Pinus resinosa*) plantation.

Chapter 4: Influence of climate and environmental variability on tree ring $\delta^{13}\text{C}$ and water use efficiency in temperate pine plantation forests.

In all three manuscripts, I reviewed the literature, conducted the study using the suggested methodology, performed data analysis, interpreted results, and wrote manuscripts. Insightful discussion with collaborators and committee members occurred throughout the course of the project. Direction was also provided at key points during the study and during data analysis and manuscript preparation. Acknowledgements specific to the production of each manuscript are provided at the end of each chapter.

TABLE OF CONTENTS

ABSTRACT	iv
ACKNOWLEDGEMENTS	vi
PREFACE	viii
TABLE OF CONTENTS	x
LIST OF TABLES	xiii
LIST OF FIGURES	xiv
Chapter 1 Introduction	1
1.1 Background	1
1.2 Study objectives	4
1.3 References	8
Chapter 2 Climate sensitivities and productivity derived from tree ring records from two white pine (<i>Pinus strobus</i>) plantation forests in southern Ontario	18
2.1 Abstract	18
2.2 Introduction	19
2.3 Materials and methods	21
2.3.1 Field site	21
2.3.2 Meteorological data	23
2.3.3 Dendrochronology	24
2.3.4 Eddy covariance measurements	26
2.3.5 Climate, dendrochronological and eddy covariance flux correlations	27
2.4 Results	27
2.4.1 Chronology characteristics.....	27
2.4.2 Climate and tree ring growth relationships.....	29
2.4.3 Dendrochronological and eddy covariance flux correlations	31
2.5 Discussion	32
2.6 Conclusion	38

2.7 Acknowledgements	39
2.8 References	41
Supplemental data: correlation coefficient values	58
Chapter 3 Tree ring growth records track drought and heat stress in an afforested red pine (<i>Pinus resinosa</i>) plantation	62
3.1 Abstract	62
3.2 Introduction	63
3.3 Materials and methods	66
3.3.1 Site description and experimental design	66
3.3.2 Meteorological and climate information	69
3.3.3 Sample collection and data processing	70
3.3.4 Climate correlations	72
3.4 Results	72
3.4.1 Chronology characteristics.....	72
3.4.2 Climate record integrity and trends.....	75
3.4.3 Climate and tree ring growth relationships 1942-2013.....	76
3.4.4 Temporal climate and growth relationships 1942-2013.....	78
3.5 Discussion	80
3.6 Conclusions	86
3.7 Acknowledgements	87
3.8 References	88
Supplemental data: correlation coefficient values	100
Chapter 4 Influence of climate and environmental variability on tree ring $\delta^{13}\text{C}$ and water use efficiency in temperate pine plantation forests	104
4.1 Abstract	104
4.2 Introduction	105
4.3 Materials and methods	108
4.3.1 Site description	108
4.3.2 Sample preparation and stable isotope analyses	112

4.3.3 Data treatment	115
4.3.4 Correlation of iWUE with climate and eddy-flux data	116
4.4 Results	118
4.4.1 Trends in tree ring isotope compositions and iWUE	118
4.4.2 Relationships of iWUE with climate and eddy-flux measurements.....	121
4.4.3 Relationships of iWUE with ring width measurements.....	123
4.5. Discussion	123
4.6 Conclusions	130
4.7 Acknowledgements	131
4.8 References	133
Chapter 5 Conclusions and suggestions for future research	149
5.1 Major findings	149
5.2 Future considerations	152
5.3 References	154

LIST OF TABLES

Table 2.1 Site characteristics of the TP39 and TP74 conifer plantations	48
Table 2.2 Summary statistics for the TP39 and TP74 site chronologies	48
Supplemental data: correlation coefficient value tables	58
Table 3.1 Summary statistics for the red pine site chronology	94
Table 3.2 Ten-year statistical means for the red pine site chronology	94
Supplemental data: correlation coefficient value tables	100

LIST OF FIGURES

Figure 1.1 Global carbon budget of sources and sinks (1959-2015)	15
Figure 1.2 Future climate impacts on ecosystem resilience	16
Figure 1.3a Location map of the Turkey Point study sites	17
Figure 1.3b Location of the study sites within the IBBAC	17
Figure 2.1 Climatograph of monthly temperature and total precipitation ..	49
Figure 2.2a Annual mean temperature and total precipitation	50
Figure 2.2b Monthly PDSI values	50
Figure 2.3a TP39 and TP74 site chronologies	51
Figure 2.3b Divergence in the two site chronologies.....	51
Figure 2.4 Monthly and multi-month RWI-climate significance	52
Figure 2.5 Growth response during extreme drought years.....	54
Figure 2.6 Monthly and multi-month RWI-GEP significance	55
Figure 2.7 RWI-GEP relationships 2003-2017	56
Figure 2.8 Modelled GEP based from RWI	57
Figure 3.1 Location of the red pine study site	95
Figure 3.2 Red pine site chronology	96
Figure 3.3 1941 to 1970 and 1981 to 2010 climatographs	97
Figure 3.4 Monthly and multi-month RWI-climate significance	98
Figure 3.5 Moving interval correlations	99
Figure 3.6 Inter-annual RWI-climate time series	100
Figure 4.1 Location map of the TP39 and TP02 study sites	140
Figure 4.2 Ring widths of the three sampled trees	141
Figure 4.3 $\delta^{13}\text{C}_{\text{tr}}$ and $\delta^{13}\text{C}_{\text{corr}}$ records of TP39-1, TP39-2, and TP02	142
Figure 4.4 Segmented-regression of the ci/ca time series of TP39-1	143
Figure 4.5a $\delta^{13}\text{C}$ -inferred iWUE records	144
Figure 4.5b Segmented-regression of the ci/ca time series of TP39-1	144
Figure 4.6a Monthly and multi-month iWUE-climate significance	145
Figure 4.6b Monthly and multi-month iWUE-fluxes significance	146

Figure 4.7 Data scatter of iWUE versus ring width 148

Chapter 1 Introduction

1.1. Background

According to the United Nations' Intergovernmental Panel on Climate Change (IPCC), Earth's climate has warmed by 0.61°C (0.55 to 0.67°C with 95% confidence interval) from 1850 to 2005 and a further temperature increase of 1.0 to 4.0°C is predicted by the end of the 21st century (Ciais et al., 2013). According to the IPCC, there is clear evidence that the observed warming trend is directly coupled to historic anthropogenic greenhouse gas (GHG) emissions (90-100% probability of likelihood) (Ciais et al., 2013). Approximately 67% of 555±85 Pg of the total carbon (C) emissions over 1750 to 2011 period came from fossil fuel combustion and cement production, while the remaining 33% came from land use changes such as deforestation, burning, and desertification (Ciais et al., 2013). From a budgetary standpoint, the Earth was able to offset GHG emissions from anthropogenic activity until about 1860 (Boden et al., 2016; Khatiwala et al., 2013; Houghton et al., 2012; Joos and Spahni, 2008). After this time, the Earth's ability to offset these emissions has been compromised and there has been increasing disparity between GHG emission sources and sinks (Figure 1.1) (Borden et al., 2016; Le Quéré et al., 2016; Houghton et al., 2012). This excess carbon dioxide therefore accumulates in the atmosphere and impacts radiative forcing which in turn contributes to further heating of the atmosphere (Van

Oldenborgh et al., 2017; Serdeczny et al., 2015). A portion (26%) of atmospheric CO₂ is absorbed into the ocean (Le Quéré et al., 2016) and is contributing to ocean acidification (Hoegh-Guldberg et al., 2017). Air temperature is directly linked to the water holding capacity of the atmosphere. The August-Roche-Magnus relationship suggests 7% increase in water holding capacity of the atmosphere with every 1°C increase in temperature (IPCC, 2013). Therefore, warmer atmospheric temperature will cause an acceleration of the hydrologic cycle and changes in regional precipitation events. Extreme weather events such as droughts, heavy precipitation and heatwaves are expected to increase.

Predictions under the IPCC Representative Concentration Pathway, RCP4.5 (i.e. 4.5Wm⁻² radiative forcing effect) suggest air temperatures are likely to increase by 1.1 to 2.6°C by the end of this century relative to the 1986-2005 average (Table SPM-2, IPCC, 2014; IPCC, 2013 Annex 1). Even if CO₂ emissions were to peak by 2020 and decline substantially thereafter as suggested by RCP2.6, global temperatures are still very likely (90-100% probability) to increase by 0.3 to 1.7°C by 2100 (IPCC, 2014, Figure SPM.7). With these expected temperature increases in the near future, forest ecosystem resilience will be adversely impacted (Figure 1.2.). Observation and modeling studies in the literature show that forest ecosystems are already becoming more vulnerable to climate change (Anderegg et al., 2018; Pan et al., 2011; Pielke et al., 2011; Allen et al. 2010; Arneeth et al., 2010; Gonzalez et al., 2010). The carbon capacity of these forests is

changing due to both alteration in climatological controls (i.e. warm temperatures and droughts) (Murthy et al., 2011; Leemans and Eickhout, 2004) and photosynthetic capacity (i.e. CO₂ fertilization effects) (Silva and Anand, 2013; Gagen et al., 2011; Charru et al., 2010; Silva et al., 2010).

Temperature increases and droughts are likely to impact the carbon cycle as forest ecosystems are a major contributor to the global terrestrial carbon sink. Forests cover 30% of the total land area and currently hold 260 to 380 PgC of the total 450 to 650 PgC of above ground biomass (Le Quéré et al., 2016; Ciais et al., 2013; Dixon et al., 1994). Forest ecosystems also store 790 PgC out of the total 1500 to 2400 PgC of below ground carbon (Le Quéré et al., 2016; Ciais et al., 2013). Currently, forest ecosystems sequester 2.3 PgC per year (Pan, et al., 2011), which is about 20% of the total carbon emissions from anthropogenic sources (i.e. sum of 2015 estimate of fossil fuel, cement production and land-use change related emissions) (Boden et al., 2016; Le Quéré et al., 2016).

Numerous studies examining climate change impacts on forest ecosystems point to a weakening of the forest carbon sink and increasing tree mortality (Figure 1.2.) (Mann et al., 2017; Silva and Anand, 2013; Allen et al., 2010; Silva et al., 2010; Prentice and Harrison, 2009), however, there are fewer studies in the literature about the effects of climate change on forest growth in managed forests and afforested settings where forests are established by tree plantations (Chum et

al., 2011; Thompson et al., 2009). Afforestation contributes approximately 7% to the global forest area and more than 31% of global forests are managed forests (FAO, 2015). These forests possess different characteristics from natural forests by having reduced species diversity, even-age tree composition and unique structures resulting from both plantation strategies and subsequently applied management or thinning methods (Thompson et al., 2009; Aussenac, 2000). Clear attribution of climatic drivers on the growth in these forests is more difficult because of changes in growth patterns due to forest management strategies (Dale et al., 2010; Ciais et al., 2008; Boisvenue and Running, 2006). Some studies, suggest that lower species diversity renders afforested or plantation stands to be less resilient to climate change as compared to natural forests (Hemery, 2008) particularly due to exogenous disturbances (forest pests, pathogens, fire) (Brasier and Webber, 2010; Dale et al., 2010). Therefore, further research is needed to identify the effects of long-term climate change on afforested or plantation and managed forest ecosystems.

1.2. Study objectives

The main goal of this dissertation is to determine the environmental controls on forest growth within different age temperate afforested or plantation forests in Great Lakes region in southern Ontario, Canada and evaluate how these environmental controls impacted growth of these stands over their life history.

Other objectives include the examination of relationships between tree ring growth and ecosystem productivity, and the evaluation of controls on tree ring carbon isotope values and intrinsic water use efficiency. These forest sites include a red pine (*Pinus resinosa*) stand established in 1931 and three white pine (*Pinus strobus* L.) stands planted during the years 1939, 1974, and 2002 located within the Norfolk Forest Complex and Important Bird and Biodiversity Area of Canada (IBBAC) zone ON009 near Lake Erie (Figure 1.3a, 1.3b.). Hereafter these sites are identified as TP31, TP39, TP74 and TP02 based on the year of planting. These sites are collectively known as the Turkey Point Flux Station and are part of Global Fluxnet and Global Water Futures initiatives (Arain and Restrepo, 2005; Peichl et al., 2010a; 2010b; Skubel et al., 2015; 2017; Chan et al., 2018).

In this study, dendrochronological methods were used to determine growth histories in three different aged pine stands (TP31, TP39, and TP74 plantations). Tree ring chronologies are reliable records to evaluate recent and historical environmental change that occur and how they impact tree growth (Schweingruber, 1988; Biondi, 1999; Esper, et al., 2002; Kipfmueller et al., 2010; Magruder et al., 2012; Magruder et al., 2013). The availability of long-term (1935 – present) meteorological data records in the region from Environment Canada data archives aided in the establishment of climate-growth relations over the entire life cycle of these stands (Environment Canada, 2017). In addition, 14 years of eddy covariance flux data: energy, water vapour and carbon dioxide CO₂

were available to establish relationships between climate, annual carbon fluxes and tree ring chronologies for different age stands to determine how growth and carbon exchanges has been affected by climate variability in these plantation forests.

In addition, growth rings were analyzed for carbon isotope composition ($\delta^{13}\text{C}$ values) to determine intrinsic water use efficiency (iWUE). The isotopic composition of tree ring material also serves as a potential record of environmental change (McCarroll and Pawellek 1998; McCarroll and Loader, 2004; Gagen et al., 2011b). Mechanistic models have been developed to describe the fractionation of carbon isotopes in trees (Farquhar et al., 1982; Farquhar and Richards, 1984; Campbell and Norman, 1998; Marshall et al., 2007), help in interpreting the climate signal, determine tree water use efficiency (Weiwei et al., 2018; Gagen et al., 2011a; 2011b; Eilmann et al., 2010; Saurer et al., 2004) and CO_2 fertilization effects (Waterhouse et al., 2012)

Specific objectives of the study are:

- 1) Determine long-term environmental effects on growth and gross ecosystem productivity of two different-age (TP39 and TP74) stands of white pine (*Pinus strobus* L.) using dendrochronological methods (Chapter 2).

- 2) Determine multiple environmental factors affecting tree ring chronologies in a mature (TP31) red pine (*Pinus resinosa*) plantation in the region (Chapter 3).
- 3) Evaluate the impacts of temperature and early growing season (May-June) precipitation on the inter-annual variability in growth (Chapter 2 and 3).
- 4) Determine water use efficiency of two different age (14- and 77-year old) white pine plantation forests using $\delta^{13}\text{C}$ of growth rings and provide some insight into past water use efficiency of these stands (Chapter 4).
- 5) Identify any shifts in $\delta^{13}\text{C}$ and iWUE that may be driven by anthropogenic carbon emissions into the atmosphere (Chapter 4).

With respect to the organization of this dissertation, introduction and background is given in Chapter 1, study results are presented in Chapters 2, 3 and 4, and conclusions are summarized in Chapter 5. Chapter references are self-contained at the end of each chapter. Because this dissertation is comprised of three manuscripts, there is a certain amount of overlap in the introduction, study site details and certain aspects of methodology.

1.3. References

Allen, C.D., Macalady, A.K., Chenchouni, H., Bachelet, D., McDowell, N., Vennetier, M., Kitzberger, T., Rigling, A., Breshears, D.D., Hogg, E.H., Gonzalez, P., Fensham, R., Zhang, Z., Castro, J., Demidova, N., Lim, J.H., Allard, G., Running, S.W., Semerci, A., and Cobb, N. 2010. A global overview of drought and heat-induced tree mortality reveals emerging climate change risks for forests. *Forest Ecology and Management* 259:4, 660-684.

Anderegg, W.R.I., Konings, A.G., Trugman, A.T., Yu, K., Bowling, D.R., Gabbitas, R., Karp, D.S., Pacala, S., Sperry, J.S., Sulman, B.N., and Zenes, N. 2018. Hydraulic diversity of forests regulates ecosystem resilience during drought. *Nature* 538:561. <https://doi.org/10.1038/s41586-018-0539-7>

Arain, M.A., and Restrepo-Coupe, N., 2004. Net ecosystem production in a temperate pine plantation in southeastern Canada. *Agricultural and Forest Meteorology* 128, 223-241.

Arneeth, A., Harrison, S.P., Zaehle, S., Tsigaridis, K., Menon, S., Bartlein, P.J., Feichter, J., Korhola, A., Kulmala, M., O'Donnell, D., Schurgers, G., Sorvari, S., and Vesala, T. 2010: Terrestrial biogeochemical feedbacks in the climate system. *Nature Geoscience* 3:8, 525-532.

Aussenac, G. 2000. Interactions between forest stands and microclimate: Ecophysical aspects and consequences for silviculture. *Annals of Forest Science* 57, 287-301.

Babst, F., Bouriaud, O., Papale, D., Gieden, B., Janssens, I., Nikinmaa, E., Ibrom, A., Wu, J., Bernhofer, C., Köstner, B., Grünwald, T., Seufert, G., Ciais, P., Frank, D. 2013. Above-ground woody carbon sequestration measured from tree rings is coherent with net ecosystem productivity at five eddy-covariance sites. *New Phytologist* 2013. doi: 10.1111/nph.12589

Biondi, F. 1999. Comparing tree ring chronologies and repeated timber inventories as forest monitoring tools. *Ecological Applications* 9:1, 216-227.

Boden, T.A., Marland, G., and Andres, R.J. 2016. Global, Regional, and National Fossil-Fuel CO₂ Emissions. Carbon Dioxide Information Analysis Center, Oak Ridge National Laboratory, U.S. Department of Energy, Oak Ridge, Tenn., U.S.A. doi 10.3334/CDIAC/00001_V2016

Brasier, C. and Webber, J. 2010: Plant pathology: Sudden larch death. *Nature* 466:7308, 824-825.

Boisvenue, C. and Running, S.W. 2006. Impacts of climate change on natural forest productivity - evidence since the middle of the 20th century. *Global Change Biology* 12:5, 862-882.

Brüggemann, N., Gessler, A., Kayler, Z., Keel, S.G., Badeck, F., Barthel, M., Boeckx, P., Buchmann, N., Brugnoli, E., Esperschütz, J. et al. 2011. Carbon allocation and carbon isotope fluxes in the plant–soil–atmosphere continuum: a review. *Biogeosciences* 8, 3457–3489.

Campbell, G.S., and Norman, J.M. 1998. An introduction to environmental biophysics. Springer-Verlag, New York.

Charru, M., I. Seynave, F. Morneau, and J.D. Bontemps, 2010: Recent changes in forest productivity: an analysis of national forest inventory data for common beech (*Fagus sylvatica* L.) in north-eastern France. *Forest Ecology and Management* 260:5, 864-874.

Chum H., Faaij, A., Moreira, J., Berndes, G., Dhamija, P., Dong, H., Gabrielle, B., Eng, A.G., Lucht, W., Mapako, M., Cerutti, O.M., McIntyre, T., Minowa, T., and Pingoud, K. 2011. Bioenergy. In: IPCC Special Report on Renewable Energy Sources and Climate Change Mitigation [O. Edenhofer, R. Pichs-Madruga, Y. Sokona, K. Seyboth, P. Matschoss, S. Kadner, T. Zwickel, P. Eickemeier, G. Hansen, S. Schlömer, C. von Stechow (eds)],. Cambridge University Press, Cambridge, United Kingdom and New York, NY, USA, pp. 209 – 332.

Dale, V.H., Tharp, M.L., Lannom, K.O., and Hodges, D.G. 2010. Modeling transient response of forests to climate change. *Science of the Total Environment* 408:8, 1888-1901.

Dixon, R.K, Trexler, M.C, Wisniewski, J, Brown, S, Houghton, R.A. and Solomon, A.M., 1994. Carbon pools and flux of global forest ecosystems. *Science* 263, 185-190.

Eilmann, B., Buchmann, N., Siegwolf, R., Saurer, M., Cherubini, P., Rigling, A. 2010. Fast response of Scots pine to improved water availability reflected in tree-ring width and $\delta^{13}\text{C}$. *Plant, Cell & Environment* 33:8, 1351-1360.

Environment Canada. 2017. Climate Data Online. <http://www.climate.weatheroffice.ec.gc.ca>

Esper, J., Cook, E., Schweingruber, F. 2002. Low-frequency signals in long tree-ring chronologies for reconstructing past temperature variability. *Science* 295:5563, 2250-2253 DOI: 10.1126/science.1066208

FAO, 2010: Global Forest Resources Assessment 2010. FAO Forestry Paper No. 163, Food and Agriculture Organization of the United Nations (FAO), Rome, Italy, 340 pp.

FAO, 2015: Global Forest Resources Assessment 2015. 2nd Edition. Food and Agriculture Organization of the United Nations (FAO) 54 pp. <http://www.fao.org/3/a-i4793e.pdf>

Farquhar, G.D., O'Leary, M.H., Berry, J.A. 1982. On the relationship between carbon isotope discrimination and the intercellular carbon dioxide concentration in leaves. *Australian Journal of Plant Physiology* 9, 121-137.

Farquhar, G.D., and Richards, R.A. 1984. Isotopic composition of plant carbon correlates with water-use efficiency of wheat genotypes. *Functional Plant Biology* 11, 539-552.

Gagen, M., Finsinger, W., Wagner-Cremer, F., McCarroll, D., Loader, N., Robertson, I., Jalkanen, R., Young, G., Kirchhefer, A. 2011a. Evidence of changing intrinsic water-use efficiency under rising atmospheric CO₂ concentrations in Boreal Fennoscandia from subfossil leaves and tree ring $\delta^{13}\text{C}$ ratios. *Global Change Biology* 14, 1064-1072.

Gagen, M., McCarroll, D., Edouard, J-L. 2004. Latewood width, maximum density, and stable carbon isotope ratios of pine as climate indicators in a dry subalpine environment. *French Alps. Arctic, Antarctic, and Alpine Research* 36:2, 166-171

Gagen M., McCarroll D., Loader N.J., Robertson I. 2011b. Stable isotopes in dendroclimatology: moving beyond 'potential'. In: Hughes M., Swetnam T., Diaz H. (eds) *Dendroclimatology. Developments in Paleoenvironmental Research*, Vol 11. Springer, Dordrecht

Gonzalez, P., Neilson, R.P., Lenihan, J.M., and Drapek, R.J. 2010. Global patterns in the vulnerability of ecosystems to vegetation shifts due to climate change. *Global Ecology and Biogeography* 19:6, 755-768.

Hemery, G.E., 2008. Forest management and silvicultural responses to projected climate change impacts on European broadleaved trees and forests. *International Forestry Review* 10:4, 591-607.

Hoegh-Guldberg O., Poloczanska, E.S., Skirving, W. and Dove, S. 2017. Coral Reef Ecosystems under Climate Change and Ocean Acidification. *Frontiers in Marine Science* 4:158. doi: 10.3389/fmars.2017.00158

Houghton, R.A., van der Werf, G.R., DeFries, R.S., Hansen, M.C., House, J.I., Le Quéré, C., Pongratz, J., and Ramankutty, N. 2012. Chapter G2 Carbon emissions from land use and land-cover change. *Biogeosciences* 9, 5125-5140.

IPCC, 2013: Annex I: Atlas of Global and Regional Climate Projections [van Oldenborgh, G.J., M. Collins, J. Arblaster, J.H. Christensen, J. Marotzke, S.B. Power, M. Rummukainen and T. Zhou (eds.)]. In: *Climate Change 2013: The Physical Science Basis. Contribution of Working Group I to the Fifth Assessment Report of the Intergovernmental Panel on Climate Change* [Stocker, T.F., D. Qin, G.-K. Plattner, M. Tignor, S.K. Allen, J. Boschung, A. Nauels, Y. Xia, V. Bex and P.M. Midgley (eds.)]. Cambridge University Press, Cambridge, United Kingdom and New York, NY, USA.

IPCC, 2013: Summary for Policymakers. In: *Climate Change 2013: The Physical Science Basis. Contribution of Working Group I to the Fifth Assessment Report of the Intergovernmental Panel on Climate Change* [Stocker, T.F., D. Qin, G.-K. Plattner, M. Tignor, S.K. Allen, J. Boschung, A. Nauels, Y. Xia, V. Bex and P.M. Midgley (eds.)]. Cambridge University Press, Cambridge, United Kingdom and New York, NY, USA.

Joos, F and Spahni, R 2008. Rates of change in natural and anthropogenic radiative forcing over the past 20,000 years. *Proceedings of the National Academy of Science* 105, 1425-1430.

Khatiwala, S., Tanhua, T., Mikaloff Fletcher, S.E., Gerber, M., Doney, S.C., Graven, H.D., Gruber, N., McKinley, G.A., Murata, A., Rios, A.F., and Sabine, C.L. 2013 Global ocean storage of anthropogenic carbon. *Biogeosciences* 10, 2169-2191.

Kipfmüller, K.F., Elliot, G.P., Larson, E.R., Salzer, M.W. 2010. An assessment of the dendroclimatic potential of three conifer species in northern Minnesota. *Tree Ring Research* 66, 113–126.

Leemans R., and Eickhout, B. 2004. Another reason for concern: regional and global impacts on ecosystems for different levels of climate change. *Global Environmental Change Part A* 14, 219 – 228.

Le Quéré, C., Andrew, R.M., Canadell, J.G., Sitch, S., Korsbakken, J.I., Peters, G.P., Manning, A. C., Boden, T.A., Tans, P.P., Houghton, R.A., Keeling, R.F., Alin, S., Andrews, O. D., Anthoni, P., Barbero, L., Bopp, L., Chevallier, F., Chini, L.P., Ciais, P., Currie, K., Delire, C., Doney, S. C., Friedlingstein, P., Gkritzalis, T., Harris, I., Hauck, J., Haverd, V., Hoppema, M., Klein Goldewijk, K., Jain, A.K., Kato, E., Körtzinger, A., Landschützer, P., Lefèvre, N., Lenton, A., Lienert, S., Lombardozi, D., Melton, J.R., Metz, N., Millero, F., Monteiro, P.M.S.,

Munro, D.R., Nabel, J.E.M.S., Nakaoka, S., O'Brien, K., Olsen, A., Omar, A.M., Ono, T., Pierrot, D., Poulter, B., Rödenbeck, C., Salisbury, J., Schuster, U., Schwinger, J., Séférian, R., Skjelvan, I., Stocker, B.D., Sutton, A. J., Takahashi, T., Tian, H., Tilbrook, B., van der Laan-Luijkx, I.T., van der Werf, G. R., Viovy, N., Walker, A.P., Wiltshire, A.J., and Zaehle, S. Global Carbon Budget. 2016. *Earth Syst. Sci. Data*, 8, 605-649, doi:10.5194/essd-8-605-2016, 2016. <http://www.earth-syst-sci-data.net/8/605/2016/>

Magruder, M., Chhin, S., Monks, A., O'Brien, J. 2012. Effects of Initial Stand Density and Climate on Red Pine Productivity within Huron National Forest, Michigan, USA. *Forests* 3, 1086-1103.

Magruder, M., Chhin, S., Palik, B., Bradford, J. 2013. Thinning increases climatic resilience of red pine. *Canadian Journal of Forest Resources* 43, 878–889.

Mann, M. E., Rahmstorf, S., Kornhuber, K., Steinman, B.A., Miller, S., Coumou, D. 2017. Influence of anthropogenic climate change on planetary wave resonance and extreme weather events. *Scientific Reports* 7, 45242; doi: 10.1038/srep45242.

Marshall, J.D., Brooks, J.R. and Lajtha, K. 2007. Sources of Variation in the Stable Isotopic Composition of Plants, in *Stable Isotopes in Ecology and Environmental Science*, Second Edition (eds R. Michener and K. Lajtha), Blackwell Publishing Ltd, Oxford, UK.

McCarroll, D., and Loader, N. 2004. Stable isotopes in tree rings. *Quaternary Science Reviews* 23, 771-801.

Murthy I. K., Tiwari, R., and Ravindranath, N.H., 2011. Climate change and forests in India: adaptation opportunities and challenges. *Mitigation and Adaptation Strategies for Global Change* 16, 161 – 175. doi: 10.1007 / s11027 - 010 - 9261-y, ISSN: 1381-2386, 1573 – 1596.

Pan, Y., Birdsey, R., Fang, J., Houghton, R., Kauppi, P., Kurz, W.A., Phillips, O.L., Shvidenko, A., Lewis, S.L., Canadell, J.G., Ciais, P., Jackson, R.B., Pacala, S., McGuire, A.D., Piao, S., Rautiainen, A., Sitch, S., and Hayes, D. 2011: A large and persistent carbon sink in the world's forests. *Science* 333:6045, 988-993.

Peichl M., Arain, M.A., 2006. Above- and belowground ecosystem biomass and carbon pools in an age-sequence of planted white pine forests. *Agricultural and Forest Meteorology* 140, 51-63.

Peichl, M., Arain, M.A., Brodeur, J.J., 2010a. Age effects on carbon fluxes in temperate pine forests. *Agricultural and Forest Meteorology* 150, 1090–1101.

Peichl, M., Arain, M.A., Ullah, S., Moore, T. 2010b. Carbon dioxide, methane, and nitrous oxide exchanges in an age-sequence of temperate pine forests. *Global Change Biology* 16, 2198-2212.

Pielke, R.A., Pitman, A., Niyogi, D., Mahmood, R., McAlpine, C., Hossain, F., Goldewijk, K.K., Nair, U., Betts, R., Fall, S., Reichstein, M., Kabat, P., and de Noblet, N. 2011. Land use/land cover changes and climate: modeling analysis and observational evidence. *Wiley Interdisciplinary Reviews: Climate Change* 2:6, 828-850.

Prentice, I. C., and S. P. Harrison, 2009: Ecosystem effects of CO₂ concentration: Evidence from past climates. *Climate of the Past* 5, 297–307.

Saurer, M., Borella, S., Schweingruber, F.H., Siegwolf, R. 1997. Stable carbon isotopes in tree rings of beech: climatic versus site-related influences. *Trees-Structure and Function* 11, 291-297.

Schweingruber, F.H., 1988. *Tree Rings: Basics and Applications of Dendrochronology*. D. Reidel Publishing Co., Dordrecht, the Netherlands. 276 pp.

Silva, L.C.R. and M. Anand, 2013: Probing for the influence of atmospheric CO₂ and climate change on forest ecosystems across biomes. *Global Ecology and Biogeography* 22, 83-92.

Silva, L.C.R., Anand, M., and Leithead, M.D. 2010. Recent widespread tree growth decline despite increasing atmospheric CO₂. *PLoS One* 5:7, e11543, doi:10.1371/journal.pone.0011543.

Skubel, R., Khomik, M., Brodeur, J., Arain, M. 2017. Short-term selective thinning effects on hydraulic functionality of a temperate pine forest in eastern Canada. *Ecohydrology* 10:1, DOI: 10.1002/eco.1780.

Skubel, R., Peichl, M., Brodeur, J., Khomik, M., Thorne, R., Trant, J., Kula, M. 2015. Age effects on the water-use efficiency and water-use dynamics of temperate pine plantation forests. *Hydrological Processes* 29:18. DOI: 10.1002/hyp.10549.

Switsur, V.R., Waterhouse, J.S., Field, E.M., Carter, A.H.C., 1996. Climatic signals from stable isotopes in oak tree-rings from East Anglia, Great Britain. In: Dean, J.S., Meko, D.,M., Swetnam, T.W. (Eds.), *Tree Rings, Environment and Humanity Radiocarbon*, pp. 637–645. Radiocarbon, Arizona.

Thompson I., Mackey, B., McNulty, S., and Mosseler, A. 2009. Forest resilience, biodiversity, and climate change: A Synthesis of the Biodiversity / Resilience /

Stability Relationship in Forest Ecosystems. Secretariat of the Convention on Biological Diversity, Montreal, Canada, 67 pp. Available at: <http://www.cakex.org/virtual-library/1233>.

Van Oldenborgh, G.J. et al. 2017. Attribution of extreme rainfall from Hurricane Harvey, August 2017, Environmental Research Letters DOI: 10.1088/1748-9326/aa9ef2 <https://phys.org/news/2017-12-climate-harvey-rainfall-percent-intense.html#jCp>

Waterhouse, J.S., Switsur, V.R., Barker, A.C., Carter, A.H.C., Hemming, D.L., Loader, N.J., Robertson, I. 2004. Northern European trees show a progressively diminishing response to increasing atmospheric carbon dioxide concentrations. Quaternary Science Reviews 23, 803–810.

Weiwei, L.U., Xinxiao, Y.U., Guodong, J.I.A., Hanzhi, L.I., Ziqiang, L.I.U. 2018. Responses of intrinsic water-use efficiency and tree growth to climate change in semi-arid areas of north China. Scientific Reports 8, Article number: 308

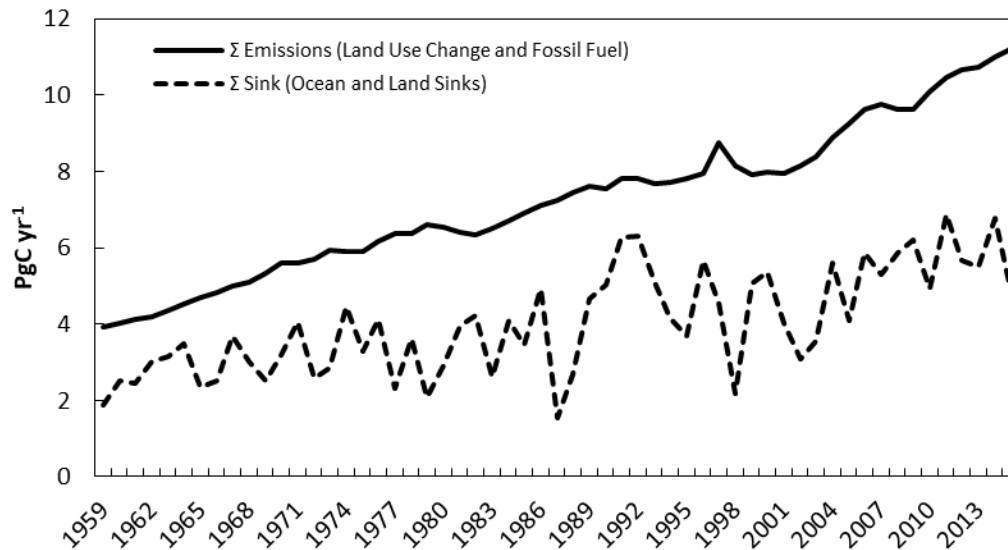


Figure 1.1. Global carbon budget (PgC yr⁻¹) including total emissions (solid line) from land use change and fossil fuel use counterbalanced with the total global carbon sinks (hatched line) in ocean and terrestrial ecosystems from 1959 to 2015 (data from Borden et al., 2016; Le Quéré et al., 2016). Note the increased disparity between carbon emissions and sinks over time. This disparity enters the atmospheric carbon pool and increases its carbon concentration.

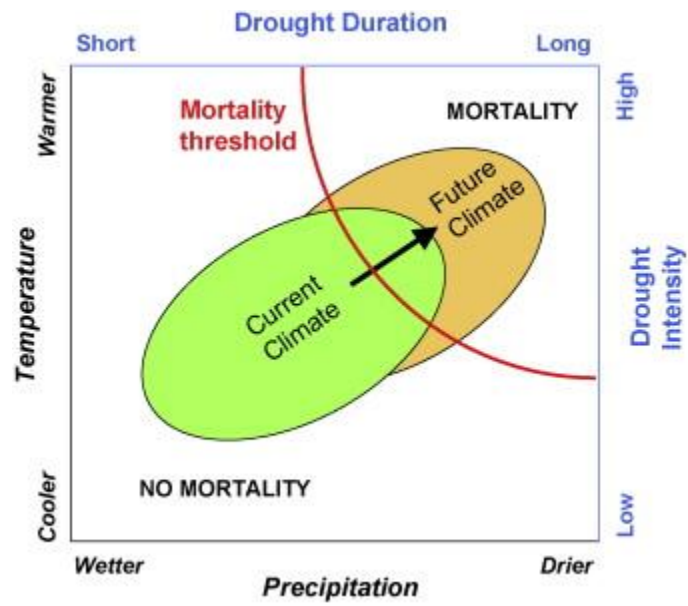


Figure 1.2. Conceptual diagram from Allen et al. (2010) showing the current climate parameters for temperature and precipitation and how future climate will impact species resilience and mortality.

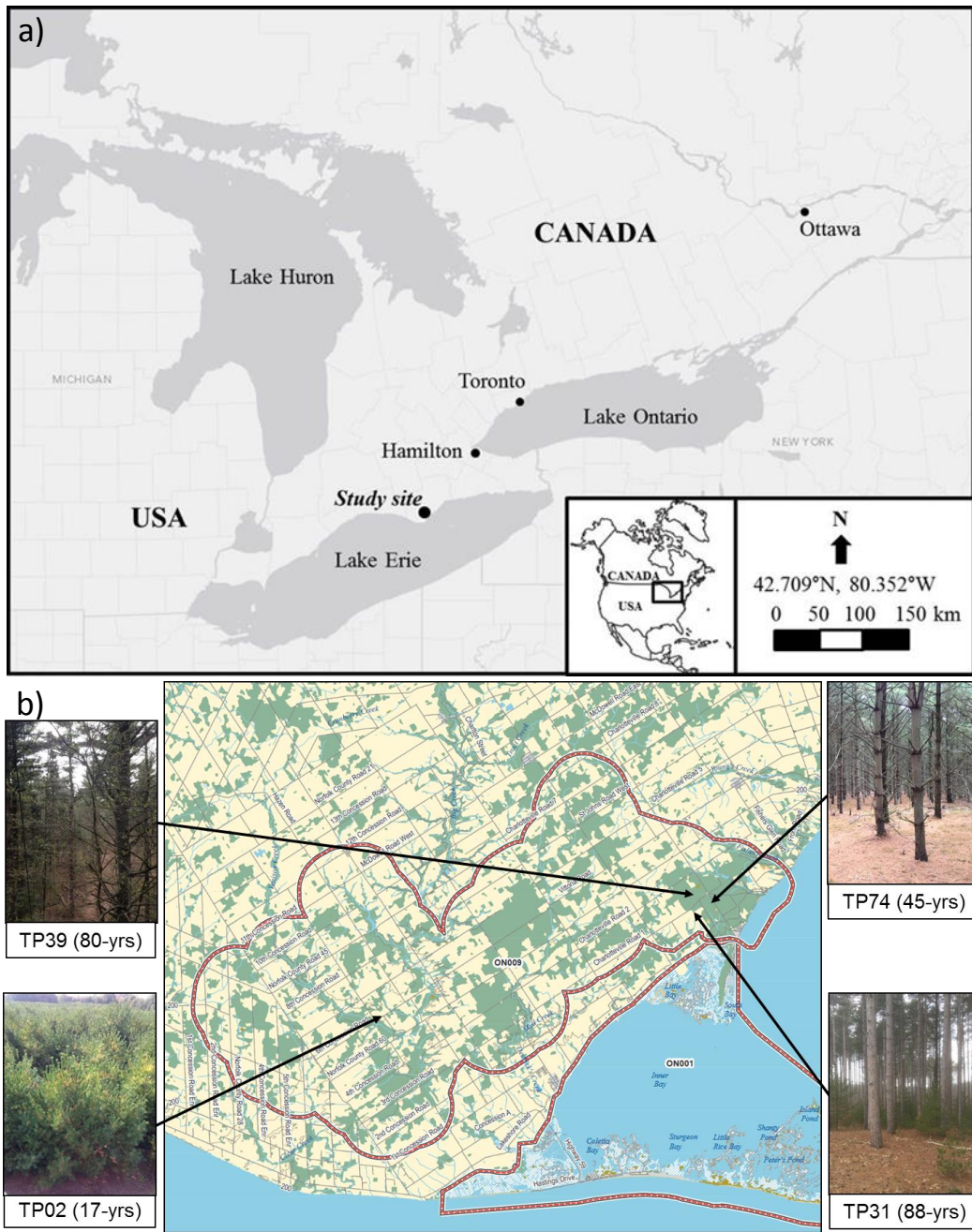


Figure 1.3. Location of the Turkey Point Flux Station Study Sites a) in southern Ontario and b) within the IBBAC zone ON009 on the north shore of Lake Erie in the Great Lakes region.

Chapter 2: Climate sensitivities and productivity derived from tree ring records from two white pine (*Pinus strobus*) plantation forests in southern Ontario

2.1 Abstract

In this study tree ring residual chronologies were constructed from wood cores sampled from two eastern white pine (*Pinus strobus* L.) plantation forests established in 1939 (TP39) and 1974 (TP74) in southern Ontario, Canada. Annual radial growth of trees was measured on each core extracted from stems at 1.3 m height. The tree ring chronologies were subsequently compared to monthly climate indices including temperature, precipitation, and Palmer Drought Severity Index (PDSI). At both sites, the computed tree ring chronologies displayed significant sensitivities to climate variables, with negative relationships for temperature and positive relationships for precipitation and the PDSI. Significant relationships between these climate variables and tree ring growth occurred at both sites during the growing season, with May-June-July being the most critical period for growth. Enhanced growth sensitivity was observed in the TP74 stand, which is likely more vulnerable to drought as compared to the TP39 stand. Tree ring growth measurements also showed strong correlation with gross ecosystem productivity (GEP) derived from eddy covariance fluxes from 2003 to 2017. The differences between stand age and density may need to be considered when evaluating tree growth in plantation forests in response to future climate change.

2.2 Introduction

Forests play a major role in the global terrestrial carbon cycle (Dixon et al., 1994; Smith et al., 2016). They store approximately 80% of above ground carbon (Goodale et al., 2002) and stem wood is the largest fraction of above-ground carbon in forest ecosystems across the globe (Peichl et al., 2007; Lorenz and Lal, 2010). Annually, forest ecosystems sequester about 2.3 PgC yr^{-1} (Pan, et al., 2011), which is about 20% of the total 11.21 PgC emitted from anthropogenic activities (Le Quéré et al., 2016; Boden et al., 2016). The volume of research on the effects of climate change on productivity in forest ecosystems is extensive (Piutti and Cescatti, 1997; Prentice and Harrison, 2009). However, the effects of climate change on growth in plantation or afforested settings are not well understood (Fernández-de-Uña et al., 2015; Dié et al., 2015). As afforestation contributes approximately 7% to the global forest area and more than half the forest across the world are managed forests (FAO, 2010), it is important to characterize how plantation forest growth will respond to changes in environmental factors. Plantation forests possess different characteristics from natural forests because they have low species diversity, even age trees and unique stand structure depending upon management or thinning techniques applied since their establishment (Thompson et al., 2009; Aussenac, 2000).

The annual growth of tree rings contains annually-resolved environmental data recorded by the forest over centuries to millenia (Fritts, 1976, Speer, 2010). Tree rings record temporal anomalies partially attributed to inter- and intra-annual climate variability (Whitehead et al., 1984; Shao et al., 2009). Zafirov (2005) used tree rings to examine the relationship between climatic factors and stem growth in plantation stands. The drivers that influence forest growth are often diverse, in particular in temperate regions, which have strong anthropogenic influences (Fritts, 1976; Gagen and McCarroll, 2004). Major environmental drivers or factors include local climate and soil conditions, species competition and management history of the forest (Biondi 1999; Acker et al., 2002). Tree rings have also been used to estimate gross primary productivity (GPP) of forest ecosystems (Babst et al., 2014). Thus, we hypothesize that tree age and stand density may be important biotic factors that may affect tree response to climate change in plantation forests. Additionally, it is hypothesized that these biotic factors may influence GPP relationships with climate in plantation forests.

This study, examined annual growth records of tree rings in two different age (78- and 43-year-old) white pine plantation stands in southern Ontario, Canada to determine how climate variables such as temperature and precipitation influence radial growth rates. Additionally, tree ring records were compared with gross ecosystem productivity (GEP) measured using the eddy covariance technique to examine the relationship between radial and stand-level growth

estimates from two very different, but commonly used techniques. Specific goals of this study were to (i) determine effects of climate variability on tree ring growth and stand-level productivity (ii) examine relationships between growth patterns derived from dendrochronology and micrometeorological (eddy covariance) techniques using CO₂ flux data from 2003 to 2017 and (iii) examine how climate stresses may have impacted the growth patterns and carbon uptake in these two different aged temperate forests since their establishment (life cycle analysis).

2.3 Materials and methods

2.3.1 Field site

The study sites are located on the north shore of Lake Erie in Norfolk County in southern Ontario (Figure 1.1). In the late 1800s and early 1900s, this area was farmed with wheat and tobacco, causing deteriorating soil conditions and desertification (Randall, 1877, Draper, 2003). In 1926, the Ontario Ministry of Natural Resources and Forestry (OMNRF) began procuring land in this region (Zavitz, 1958; Kelly, 1974) to afforest the degraded agricultural lands (Draper, 2003). The study sites consist of two pine plantation forests established in 1939 and 1974 and here after referred to as TP39 and TP74, respectively (Table 2.1).

These sites are part of Turkey Point Flux Station (TPFS), Global Water Futures initiative as well as Global Fluxnet where they are known as CA-TP3 and CA-TP4. The sites are located within 2 km of each other and experience very similar climatic conditions. The TP39 stand consists of 82% eastern white pine (*Pinus strobus* L.), 11% balsam fir (*Abies balsamea* L. Mill) and 7% native Carolinian species (Thorne and Arain, 2015). Stem density at TP39 was 425 ± 172 stems·ha⁻¹ with at least 4 to 6 m spacing between mature trees (Peichl, et al., 2010a). TP39 stand was thinned twice in 1983 and 2012. Each time about 30% of the trees was systematically harvested. Stem wood was removed while remaining material was left at the site. These harvestings were conducted to open the canopy to improve light and water availability as well as stimulate growth in the remaining trees (Thorne and Arain, 2015). The TP74 stand consists predominately of white pine trees with stand density of 1633 ± 166 stems ha⁻¹ (Peichl, et al., 2010a). TP74 has not been thinned since its establishment. Table 2.1 provides additional site information.

The soil at all the sites is highly porous sandy brunisolic grey-brown luvisol in the Canadian System of Soil Classification (Presant and Acton, 1984). These soils are characterized by lacustrine sand-sized grains, which allow for good drainage and low water-holding capacity. The organic hummus-litter layer is approximately 5 cm thick. Topography of the study area consists of gently rolling sand dunes. Based on field measurements at TP39 from 2005 to 2017, ground

water level at the site ranges from 5 to 9 m. Historical water table elevation records from 400 wells within 10 km² area show a mean water level 11.8 ± 5.6 m (Well Records Ontario 1953-2006). Approximately two-thirds of root biomass is reported to be in the upper 0 – 15 cm depth range, with 90% of root volume within the upper 1 m of the soil profile (Peichl et al., 2007; McLaren et al., 2008). Arain and Restrepo-Coupé (2005) and Peichl et al. (2010a; 2010b) contain additional information about the sites.

2.3.2 Meteorological data

The climate in the region is characterized as humid temperate with cold winters and warm summers (Figure 2.1). This region is one of the warmest in Canada. Meteorological data was acquired from the Ministry of Environment and Climate Change Canada for the Delhi weather station (42.871°N, 80.550°W; <http://climate.weather.gc.ca/>), approximately 24 km northwest of the study area. Mean annual temperature is 8.2°C for the period 1935 – 2017 with mean daily maximum temperature of 21°C for the hottest month (July) and mean minimum daily temperature of –5.4°C occurring in January. Mean annual precipitation is 936 mm and is evenly distributed throughout the year, with the autumn months being slightly wetter (85 mm) than the winter months (70 mm). However, there was high year-to-year variability in precipitation. Monthly temperature and precipitation data from 1935 to 2017 are shown in Figure 2.2. For this study,

potential evaporation was calculated following Thornthwaithe (1948). The mean ratio of annual precipitation (P) to potential evapotranspiration (PE) (P/PE) was also calculated as an index of water availability at these sites. The mean annual P/PE ratio over the available climate record from 1935 to 2017 is approximately 1.67, suggesting precipitation is generally abundant in the region on an annual basis, but inter-annual variability is large. In order to identify drought periods, monthly and annual values of the Palmer Drought Severity Index (PDSI) was calculated. The input variables are monthly mean temperature, precipitation, latitude of the meteorological station, and available water content (assumed to be a maximum of 35 mm for these sandy soils). Potential evapotranspiration (PET) was calculated according to the Thornthwaite (1948) method and the calibration period was taken to be for the full available record 1935-1990. Tables of monthly water balance, Z-Index, PET, PDSI, and PDHI (Palmer Hydrological Drought Index) (Jacobi et al., 2013). The PDSI outputs were used in further pairwise correlation analyses as a measure of drought index.

2.3.3 Dendrochronology

Tree cores were collected from both stands in May of 2018 using a 5-mm Haglöff increment borer at a height of 1.3m above the ground surface. Selected trees were sampled twice: collecting one core from each of the east and south sides of the tree trunk. For TP39, 32 series were obtained from 16 trees located in

National Forest Inventory (NFI) plots of 10 m radius that were established in 2004. For TP74, 42 series were obtained from 21 trees located within NFI plots that were also established in 2004. In addition to the cores, five cross sectional trunk samples from both sites was obtained from dominant trees. These trees were randomly selected and harvested in late August in 2004, as part of a study on biomass allometry (Peichl and Arain, 2007). The felled trees were cut into slices to form cross-sections approximately 3 cm thick. Core and trunk samples were sanded and prepared according to standard dendrochronological practices (Stokes and Smiley, 1968; Fritts, 1976).

Annual ring-width measurements were made using a Velmex measuring system with a linear encoder at a measurement precision of 0.001 mm. Samples were visually cross dated by counting inwards from the cambium. Visual cross dating was confirmed using measurement data that was quality checked against a master chronology constructed using the computer software program COFECHA (Holmes, 1983). Following successful cross-dating, the computer program ARSTAN (Cook, 1985) was used to generate a residual mean ring width chronology (RWI) for each site. These residual chronologies were generated using a 40-year cubic spline to remove 50% of 40-year variance while retaining 99% of the variance acting at 12.67 years. This was necessary to remove long-term noise variance (e.g. age effects) from the measured series and to preserve signals acting on the frequency of interest (Speer, 2010). The residual chronology has had all

autocorrelation stripped from the series. This makes it a suitable chronology to assess climate effects on growth as one of the assumptions in correlation analyses is that the series are not autocorrelated. These chronologies were used in our comparisons with monthly climate indices acting on decadal frequency or less.

2.3.4. Eddy covariance flux measurements

Half-hourly fluxes of energy, water vapour and carbon dioxide (CO₂) were measured from 2003 to 2017 using open-path (2003-2007 at TP74 only) and closed-path eddy covariance (EC) systems at both sites. In both EC systems, air was sampled at 20 Hz on top of towers at 28 and 18 m heights at the TP39 and TP74 sites, respectively. See Arain and Restrepo-Coupé (2005) and Peichl et al. (2010a, 2010b) for further information on EC instrument specifications and site set-up. Flux data was quality-controlled following Fluxnet-Canada protocols. Small gaps (less than a few hours) in flux data due to instrument malfunction, power failure and instrument calibration were filled using linear interpolation. In both EC systems, half-hourly net ecosystem productivity (NEP) was calculated by adding CO₂ flux and the rate of CO₂ storage change in the air column below the EC sensors. Ecosystem respiration (RE) was calculated as a non-linear relationship between nighttime NEP and soil temperature at 5 cm depth (Arain and Restrepo-Coupé, 2005). GEP was calculated by adding NEP and RE values during the growing season. Missing GEP values were filled using a model

following Richardson et al. (2007). Error in GEP was determined to be about ± 25 $\text{g C m}^{-2} \text{y}^{-1}$ for TP39, and ± 50 $\text{g C m}^{-2} \text{y}^{-1}$ for the TP74 site.

2.3.5. Climate, dendrochronological and eddy covariance flux correlations

To identify long-term climate-growth relations, the residual growth chronologies from both TP39 and TP74 were compared to local climate records of temperature (T), precipitation (P) and PDSI. For TP39, the period of correlation was 1944 to 2017 and for TP74, the period of correlation was 1981 to 2017. Monthly values of GEP derived from eddy covariance (EC) data were compared to the tree ring record for the period 2003 to 2017. Climate versus tree ring-growth and EC fluxes versus tree ring growth relationships were determined using pairwise linear Pearson's correlation coefficients for all months and all combination of months for the growing season year. Relationships between GEP and tree ring growth were examined further to generalize GEP values over the length of the available chronologies for both sites.

2.4 Results

2.4.1. Dendrochronology characteristics

Summary statistics for the TP39 and TP74 chronologies are shown in Table 2.2, while the mean ring width index for both chronologies is shown in Figure 2.3a. For TP39, the maximum sample size was 37 series, while for TP74 the maximum sample size was 46 series. For both chronologies, the higher sample size prior to 2004 was due to the inclusion of five series from trees harvested in 2004.

For this study, the minimum number of series used to construct the annual growth index values for correlation analysis was 12 series per year. This minimum number was chosen to exclude index values derived from small sample pools. Given this minimum sample size requirement, the sample size used to construct the mean chronology was considered too low until 1942 for TP39 and until 1981 for TP74 site (Figure 2.3a).

Summary statistics for the two site chronologies are presented in Table 2.2, with the mean ring width index plotted versus year in Figure 2.3a. The mean annual ring width was 2.65 mm yr^{-1} at TP39, and 0.46 mm yr^{-1} at TP74. Autocorrelation was described by a first-order autoregressive model for both growth series which were 0.90 and 0.77 for TP39 and TP74, respectively. Autocorrelation was removed from the growth series to produce the site residual chronologies. Series inter-correlation estimated as the average correlation of each individual series to the master chronology was 0.40 for TP39 and 0.46 for TP74.

RBAR or a running average correlation between all series was 0.47 for TP39 and 0.41 for TP74. Mean sensitivity for the chronology was 0.24 and 0.29 for TP39 and TP74 sites, respectively. However, the usefulness of mean sensitivity as a statistic of growth response had been called into question by some studies in the literature (e.g. Bunn et al., 2013).

The site chronologies were positively correlated with one another for the period 1981- 2017 ($r=0.49$; $p < 0.10$), indicating some agreement between the ring width chronologies at these two different aged sites (Figure 2.3b). The average first difference between the two chronologies is low for this period (-0.011). However, there were notable differences between the two site chronologies in specific yearly intervals (Figure 2.3b). For example, between 1982- 1986, TP74 was characterized by positive ring widths while TP39 was generally complacent. This interval includes 1983 when the largest difference in ring growth was observed between two sites (-0.414 RWI difference). The difference between the two chronologies in the early 1980s may be due to sample depth, which was higher in the TP39 record. TP39 was thinned in 1983, which may have also contributed to this difference.

2.4.2 Climate and tree ring growth relationships

The inter-annual variability in the detrended ring width indices was compared to monthly values of temperature, precipitation, and PDSI for each site as shown in Figure 2.4. Correlation coefficient values of all climate-growth relations are shown in the supplemental data at the end of this chapter.

All significant ($p \leq 0.05$) relationships between mean monthly temperature and ring width indices were negatively correlated for individual months and combination of months (Figure 2.4; supplemental data). For TP39, the most significant correlation occurred during the June-July period ($r = -0.26$, $p < 0.05$). Temperature during combined months were equally significant (June-August $r = -0.26$, $p < 0.05$ and June-September $r = -0.23$, $p < 0.05$). For TP74, the most significant negative correlation between temperature and growth was for the month of June ($r = -0.36$, $p < 0.05$).

All significant ($p < 0.05$) total monthly precipitation and mean PDSI correlations with ring width indices were positive for both TP39 and TP74 chronologies (Figure 2.4; supplemental data). The most significant correlations for precipitation occurred in the late spring to mid-summer (May-July; $r = 0.28$, $p < 0.05$) portion of the growing season. In addition, significant correlations were also apparent between ring width indices and August precipitation at TP74 ($r = 0.39$, $p < 0.05$). April to July PDSI was significantly correlated ($r = 0.26$, $p < 0.05$)

with tree growth at TP39 and for all possible growing season month combinations at TP74 site.

June-July PDSI was < -2.0 during seven years of the chronology overlap period (1981 to 2017). Growth during these seven years was generally lower at TP74 relative to TP39 during these seven years (Figure 2.5). This trend was reversed in 1987 with the growth of trees at TP74 being higher than at the older TP39 site. These results complement the correlation analysis in that ring growth of TP74 responds more readily to drought.

2.4.3. Dendrochronological and eddy covariance flux correlations

Tree ring records were found to be non-significantly related to NEP at monthly or multi-monthly growing season scales (not shown), but were significantly related to GEP. The correlations between tree growth and GEP are shown in Figure 2.6 and in supplemental data. The relationship between tree growth and GEP was further examined in an attempt to generalize what GEP values may have been over the growth history of sites. The monthly GEP versus tree growth correlation values from both the TP39 and TP74 sites were cross examined. The intra-annual period where highest correlation values occurred in both sites occurred in April-May-June-July (AMJJ) $r=0.70$, $p<0.01$. Therefore

GEP values over the AMJJ period (hereinafter referred to as GEP) were used to represent each year of the observational period from 2003 to 2017.

The RWI and GEP relationships at both sites are shown in Figures 2.7. Regression models of GEP versus RWI were developed using chronologies from 2003 to 2017 for TP39 (Figure 2.7a) and TP74 (Figure 2.7b). The equations $GEP = 711.2 * RWI^2 - 1163.4 * RWI + 1219.8$ (TP39) and $GEP = 1163.1 * RWI^2 - 1621.2 * RWI + 1245.4$ (TP74) were used to produce modelled values of GEP over the entire growth period when tree ring records were available for both sites. The correlation between modelled GEP and observed GEP values using eddy covariance technique was $r = 0.72$ ($p < 0.01$) for TP39 and $r = 0.73$ for TP74 over the 2003 to 2017 period. Finally, modelled GEP values were used to produce a generalization of GEP over the full chronologies for TP39 (1944 to 2017; Figure 2.8a) and TP74 (1981 to 2017; Figure 2.8b). Uncertainty in GEP estimates was determined for both sites by adding the error in eddy covariance flux measurements ($\pm 25 \text{ g C m}^{-2} \text{ y}^{-1}$ for TP39, and $\pm 50 \text{ g C m}^{-2} \text{ y}^{-1}$ for the TP74) and standard error in tree growth derived GEP values. The sum error in tree ring reconstructed GEP is shown in Figure 2.7 as red error bars.

2.5 Discussion

The overlapping chronologies over 1981 to 2017 revealed differences in tree growth between the TP39 and TP74 sites, which may be due to site-specific factors. The divergence of chronologies from 1982 to 1986, if it is not due to sampling differences, may be related to age difference between the two stands and structural changes at TP39 sites caused by a thinning treatment in 1983. Tree growth response to thinning disturbances has been observed and documented in other conifer plantations in southern Ontario and the northern United States (Bebber et al. 2004; Bevilaqua et al. 2005; Powers et al., 2009). Significant increases in stem radial growth occurred after 3 to 4 years after harvest disturbance (Bebber et al., 2004). Similar trends in tree growth were observed in a red pine stand in Minnesota after 3 years post-thinning (Powers et al., 2009). Peak responses in tree growth did not occur until 8-13 years after disturbance in a natural white pine forest near Chalk River, Ontario (Bevilaqua et al. 2005). Our study results showed that at TP39 site, low and steady-state growth lasted until 1989, approximately 6 years after thinning, which is well within observed response intervals of previous studies. Stand age was also a factor in the divergence observed between the two chronologies in our study. Trees at the TP39 site were 42 years old in 1981 compared to the 7 years old for the TP74 trees.

It is generally a valid assumption in dendrochronological studies that climate-growth relationships are age independent if the geometric constraint of adding a volume of wood to an increasing radius is removed (Cook et al., 1990).

However studies that examine tree physiology within a species have shown differing response functions between older and younger members of that species across age categories (e.g. Carrer and Urbinati, 2004; Esper et al., 2008; Primicia et al., 2015). As trees age they respond differently environmental factors (Zobel and Sprague, 1998; Bond et al., 2000; Wendling et al., 2014). The environmental signal in tree ring growth records is a complex interaction between environmental factors and physiological response (Carrer and Urbinati, 2004). The destination of translocated photosynthates and their storage rates has been found to change with aging (Ryan et al., 1997). In addition, reduced hydraulic resistances in younger, smaller trees (Ryan and Yoder, 1997) affects stomatal conductance which increase photosynthetic rate as compared to older members of a species (Bond, 2000). The observed differences in ring width to PDSI due to aging (e.g. hydraulic conductance, photosynthetic rate) could explain the higher responsiveness of the younger trees with high competition during drought, as an indirect influence of temperature on water availability to individual trees.

Previous studies have investigated the influence of temperature variability on wood production in forest ecosystems (Gordon and Larson, 1968; Jenkins, 1974; Kellomäki, 1979; Catesson, 1997). In temperate forests, negative correlations between tree growth and temperature have been observed, with a number of causes of these climate-growth relations being proposed. For example, higher temperatures cause reduction in photosynthetic rates and hence lower

radial growth (Oribe et al., 2003; Rennenberg et al., 2006). Stem heating may also impact growth processes in the cambium (Oribe et al., 2003), while photosynthetic rate of canopy shoots has also been linked to growth processes in the cambium (Kellomäki, 1979). Low water availability and drought conditions have also been identified as important factors causing decreases in tree photosynthetic rates and growth due to decreases in stomatal conductance (Rennenberg et al., 2006). Additionally, rubisco and photochemical pigments such as chlorophyll are degraded during prolonged droughts, which can further reduce photosynthetic rates (Waring and Running, 2007). In temperate regions, drought is often temperature driven. Therefore, reduction in growth may be caused by both reduced availability of water and heat stress (Adams et al., 2009).

Stand age and management are likely controlling factors on the observed differences in drought responses during the common period of overlap (1981-2017) (Figure 2.4; 2.5), with growth at the TP74 stand likely more vulnerable to drought as compared to the TP39 stand. Tree vulnerability to drought stress has been found to vary by stand age due to physical and environmental microclimate differences, with younger trees being more vulnerable (Law, 2014). The greater sensitivity of younger trees to drought may be due to relatively limited root networks (van Mantgem, 2009) that make them more vulnerable to acute water stress. Small trees also have limited carbohydrate reserves that render them more vulnerable to carbon stress (Niinemets, 2010). Stand density has also been used as

a predictor of drought mortality risk (Ganey and Vojta, 2011), which has important implications for forest management (Clifford et al., 2011). Thinning significantly influences mortality as a function of stand density (Powers et al., 2010). Stand density is also likely to have a significant positive relationship on tree mortality at a global scale, as shown in a drought and heat assessment of 248 sites (Zhang et al., 2017).

Availability and use of long-term (2003- 2017) eddy covariance flux data was a unique aspect of this study. This allows for more degrees of freedom in Pearson correlation analysis for both sites. Babst et al (2014) used allometric models to scale up tree ring records to produce estimates of ecosystem growth estimates, but these relationships were strongest with NEP. However, Rocha (et al., 2006) did not find any significant relationship between tree ring growth and EC-inferred estimates of productivity. Rocha suggests that the lack of relationship between ring growth and EC estimates of productivity in old growth (150-year old) black spruce (*Picea mariana* [Mill.]) may be due to ring growth being controlled by something other than carbon uptake, and may be controlled by respiration rates or inter-annual changes in carbohydrate pools or translocation of photosynthates. Ring growth was confirmed to be related to EC-inferred estimates of productivity in a mixed hardwood site in central Japan (Ohtsuka et al., 2009) with the explanation that inter-annual variability of ecosystem carbon exchange was directly responsible for much of the inter-annual variation in autotrophic

production and carbon accumulation in the woody part of the ecosystem. Additionally, stem diameter changes were found to be highly correlated to site NEP and other EC-inferred estimates of productivity in a Norway spruce (*Picea abies* (L) forest in the Swiss Alps (Zweifel et al., 2010) and a coniferous (red spruce (*Picea rubens*) and eastern hemlock (*Tsuga canadensis*) forest in central Maine (US) (Teets et al., 2018). Year-to-year relationships should be treated with caution, as water limitations may reduce current photosynthetic rates may limit growth in following years (Zweifel et al., 2010; Teets et al., 2018).

Direct comparison between tree growth and EC measurements may not address all factors that are unique to each data set, which likely led to some discrepancies seen over the observational record. Other studies that have attempted to link tree growth with EC fluxes have also recognized challenges for such comparisons (Babst et al., 2014). Ring width measurements are a measure of biomass allocation to tree stems, while EC fluxes represent carbon assimilation or loss from an entire stand and are dependent on the flux footprint (Baldocchi, 2003). Biomass accumulation is not limited to the stems and biomass accumulation in roots or foliage may not be captured through a relative increase in stem size and thereafter EC fluxes capture overall biomass production more completely (Brüggermann et al., 2011). Another challenge is constraining uncertainty in RWI estimated GEP values. Incompatibility between the measured EC and ring width measurements arise from variations in the EC flux footprint

size, which may vary in size and location due to prevailing wind direction (Chen et al., 2009). In order to eliminate this error, all trees within the flux footprint would need to be sampled, and the footprint shape during the calibration period (i.e. April-May-June-July) would have to be mapped fully. As both of our sites are homogenous, even-aged stands of white pine, error originating from this source should be rather minimal. Another challenge for the modelled GEP is the 14-year (2003- 2017) calibration period (Figure 2.7; 2.8), where mechanisms driving ecosystem productivity were undoubtedly different from earlier decades covered by ring width data.

Despite these challenges, our study shows a significant relationship between tree ring growth and GEP in these two different age stands. This relationship will be helpful for up-scaling of biometric measurements to stand level to examine the past climate drivers of ecosystem productivity. Direct measurements of root growth, foliar biomass, and other components of tree growth and biomass accumulation should be combined with tree ring records to produce a more comprehensive measure of inter-annual biomass accumulation in trees.

2.6 Conclusions

This study evaluated relationships between tree ring chronologies and environmental controls such as temperature, precipitation, and PDSI in two different age (78-year and 43-year-old) white pine plantation forests in southern Ontario, Canada. At both sites, tree ring chronologies displayed significant growth sensitivities to climate, with negative relationships for temperature and positive relationships for precipitation and PDSI. As expected, the most significant relationships between tree growth and climate variables occurred during the growing season, where May-June-July was the most critical period for growth at both sites. Drought sensitivity was different between the two stands, with the younger TP74 stand showing higher sensitivity over the long term (36 years) and during moderate to extreme drought years. Stand age and management are likely responsible for the observed differences in tree growth in response to drought. GEP values derived from eddy-flux measurements from 2003- 2017 showed a significant relationship with tree growth as represented by ring width measurements at both sites. This study shows that tree rings are a strong indicator of climate impacts in white pine forests, which is a common afforestation species in the region.

2.7 Acknowledgements

This study was supported by the Natural Sciences and Engineering Research Council (NSERC) of Canada, Global Water Futures initiative and

Ontario Ministry of Environment and Climate Change. In-kind support from the Canadian Foundation of Innovation (CFI), the Ontario Innovation Trust (OIT), McMaster University, and the McMaster Centre for Climate Change is also acknowledged. Thanks to Matthias Peichl and Michelle Kula for access to sample archives and biometrics information for the site. Additional thanks to Felix Chan for assistance with sample preparation and to Myroslava Khomik and Joshua McLaren for data analytical assistance.

2.8 References

Acker, S.A., Halpern, C.B., Harmon, M.E., Dyrness, C.T. 2002. Trends in bole biomass accumulation, net primary production and tree mortality in *Pseudotsuga menziesii* forests of contrasting age. *Tree Physiology* 22, 213–217.

Adams, H.D., Guardiola-Claramonte, M., Barron-Gafford, G.A., Villegas, J.C., Breshears, D.D., Zou, C.B., Troch, P.A., Huxman, T.E. 2009. Temperature sensitivity of drought induced tree mortality portends increased regional die-off under global-change-type drought. *Proceedings of the National Academy Of Sciences USA* 106, 7063–7066.

Arain, M.A., and Restrepo-Coupe, N., 2004. Net ecosystem production in a temperate pine plantation in southeastern Canada. *Agricultural and Forest Meteorology* 128, 223-241.

Babst, F., Bouriaud, O., Papale, D., Gieden, B., Janssens, I., Nikinmaa, E., Ibrom, A., Wu, J., Bernhofer, C., Köstner, B., Grünwald, T., Seufert, G., Ciais, P., Frank, D. 2013. Above-ground woody carbon sequestration measured from tree rings is coherent with net ecosystem productivity at five eddy-covariance sites. *New Phytologist* 2013. doi: 10.1111/nph.12589

Baldocchi D. 2003. Assessing the eddy-covariance technique for evaluating carbon dioxide exchange rates of ecosystems: past, present and future. *Global Change Biology* 9, 1–14.

Bebber, D. P., Thomas, S. C., Cole, W. G., Balsillie, D. 2004. Diameter increment in mature eastern white pine *Pinus strobus* L. following partial harvest of old-growth stands in Ontario, Canada. *Trees*, 18:1, 29-34.

Bevilacqua, E., Puttock, D., Blake, T. J., Burgess, D. 2005. Long-term differential stem growth responses in mature eastern white pine following release from competition. *Canadian Journal of Forest Research*, 35:3, 511-520.

Biondi, F. 1999. Comparing tree-ring chronologies and repeated timber inventories as forest monitoring tools. *Ecological Applications* 9:1, 216-227.

Boden, T.A., G. Marland, and R.J. Andres. 2016. Global, regional, and national fossil-fuel CO₂ emissions. Carbon Dioxide Information Analysis Center, Oak Ridge National Laboratory, U.S. Department of Energy, Oak Ridge, Tenn., U.S.A. doi 10.3334/CDIAC/00001_V2016

Bond, B.J. 2000. Age-related changes in photosynthesis of woody plants. *Trends in Plant Science* 5, 349–353.

- Brüggemann, N., Gessler, A., Kayler, Z., Keel, S.G., Badeck, F., Barthel, M., Boeckx, P., Buchmann, N., Brugnoli, E., Esperschütz, J. et al. 2011. Carbon allocation and carbon isotope fluxes in the plant–soil–atmosphere continuum: a review. *Biogeosciences* 8, 3457–3489.
- Bunn, A.G., Jansma, E., Korpela, M., Westfall, R.D., Baldwin, J. 2013. Using simulations and data to evaluate mean sensitivity (ξ) as a useful statistic in dendrochronology. *Dendrochronologia* 31, 250-254.
- Carrer, M., Urbinati, C. 2004. Age – dependent tree – ring growth responses to climate in *Larix decidua* and *Pinus cembra*. *Ecology* 85:3, 730-740.
- Catesson, A.M. 1994. Cambial ultrastructure and biochemistry: changes in relation to vascular tissue differentiation and the seasonal cycle. *International Journal of Plant Sciences* 155, 251–261
- Chan, F.C.C., Arain, M.A., Khomik, M., Brodeur, J., Peichl, M., Restrepo-Coupé, N., Thorne, R., Beamesderfer, E., McKenzie, S., Xu, B., Croft, H., Pejam, M., Trant, J., Kula, M., Skubel, R. 2018. Carbon, water and energy exchange dynamics of a young pine plantation forest during the initial fourteen years of growth. *Forest Ecology and Management* 410, 12-26.
- Chen, J.M., Govind, A., Sonnentag, O., Zhang, Y., Barr, A. and Amiro, B., 2006. Leaf area index measurements at Fluxnet-Canada forest sites. *Agricultural and Forest Meteorology* 140, 257-268.
- Chen, B., Black, T., Coops, N., Hilker, T., Trofymow, J., Morgenstern, K. 2009. Assessing tower flux footprint climatology and scaling between remotely sensed and eddy covariance measurements. *Boundary-Layer Meteorology* 130, 137–167.
- Clifford, M.J., Cobb, N.S., Buenemann, M. 2011. Long-term tree cover dynamics in a pinyon-juniper woodland: climate-change-type drought resets successional clock. *Ecosystems* 14, 949-962.
- Cook, E.R. 1985. A time series analysis approach to tree-ring standardization. Ph.D. dissertation, University of Arizona, Tucson, Arizona.
- Cook, E.R., Briffa, K., Shiyatov, S., Mazepa, V. 1990. Tree ring standardization and growth-trend estimation. Pages 104–123 in E. R. Cook and L. A. Kairiukstis, editors. *Methods of dendrochronology*. Kluwer Academic Publishers, Dordrecht, The Netherlands.

Dié, A., De Ridder, A., Cherubini, P., Kouamé, F., Verheyden, A., Kitin, P., Toirambe, B., Van den Bulcke, J., Van Acker, J., Beeckman, H. 2015. Tree rings show a different climatic response in a managed and non-managed plantation of teak (*Tectona grandis*) in West Africa. *IAWA Journal* 36:4, 409-427.

Draper, W.B., Gartshore, M.E. and Bowles, J.M. 2003. St. Williams Crown Land life science inventory. Ontario Ministry of Natural Resources.

Environment Canada., 2017. Climate Data Online. <http://www.climate.weatheroffice.ec.gc.ca>

Esper, J., Niederer, R., Bebi, P., Frank, D. 2008. Climate signal age effects – evidence from young and old trees in the Swiss Engadin. *Forest Ecology and Management* 255:11, 3783-3789.

FAO, 2010: Global Forest Resources Assessment 2010. FAO Forestry Paper No. 163, Food and Agriculture Organization of the United Nations (FAO), Rome, Italy, 340 pp.

Fernández-de-Uña, L., Cañellas, I., Gea-Izquierdo, G. 2015. Stand competition determines how different tree species will cope with a warming climate. *PLoS ONE* 10:3: e0122255. <https://doi.org/10.1371/journal.pone.0122255>

Fritts, H.C. 1976. *Tree Rings and Climate*. Academic Press Inc. London.

Ganey, J.L. and Vojta, S.C. 2011. Tree mortality in drought-stressed mixed-conifer and ponderosa pine forests, Arizona, USA. *Forest Ecology and Management* 261, 162-168.

Goodale, C.L., Heath, L.S., Houghton, R.A., Jenkins, J.C., Kohlmaier, G.H., Kurz, W., Liu, S., Nabuurs, G.J., Nilsson, S., Shvidenko, A.Z., Apps, M.J., Birdsey, R.A., Field, C.B. 2002. Forest carbon sinks in the Northern Hemisphere. *Ecological Applications* 12:3, 891-899.

Holmes, R.L. 1983. Computer-assisted quality control in tree-ring dating and measurement. *Tree-Ring Bulletin* 43, 69–75.

Jacobi, J., Perrone, D., Duncan, L.L., and Hornberger, G. 2013. A tool for calculating the Palmer drought indices. *Water Resources Research* 49, 6086-6089.

Kelly, K. 1974. Damaged and efficient landscapes in rural and southern Ontario 1880–1900. *Ontario History* 66, 1–14.

Law, B.E. 2014. Regional analysis of drought and heat impacts on forests: current and future science directions. *Global Change Biology* 20, 3595-3599.

Le Quéré et al., 2016. Global carbon budget 2016. *Earth Systems Scientific Data* 8, 605–649. Doi: 10.5194/essd-8-605-2016.

Lorenz, K., and Lal, R. 2010. *Carbon Sequestration in Forest Ecosystems*. Springer Netherlands. DOI 10.1007/978-90-481-3266-9

McLaren, J.D., Arain, M.A., Khomik, M., Peichl, M. and Brodeur, J., 2008. Water flux components and soil water –atmospheric controls in a temperate pine forest growing in a well-drained sandy soil. *Journal of Geophysical Research: Biogeosciences* 113, G04031.

Niinemets U. 2009. Responses of forest trees to single and multiple environmental stresses from seedlings to mature plants: Past stress history, stress interactions, tolerance and acclimation. *Forest Ecology and Management* 260, 1623-1639.

Ohtsuka, T., Saigusa, N., Koizumi, H. 2009. On linking multiyear biometric measurements of tree growth with eddy covariance – based net ecosystem production. *Global Change Biology* 15:4, 1015-1024.

Oribe, Y., Funada, R., Kubo, T. 2003. Relationships between cambial activity, cell differentiation and the localization of starch in storage tissues around the cambium in locally heated stems of *Abies sachalinensis* (Schmidt) Masters. *Trees* 17:185-192.

Pan, Y., Birdsey, R., Fang, J., Houghton, R., Kauppi, P., Kurz, W.A., Phillips, O.L., Shvidenko, A., Lewis, S.L., Canadell, J.G., Ciais, P., Jackson, R.B., Pacala, S., McGuire, A.D., Piao, S., Rautiainen, A., Sitch, S., and Hayes, D. 2011: A large and persistent carbon sink in the world's forests. *Science*, 333:6045, 988-993.

Parresol, B.R. and Vissage, J.S., 1998. White pine site index for the southern forest survey. U.S. Department of Agriculture, Forest Service, Southern Research Station, Asheville, NC. 8 pp

Peichl, M., Arain, M.A. 2007. Allometry and partitioning of above- and belowground tree biomass in an age-sequence of white pine forests. *Forest Ecology and Management* 253, 68-80.

Peichl, M., Arain, M.A. and Brodeur, J.J., 2010a. Age effects on carbon fluxes in temperate pine forests. *Agricultural and Forest Meteorology* 150, 1090-1101.

Peichl, M., Arain, M.A., Ullah, S., and Moore, T.R. 2010b. Carbon dioxide, methane, and nitrous oxide exchanges in an age-sequence of temperate pine forests. *Global Change Biology* 16, 2198-2212.

Piutti, E., and Cescatti, A. 1997. A quantitative analysis of the interactions between climatic response and intraspecific competition in European beech. *Canadian Journal of Forest Research* 27, 277–284.

Powers, M. D., Pregitzer, K. S., Palik, B. J., Webster, C. R. 2009. Wood $\delta^{13}\text{C}$, $\delta^{18}\text{O}$ and radial growth responses of residual red pine to variable retention harvesting. *Tree Physiology*, 30:3, 326-334.

Prentice, I. C., and S. P. Harrison, 2009: Ecosystem effects of CO_2 concentration: Evidence from past climates. *Climate of the Past* 5, 297–307.

Presant, E.W., Acton, C.J., 1984. The soils of the regional municipality of Haldimand-Norfolk. Volume 1, Report No. 57. Agriculture Canada, Ministry of Agriculture and Food, Guelph, Ontario, 100pp.

Primicia, I., Camarero, J., Janda, P., Čada, V., Morressey, R., Trotsiuk, V., ... Svoboda, M. 2015. Age, competition, disturbance and elevation effects on tree and stand growth response of primary *Picea abies* forest to climate. *Forest Ecology and Management* 354, 77-86.

Randall, J.S. 1877. Map of the Township of Charlotteville. In: *Historical Atlas of Haldimand and Norfolk Counties, Ontario*. Illustrated. H.R. Page Co. 1877, 1879.

Rennenberg, H., Loreto, F., Polle, A., Brill, F., Fares, S., Beniwal, R.S., and Gessler, A. 2006. Physiological responses of forest trees to heat and drought. *Plant Biology* 8, 556–571

Rocha, A., Goulden, M., Dunn, A., Wofsy, S. 2006. On linking interannual tree ring variability with observations of whole – forest CO_2 flux. *Global Change Biology* 12:8, 1378-1389.

Ryan, M., Binkley, D., Fownes, J. 1997. Age related decline in forest productivity: pattern and process. *Advances in Ecological Research* 27, 213–262.

Ryan, M.G., Yoder, B.J., 1997. Hydraulic limits to tree height and tree growth. *BioScience* 47, 235–242.

Shao, Q., Huang, L., Liu, J., Yang, H., Chen, Z. 2009. Dynamic analysis on carbon accumulation of a plantation in Qianyanzhou based on tree ring data. *Journal of Geographic Sciences* 19, 691-706.

Skubel, R., Khomik, M., Brodeur, J., Arain, M. 2017. Short-term selective thinning effects on hydraulic functionality of a temperate pine forest in eastern Canada. *Ecohydrology* 10:1, DOI: 10.1002/eco.1780.

Smith, P. et al. 2015. Biophysical and economic limits to negative CO₂ emissions. *Natural Climate Change* 6, 42–50.

Speer, J.H. 2010. *Fundamentals of Tree-Ring Research*. University of Arizona Press. Tucson, USA.

Teets, A., Fraver, S., Hollinger, D., Weiskittel, A., Seymour, R., Richardson, A. 2018. Linking annual tree growth with eddy-flux measures of net ecosystem productivity across twenty years of observation in a mixed conifer forest. *Agricultural and Forest Meteorology* 249, 479-487.

Thompson I., B. Mackey, S. McNulty, and A. Mosseler. 2009. Forest resilience, biodiversity, and climate change: A synthesis of the biodiversity / resilience / stability relationship in forest ecosystems. Secretariat of the Convention on Biological Diversity, Montreal, Canada, 67 pp. [http:// www.cakex.org/virtual-library/1233](http://www.cakex.org/virtual-library/1233).

Thornthwaite, C.W. 1948. An approach toward a rational classification of climate. *Geographical Review* 38:1, 55-94.

van Mantgem, P.J., Stephenson, N.L., Byrne, J.C., Daniels, L.D., Franklin, J.F., Fulé, P.Z., et al. 2009. Widespread increase of tree mortality rates in the western United States. *Science* 323, 521-524. doi: 10.1126/science.1165000 PMID: 19164752

Waring, R,W, and Running, S.W. 2007. *Forest ecosystems – analysis at multiple scales*. Elsevier Academic, Burlington, MA

Well Records Ontario 1953-2006. Government of Ontario, Ministry of the Environment, Conservation and Parks. <https://www.ontario.ca/page/well-records>

Wendling, I., Trueman, S.J., Xavier, A. 2014 Maturation and related aspects in clonal forestry – Part I: concepts, regulation and consequences of phase change. *New Forests* 45, 449–471.

Whitehead, D., Jarvis, P.G., Waring, R.H. 1984. Stomatal conductance, transpiration, and resistance to water uptake in a *Pinus sylvestris* spacing experiment. *Canadian Journal of Forest Research* 14, 692–700.

Zafirov, N. 2006. Dendroecological analysis of Scots pine (*Pinus sylvestris* L.) stands in Vitosha Mountain, Bulgaria. *Tree Rings in Archaeology, Climatology and Ecology* 4, 188-194.

Zhang Q, Shao M, Jia X, Wei X. 2017. Relationship of climatic and forest factors to drought- and heat-induced tree mortality. *PLoS ONE* 12:1. e0169770. doi:10.1371/journal.pone.0169770

Zavitz, E.J. 1958. 1909: Report on the restoration of waste lands in southern Ontario. In: Zavitz, E.J. 1958. *Fifty Years of Reforestation in Ontario*. Ontario Department of Lands and Forests. Ontario Department of Agriculture, Toronto.

Zobel, B.J., Sprague, J.R. 1998. *Juvenile Wood in Forest Trees*. Springer-Verlag. Berlin. Zweifel, R., Eugster, W., Etzold, S., Dobbertin, M., Buchmann, N., Häsler, R. 2010. Link between continuous stem radius changes and net ecosystem productivity of a subalpine Norway spruce forest in the Swiss Alps. *New Phytologist* 187:3, 819-830.

Table 2.1. Biometric characteristics 2017 of TP39 and TP74 sites as of 2017. TP39 represents the site planted in 1939 and TP74 represents the site planted in 1974.

Stand ID	TP39	TP74
Geographical position	42°42'366 N 80°21'265 W	42°42'264 N 80°20'547 W
Previous land use and management practices	<i>Oak savanna cleared for afforestation; harvested in 1983 and 2012</i>	<i>Oak savanna cleared for afforestation; not disturbed</i>
Dominant tree species	<i>P. strobus</i> L.	<i>P. strobus</i> L.
Stand age (yr) (2017)	78	43
Mean height (m) *	22.0 ± 1.9	13.5 ± 3.9
DBH ± SD (cm) (2017)	34.6 ± 3.1	18.3 ± 5.6
Crown width (m) **	4.5	3.4
Density stems (ha ⁻¹) **	425 ± 172	1633 ± 166
Max. leaf area index (LAI) (m ² m ⁻²) ****	8.0	5.9
Site index at age 25(SI ₂₅) ***	26	28

* measured in 2014; ** measured in 2004; ***Chen et al. (2006); **** based on site index curves by Parresol and Vissage (1998)

Table 2.2 Summary statistics for the tree ring chronologies constructed from sampled trees at the TP39 and TP74 sites.

Statistic	TP39	TP74
Time interval	1944-2017	1981-2017
Number of series	37	47
Series intercorrelation	0.397	0.462
Mean ring width (mm)	2.65	0.46
Autocorrelation	0.903	0.767
Expressed population signal (EPS)	0.951	0.950
Running RBAR	0.473	0.410

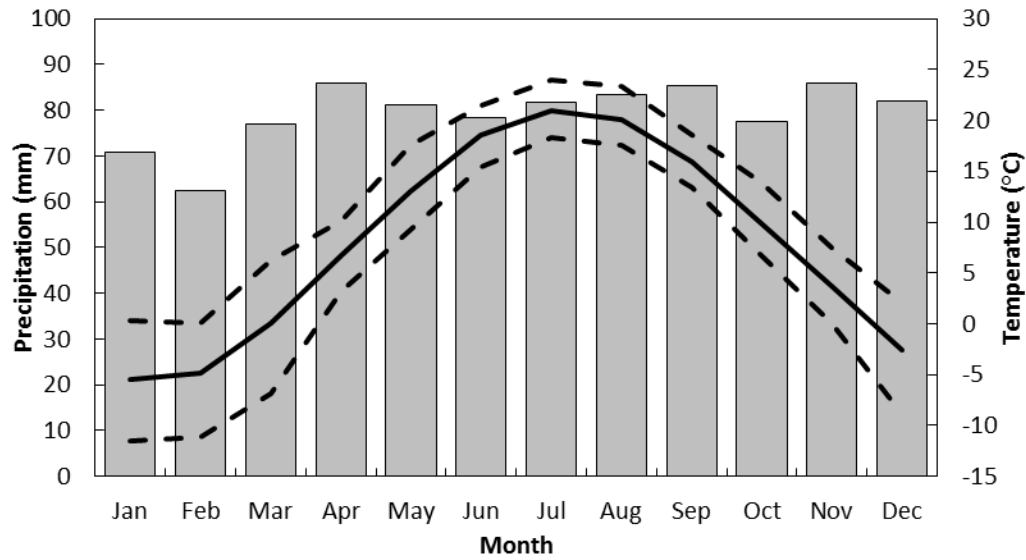


Figure 2.1 Monthly total precipitation (bars) and monthly mean (solid line), maximum and minimum (dashed lines) temperature at Delhi weather station (1935-2017) (Environment Canada).

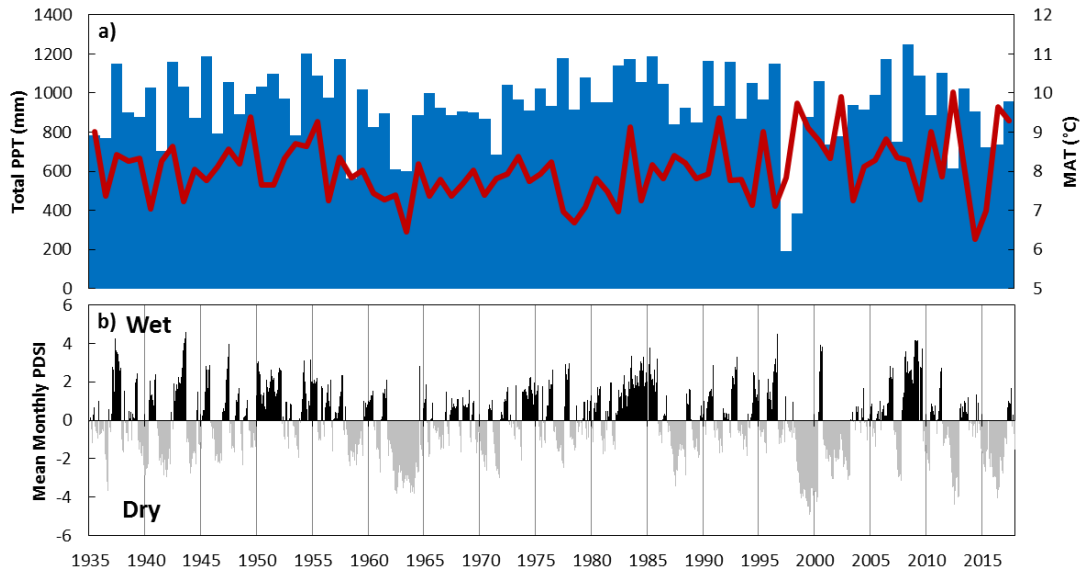


Figure 2.2. a) Mean annual temperatures (MAT) (red line) and total precipitation (PPT) (blue columns) from Environment Canada’s Delhi station data archives 1935-2017. b) Monthly PDSI values calculated from monthly climate data. Missing climate data from the Delhi station archive was filled using other station data (see section 3.4.2).

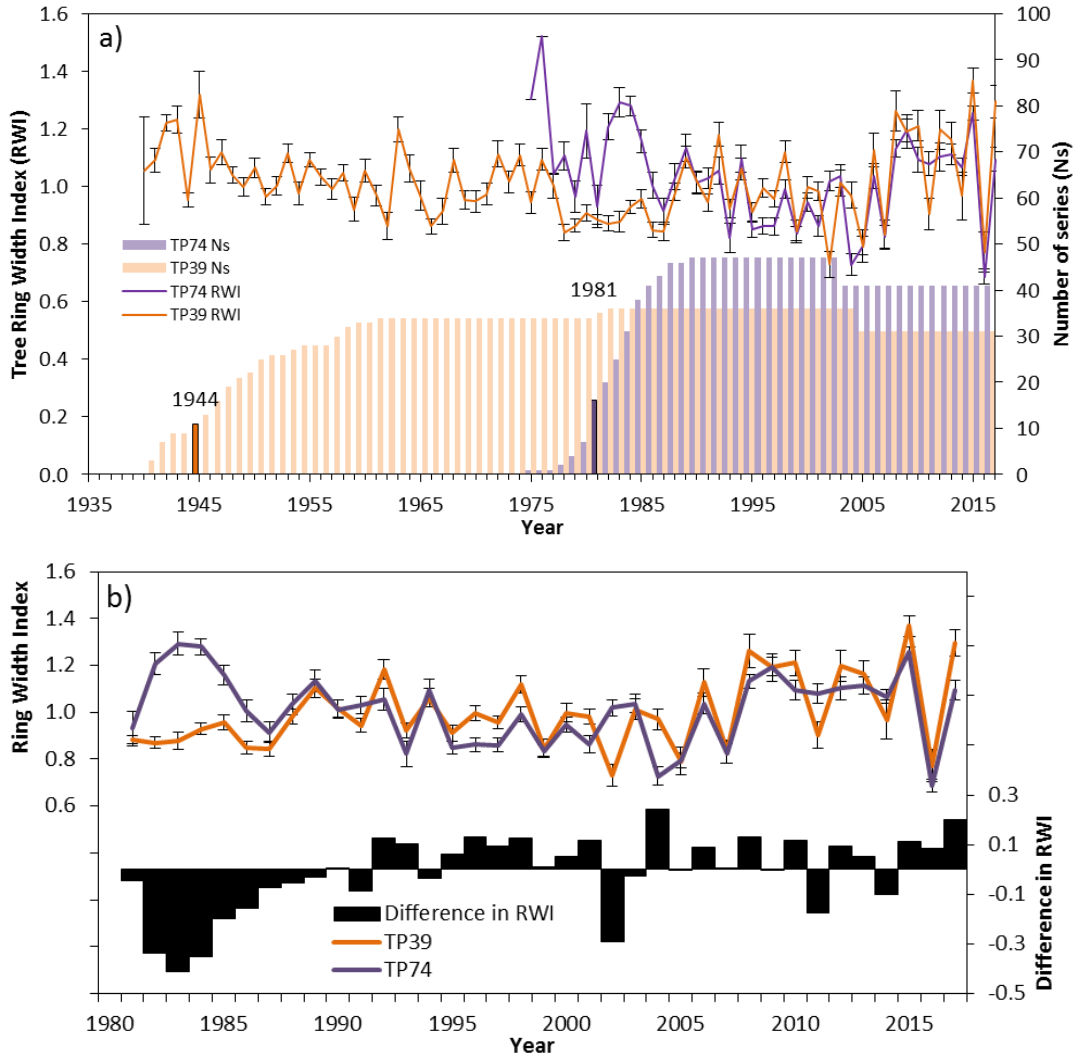


Figure 2.3. Mean ring width indices (RWI) constructed from tree ring series for a) the TP39 and TP74 stands. The error bars on the RWI correspond to annual values of standard error between the individual series. The shaded region in a) corresponds to sample depth, as plotted on the right axis. The starting year of the chronologies where sufficient sample depth was achieved is indicated by darker vertical bars at 1944 (TP39) and 1981 (TP74). In b), differences between the two site RWI chronologies are shown for the period of overlap 1981-2017. The vertical bars in b) indicate first difference in the two site chronologies.

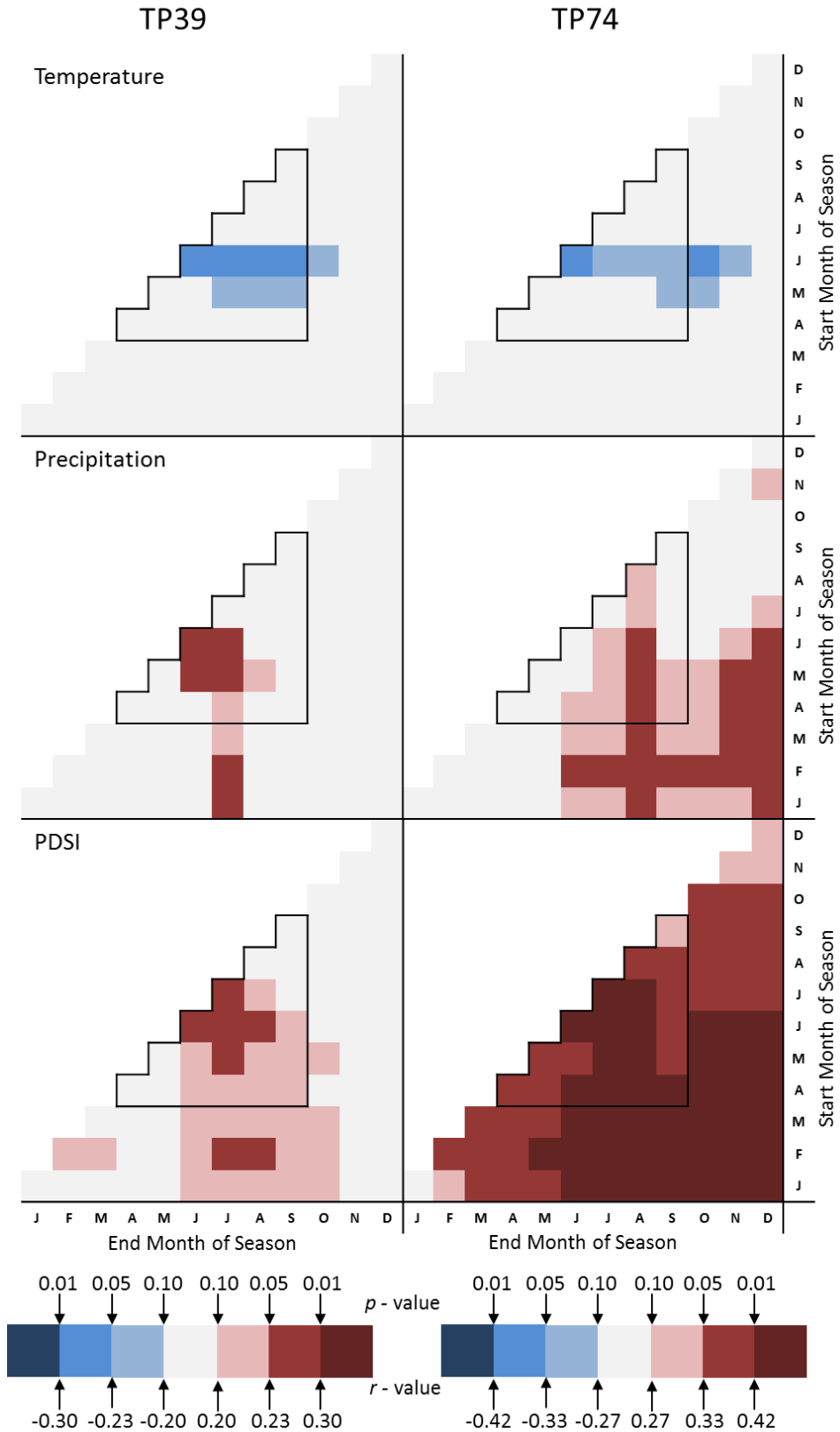


Figure 2.4. Significance of critical r -values between TP39 and TP74 ring width index (RWI) with climate variables in mean temperature, total precipitation and PDSI. The period of correlation was 1944-2017 for TP39 and 1981-2017 for TP74. Relationship significance for individual months are shown on the corner-to-corner diagonals (e.g. 1st line January to 12th line December) whereas significance over month combinations extend to the right (e.g. 1st line, 3rd block would represent the January – March significance). The area of the charts that corresponds to correlations during the growing season (April-September) is indicated by the stair-step box. Pearson correlation coefficient significance is shown as $p < 0.10$; $p < 0.05$; $p < 0.01$; two-tailed for all relationships. Critical values are shown in Supplemental Data.

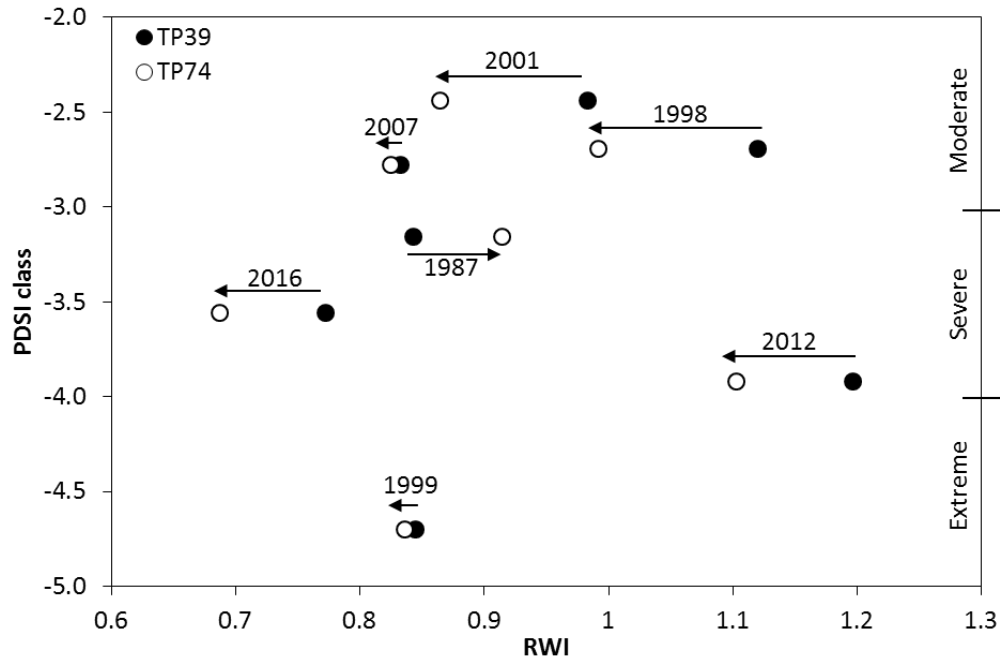


Figure 2.5. Growth response of TP74 (hollow) relative to TP39 (black) during the seven years with lowest JJ PDSI over the 1981 to 2017 period. Descriptive qualifiers of the PDSI class as described in Thornthwaite (1948) are shown on the right axis. Note that for six of these years, TP74 showed lower growth relative to TP39.

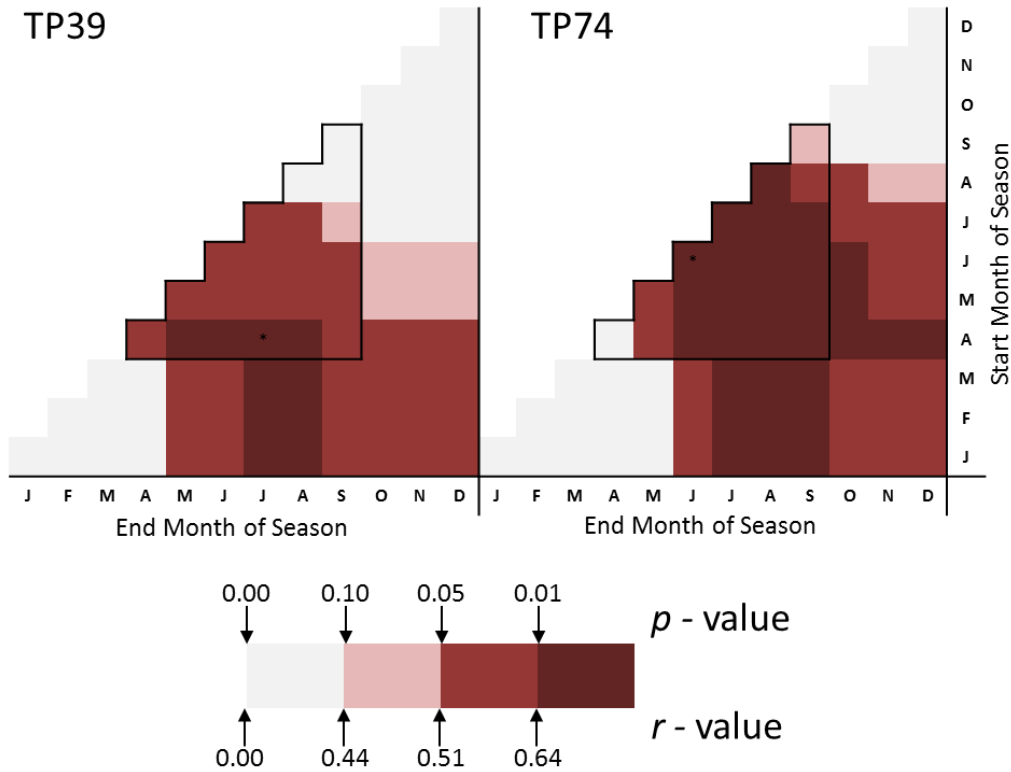


Figure 2.6. Significance of critical r -values between TP39 and TP74 ring width index (RWI) with AMJJ GEP. The period of correlation was 2003-2017 for both TP39 and TP74. Relationship significance for individual months are shown on the corner-to-corner diagonals (e.g. 1st line January to 12th line December) whereas significance over month combinations extend to the right (e.g. 1st line, 3rd block would represent the January – March significance). The area of the charts that corresponds to correlations during the growing season (April-September) is indicated by the stair-step box. Pearson correlation coefficient significance is shown as $p < 0.10$; $p < 0.05$; $p < 0.01$; two-tailed for all relationships. Critical values are shown in Supplemental Data.

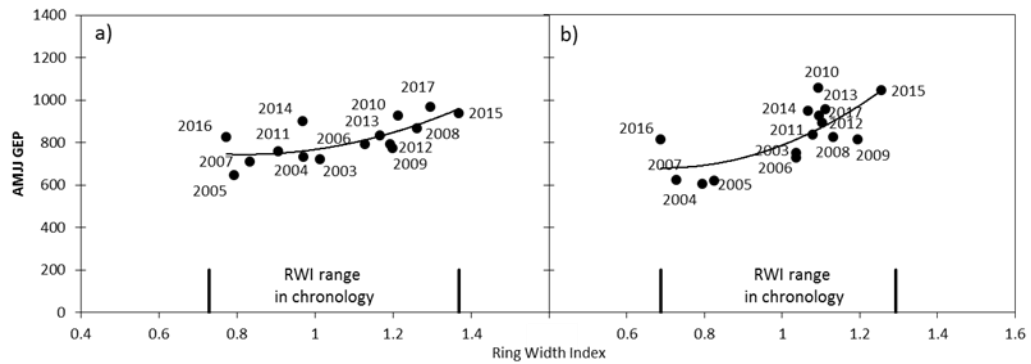


Figure 2.7. Polynomial curve relationships in tree ring RWI and observed AMJJ GEP collected from site eddy covariance for the observational period 2003-2017 for a) TP39 and b) TP74. Bars on the x-axis in a) and b) also show the range in RWI values in each chronology.

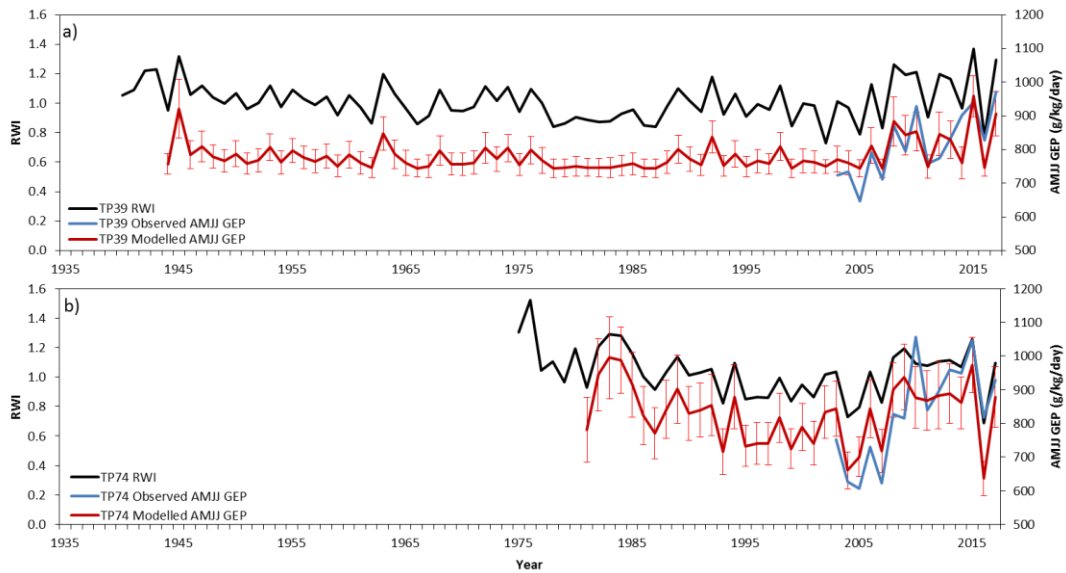


Figure 2.8. Modelled AMJJ GEP from tree ring data (red line) over the available years represented by tree ring chronologies (black line) for a) TP39 and b) TP74, with observed GEP (blue line). Error bars in GEP show the combined error in GEP calculations from RWI standard error and measured flux error.

Supplemental data: correlation coefficient values

This section contains all correlation values for the Pearson’s correlation analysis between the TP39 and TP74 tree ring chronologies (RWI) with climate (temperature, precipitation and PDSI) and stand ecosystem (GEP) variables. As in Figure 2.4 the vertical scale corresponds to the starting month of the correlation and the horizontal month corresponds to the ending month of the correlation.

TP39

TP39: Temperature with RWI

J	F	M	A	M	J	J	A	S	O	N	D		
											-0.0139	D	
										0.0497	0.0145	N	
									-0.0281	0.0172	0.0011	O	
								-0.0232	-0.0353	0.0037	-0.0061	S	
							-0.1422	-0.1065	-0.0943	-0.0532	-0.0485	A	
							-0.1671	-0.1847	-0.1577	-0.1451	-0.1017	-0.0883	J
						-0.2434	-0.2586	-0.2550	-0.2310	-0.2063	-0.1644	-0.1391	J
				-0.0218	-0.1616	-0.1987	-0.2144	-0.2033	-0.1905	-0.1532	-0.1322	M	
			0.1819	0.1026	-0.0193	-0.0790	-0.1134	-0.1108	-0.1127	-0.0846	-0.0777	A	
		0.1244	0.1824	0.1477	0.0673	0.0111	-0.0262	-0.0301	-0.0364	-0.0200	-0.0231	M	
	-0.0690	0.0313	0.0868	0.0731	0.0149	-0.0213	-0.0484	-0.0507	-0.0553	-0.0409	-0.0422	F	
0.0308	-0.0215	0.0395	0.0857	0.0744	0.0256	-0.0059	-0.0296	-0.0325	-0.0369	-0.0258	-0.0282	J	

TP39: Precipitation with RWI

J	F	M	A	M	J	J	A	S	O	N	D	
											-0.13145	D
										-0.13590	-0.17088	N
									0.00918	-0.07269	-0.11983	O
								-0.12334	-0.08750	-0.13846	-0.16621	S
							-0.09893	-0.15562	-0.13117	-0.17219	-0.18809	A
						0.16298	0.03552	-0.05128	-0.04208	-0.08924	-0.11712	J
					0.24393	0.29630	0.18089	0.06501	0.06590	0.01167	-0.02765	J
				0.13124	0.23371	0.28401	0.20485	0.10341	0.10480	0.05194	0.01135	M
			-0.09853	0.02923	0.15208	0.20559	0.14129	0.06426	0.06574	0.02168	-0.01257	A
		0.04993	-0.02559	0.05020	0.15762	0.21006	0.14856	0.07752	0.07732	0.03447	0.00086	M
	0.15939	0.12283	0.05167	0.10101	0.19361	0.23838	0.17634	0.10738	0.10584	0.06413	0.02965	F
0.02379	0.11842	0.11320	0.05377	0.10044	0.18958	0.23093	0.17343	0.10969	0.10704	0.06663	0.03332	J

TP39: PDSI with RWI

J	F	M	A	M	J	J	A	S	O	N	D	
											-0.04442	D
										-0.01969	-0.03352	N
									0.11575	0.05161	0.01914	O
								0.05060	0.08836	0.05599	0.03062	S
							0.14456	0.10353	0.11573	0.08739	0.06194	A
						0.26390	0.21879	0.16976	0.16708	0.13798	0.11090	J
					0.24990	0.26410	0.23722	0.19800	0.19268	0.16619	0.14052	J
				0.17734	0.21993	0.24314	0.22909	0.20050	0.19623	0.17327	0.15045	M
			0.12989	0.15964	0.19917	0.22579	0.21858	0.19715	0.19392	0.17359	0.15313	A
		0.19330	0.16754	0.17800	0.20675	0.22974	0.22413	0.20606	0.20249	0.18337	0.16397	M
	0.21596	0.20940	0.18858	0.19344	0.21604	0.23589	0.23110	0.21513	0.21153	0.19339	0.17481	F
0.05651	0.14137	0.16590	0.16241	0.17342	0.19793	0.21989	0.21879	0.20623	0.20406	0.18765	0.17065	J

TP39: GEP with RWI

J	F	M	A	M	J	J	A	S	O	N	D	
											0.3410	D
										0.1338	0.1988	N
									-0.0369	0.0467	0.1017	O
								0.0615	0.0127	0.0590	0.0973	S
							0.4136	0.3436	0.2636	0.2642	0.2781	A
						0.5734	0.5316	0.4796	0.4157	0.4122	0.4202	J
					0.5319	0.5971	0.5639	0.5184	0.4656	0.4608	0.4663	J
				0.5328	0.5885	0.6261	0.5955	0.5514	0.5026	0.4945	0.4980	M
			0.5576	0.6723	0.6590	0.6874	0.6530	0.6106	0.5635	0.5533	0.5560	A
		0.0214	0.3857	0.5461	0.6136	0.6779	0.6481	0.6064	0.5615	0.5512	0.5536	M
	N/A	0.0214	0.3857	0.5461	0.6136	0.6779	0.6481	0.6064	0.5615	0.5512	0.5536	F
N/A	N/A	0.0214	0.3857	0.5461	0.6136	0.6779	0.6481	0.6064	0.5615	0.5512	0.5536	J

TP74

TP74: Temperature with RWI

J	F	M	A	M	J	J	A	S	O	N	D	
											0.0415	D
										-0.0208	0.0208	N
									-0.1283	-0.1057	-0.0279	O
								-0.1669	-0.1922	-0.1484	-0.0705	S
							-0.2135	-0.2538	-0.2524	-0.2046	-0.1263	A
						-0.1375	-0.2096	-0.2471	-0.2700	-0.2261	-0.1552	J
					-0.3576	-0.2935	-0.3033	-0.3256	-0.3320	-0.2988	-0.2279	J
				-0.0250	-0.2335	-0.2406	-0.2738	-0.3033	-0.3093	-0.2773	-0.2112	M
			0.1558	0.0673	-0.0931	-0.1335	-0.1841	-0.2189	-0.2423	-0.2155	-0.1634	A
		-0.1884	-0.0825	-0.0716	-0.1692	-0.1852	-0.2176	-0.2417	-0.2596	-0.2416	-0.2066	M
	-0.1338	-0.1819	-0.1231	-0.1176	-0.1831	-0.1948	-0.2189	-0.2383	-0.2544	-0.2435	-0.2199	F
-0.1331	-0.1653	-0.1938	-0.1518	-0.1472	-0.1980	-0.2050	-0.2234	-0.2401	-0.2545	-0.2510	-0.2351	J

TP74: Precipitation with RWI

J	F	M	A	M	J	J	A	S	O	N	D	
											0.2294	D
										0.2113	0.2883	N
									-0.0149	0.1381	0.2382	O
								-0.0516	-0.0523	0.0839	0.1785	S
							0.2907	0.1457	0.1176	0.2010	0.2571	A
						0.1656	0.2966	0.2091	0.1912	0.2477	0.2910	J
					0.2266	0.2802	0.3720	0.2728	0.2627	0.3100	0.3468	J
				0.2302	0.2730	0.3192	0.3930	0.3086	0.3034	0.3403	0.3686	M
			0.1477	0.2633	0.2994	0.3280	0.3997	0.3181	0.3115	0.3485	0.3744	A
		-0.0028	0.1065	0.2183	0.2902	0.3284	0.3901	0.3190	0.3153	0.3447	0.3656	M
	0.2471	0.1469	0.2115	0.2721	0.3371	0.3638	0.4097	0.3438	0.3406	0.3671	0.3780	F
-0.1212	0.0822	0.0582	0.1148	0.2031	0.2785	0.3137	0.3603	0.3058	0.2995	0.3284	0.3425	J

TP74: PDSI with RWI

J	F	M	A	M	J	J	A	S	O	N	D	
											0.3023	D
										0.3097	0.3146	N
									0.3945	0.3643	0.3534	O
								0.3001	0.3675	0.3676	0.3623	S
						0.4326	0.4302	0.3987	0.3968	0.3968	0.3903	A
					0.4468	0.4535	0.4473	0.4182	0.4306	0.4300	0.4252	J
				0.3761	0.4227	0.4415	0.4431	0.4225	0.4334	0.4333	0.4293	M
			0.4053	0.4102	0.4417	0.4579	0.4584	0.4408	0.4488	0.4472	0.4424	A
		0.4127	0.4185	0.4238	0.4515	0.4688	0.4703	0.4566	0.4630	0.4603	0.4549	M
	0.4031	0.4147	0.4206	0.4278	0.4532	0.4708	0.4737	0.4635	0.4693	0.4667	0.4616	F
0.1915	0.3083	0.3539	0.3762	0.3947	0.4251	0.4486	0.4572	0.4527	0.4601	0.4587	0.4548	J

TP74: GEP with RWI

J	F	M	A	M	J	J	A	S	O	N	D	
											0.4194	D
										0.0530	0.1600	N
									0.1280	0.1067	0.1555	O
								0.5123	0.3567	0.3019	0.3171	S
							0.6784	0.6403	0.5461	0.4971	0.4967	A
						0.6427	0.6967	0.6789	0.6116	0.5783	0.5772	J
					0.7745	0.7284	0.7378	0.7211	0.6676	0.6407	0.6387	J
				0.5743	0.7174	0.7089	0.7194	0.7058	0.6605	0.6371	0.6352	M
			0.2957	0.5327	0.6802	0.7060	0.7188	0.7077	0.6660	0.6439	0.6420	A
		-0.1235	0.1163	0.3728	0.5913	0.6628	0.6861	0.6779	0.6397	0.6187	0.6172	M
	N/A	-0.1235	0.1163	0.3728	0.5913	0.6628	0.6861	0.6779	0.6397	0.6187	0.6172	F
N/A	N/A	-0.1235	0.1163	0.3728	0.5913	0.6628	0.6861	0.6779	0.6397	0.6187	0.6172	J

TP39 with TP74:

GEP with RWI

J	F	M	A	M	J	J	A	S	O	N	D			
											0.3802	D		
										0.0934	0.1794	N		
								0.2869	0.0455	0.0767	0.1286	O		
							0.5460	0.4920	0.1847	0.1805	0.2072	S		
							0.6081	0.6141	0.4048	0.3807	0.3874	A		
							0.6532	0.6627	0.5793	0.5137	0.4952	0.4987	J	
							0.5536	0.6530	0.6675	0.6197	0.5666	0.5507	0.5525	J
							0.6025	0.6696	0.6286	0.5816	0.5658	0.5666	0.5666	M
			0.4266				0.6967	0.6859	0.6591	0.6148	0.5986	0.5990	0.5990	A
		-0.0511	0.2510	0.4594	0.6024	0.6703	0.6671	0.6421	0.6006	0.5849	0.5854	0.5854	0.5854	M
	N/A	-0.0511	0.2510	0.4594	0.6024	0.6703	0.6671	0.6421	0.6006	0.5849	0.5849	0.5854	0.5854	F
N/A	N/A	-0.0511	0.2510	0.4594	0.6024	0.6703	0.6671	0.6421	0.6006	0.5849	0.5849	0.5854	0.5854	J

Chapter 3 Tree ring growth records track drought and heat stress in an afforested red pine (*Pinus resinosa*) plantation

3.1 Abstract

Annual stem growth of *Pinus resinosa* (red pine) was measured from 95 tree cores sampled in an evenly-aged plantation forest established in 1931 in southern Ontario, Canada. A ring-width chronology was constructed to examine climate controls on growth. The chronology length is 72 years and spans the period AD 1942 to 2013. The ring-width chronology shows promise as a potential predictor of past temperature and drought based on significant relationships with temperature, precipitation, and Palmer Drought Severity Index. Temperature was consistently negatively correlated to growth, while precipitation and PDSI were consistently positively correlated to growth. Temperatures during the month of May were likely critical to control annual tree growth. Drought signals observed in the recent years of the growth record may be a temperature- or age-driven response, as precipitation has not significantly changed over the period covered by the chronology. The climate resilience of red pine, which is a common constituent of forest plantations of southern Ontario, may be weakened as growing season temperatures are projected to continue to increase in coming decades. The climate-growth relationships identified here will be beneficial to make informed management decisions regarding climate weakness of red pine plantation forests.

3.2 Introduction

Temperate forest ecosystems are becoming more vulnerable to climate change impacts, which may be significant because forest ecosystems constitute a major portion of land surface area and are a major contributor to the carbon sink (Gonzalez et al., 2010). Extensive research suggests climate change is increasing tree mortality due to increased warming and drought (Prentice and Harrison, 2009; Allen et al., 2010; Silva et al., 2010; Silva and Anand, 2013). Climate change impacts on forest ecosystems also include intense weather events and increased drought frequency and intensity, both of which are generally expected to reduce forest productivity (Spittlehouse and Stewart, 2003; Allen et al., 2010). Increased temperatures have been shown to have important effects on forest productivity through the reduction in radial growth of trees in the Great Lakes region (Kilgore and Telewski, 2004; St. George et al., 2008; Magruder et al., 2012; Magruder et al., 2013). Prolonged drought has been shown to weaken forest ecosystems to disease and insect outbreaks within the region (Flannigan and Woodward, 1993; McLaughlin, 2001; Fernández-de-Uña et al., 2015; Mann et al., 2017).

Plantation forests possess unique characteristics as compared to natural forests (FAO, 2010) by having reduced species diversity (Thompson et al., 2009;

Aussenac, 2000). Forests in southern Ontario have a long history of being heavily modified and the composition of many forest stands today is much different than their natural counterparts. Prior to European settlement, the native forest canopy of this region existed as a hardwood-dominated ecosystem. Settlement of southern Ontario and eastern North America initiated large-scale disturbance of the native forests through intense logging and land-clearing practices (Zavitz, 1960; Parker et al., 2003). These activities have profoundly reduced the distribution and integrity of native forests (Clawson, 1979; Frelich, 1995) and reduced forest cover in the region from 90% to 11% (MAB, 2000). From the 1880s into the 1910s, agricultural cultivation reduced soil organic matter content, fertility, and productive quality of the environment (Kelly, 1974). After this brief farming period, the glacial soils were nutritionally exhausted and abandoned to wind and water erosion (Zavitz, 1958; 1960). In the early 1920s and over the next couple decades, the landscape was reforested to 19% (MAB, 2000). In southern Ontario, red pine (*Pinus resinosa*) was used extensively to afforest the declining agricultural fields in many areas (Zavitz, 1960). As of 2000, the land area of southern Ontario is 16.0% forested (1.3% coniferous, 4.4% mixed, and 10.3% deciduous) (Natural Resources Canada, 2009). Coniferous forests, which cover about 8.1% of the total land area of southern Ontario, were established through plantation in the Carolinian Life Zone of extreme southern Ontario. Therefore, given that forest plantations are a common constituent of forest throughout southern Ontario, we need to better understand the climatic and environmental

controls on these pine plantation systems to determine how they may respond to climate change in the future (McLaughlin, 2001; Erbilgin and Raffa, 2002).

Dendrochronology has been used to identify environmental controls on tree growth (e.g. Bebber et al., 2004; Bevilacqua et al., 2009; Powers et al. 2009; Bottero et al., 2016). The nature of trees and the fact that they form annual growth rings has allowed precise and absolute dating of events pertaining to climate and ecosystem change. In managed forest stands tree rings have been used to reconstruct the growth response stimulus of trees to silvicultural forest management as well as climatic variances such as drought and long-term changes in temperature (Cutter et al., 1991; Biondi, 1999; Pukkala et al., 2011; Diaconu et al., 2015; Bottero et al., 2016 and Sohn et al., 2016). As forest areas are becoming increasingly disturbed by anthropogenic activity, it is important to identify how tree growth has responded to climatic and environmental change (Gregory et al., 1991; Biondi and Waikul, 2004; Magruder et al., 2012; Magruder et al., 2013). This information will assist in making informed forest management decisions that enhance timber production, while also promoting ecosystem resilience.

In this paper, we present a tree ring record of an 87-year-old afforested red pine plantation located in southern Ontario with the purpose of identifying the primary climate controls on the growth of red pine trees in this plantation setting. We examined the relationship between climate variables and radial growth using

Pearson's correlations and moving interval correlation functions. The results identify temporal shifts in climate and tree ring growth response. This study serves as a framework for more rigorous studies of management at this southern Ontario red pine plantation.

3.3 Materials and methods

3.3.1 Site description and experimental design

The St. Williams Conservation Reserve (SWCR) consists of 1034 ha of Crown Land in Norfolk County, southern Ontario (SWCRMP, 2007). The SWCR formerly operated as the St. Williams Provincial Forest until becoming regulated by the Ontario Ministry of Natural Resources and Forestry (OMNRF) in cooperation with the St. Williams Conservation Reserve Community Council (SWCRCC) in June, 2008. The SWCR occupies one of the largest blocks of forestland in the Carolinian Forested Ecozone of southern Ontario and is recognized for its biodiversity with a high concentration of species at risk ($n \geq 90$) (SWCRMP, 2007). Several forest types occur within the SWCR, including oak savanna, Carolinian forest, and conifer plantations, in addition to wetland habitats near Lake Erie.

The study site, informally referred to as TP31, is a 14-ha red pine plantation block in the Turkey Point Tract of the SWCR (42°42'N, 80°21'W) located at elevation 220 m above sea level (Figure 3.1a). This red pine plantation is part of the Turkey Point Observatory or Turkey Point Flux Station (TPFS) (Figure 1.1b). It is also associated with the Global Water Futures Program and Global Fluxnet.

Late 18th century surveyors' timber records describe this area as mixed tamarack-cedar swamp, with white and black oak (*Quercus* spp.) stands occupying high ground or topographic ridges (e.g. Walsh 1795; Hambly 1796). In the late 1800s and early 1900s, the area was farmed for wheat and tobacco, causing deteriorating soil conditions and desertification (Draper, 2003). In 1909 and 1922 the site and adjacent lots were not shown as vegetated according to period topographic maps of the area (Canada Department of the Militia and Defence, 1908; 1922). In 1926, the Ontario Ministry of Natural Resources and Forestry (OMNRF) began procuring property in this region (Zavitz, 1958; Kelly, 1974) to afforest the degraded agricultural lands (Draper, 2003). As part of the OMNRF ecosystem restoration program, afforestation at TP31 was established in 1931 by planting red pine seedlings in furrowed rows approximately 2 m apart. The site continues to be managed by OMNRF with the assistance of the SWCRCC and is being developed under the shelterwood silviculture system. As of 2016, the mean tree diameter of measured red pine trees (n = 409) at 1.3 m

above the ground surface at breast height (DBH1.3) was 30.8 ± 5.1 cm and mean tree height was 21.7 ± 5.7 m (± 1 SD). TP31 is characterized by undulating terrain of lacustrine-sourced sand. Ground water generally lies at a minimum depth of 5 to 6 m based on ground water measurements in a well at the site. The organic litter layer is approximately 5 cm thick.

Variable retention harvest (VRH) is a method for restoration of conifer plantations to native forest types. Research of natural stands of red pine and other conifers suggest VRH as a way to create spatially heterogeneous residual canopy tree patterns that more closely emulate natural disturbance patterns and stand development processes (Harrington et al., 2005; Aukema and Carey, 2008; Pukkala et al., 2011). Research scientists from the OMNRF came to an agreement with the SWCRCC to establish a suitable area for the VRH trial, which includes the 1931 red pine plantation. In February of 2014, five different treatments were randomly applied to 0.89 ha blocks in the experimental area. During application, the area was harvested using feller-bunchers and forwarders. Harvested trees were removed for timber, but the smaller diameter portion of the stem tops were left on site. The branches were also stripped from the stems, and left on site. The four treatment applications are labeled as follows: (55D) where 55% of the canopy was retained with uniform density throughout the plot; (33D) where 33% of the canopy was retained with uniform density; (55A) where 55% of the pre-canopy was retained in large circular groves; and (33A) where 33% of the canopy was

retained in large circular groves. The remaining three plots, where no canopy was removed, were retained as reference control plots (CN). This randomized experimental design enables a quantitative assessment of VRH effects on understory and canopy growth.

3.3.2 Meteorological and climate information

The climate of southern Ontario is sub-humid temperate and relatively moderate compared to the rest of Canada. Historical climate data (1935-2017) are available from the Delhi weather station, located approximately 20 km north of the study site (Environment and Climate Change Canada). Mean annual temperature is 8.2 °C (1981-2010), with the mean temperature of the hottest month (July) being 21.1 °C (1981-2010). The mean temperature of the coldest month (January) is -5.1 °C (1981-2010). Mean annual rainfall is 976 mm (1981-2010) and is evenly distributed throughout the year (Environment and Climate Change Canada). The inter-annual variation of precipitation is high at ± 164 mm (± 1 standard deviation) (1981-2010).

In order to identify drought periods, monthly and annual values of the Palmer Drought Severity Index (PDSI) was calculated. The input variables are monthly mean temperature, precipitation, latitude of the meteorological station, and available water content (assumed to be a maximum of 35 mm for these sandy

soils). Potential evapotranspiration (PET) was calculated according to the Thornthwaite (1948) method and the calibration period was taken to be for the full available record 1935-1990. Tables of monthly water balance, Z-Index, PET, PDSI, and PDHI (Palmer Hydrological Drought Index) (Jacobi et al., 2013). The PDSI outputs were used in further pairwise correlation analyses as a measure of drought index. Positive values of the PDSI indicate wetter and cooler conditions, while negative PDSI values are indicative of drought conditions (warmer and drier).

The integrity of the Delhi station climate record (1935-2017) was compared to measurements made by the CA-TP4 flux tower site (2003-2017) located on the north side of the red pine site (Peichl et al., 2010; Skubel et al., 2017). The Delhi station climate record was also compared to those from other Environment Canada stations in the vicinity, namely Foldens, Port Dover, Simcoe, and St. Williams; all located within 50 km of the study site.

3.3.3 Sample collection and data processing

In total, 95 tree cores were collected from the even-aged red pine plantation in March of 2017 using a 5-mm Haglöff increment borer at 1.3 m height above the ground surface (DBH_{1.3}). Five to seven trees were sampled along two corner-to-corner transects in each of the fourteen plots. Core samples were

prepared according to standard dendrochronological practices (Stokes and Smiley, 1968; Fritts, 1976). Prepared cores were visually cross-dated and ring widths were measured using a Velmex measuring system with a linear encoder and a measurement precision of 0.001 mm. Visual cross-dating was confirmed using measurement data that was quality checked using the computer software program COFECHA (Holmes, 1983). Following successful cross-dating, the computer software program ARSTAN (Cook, 1985) was used to generate a residual site master chronology. This chronology was generated using a 40-year cubic spline to remove 50% of the 40-year variance, while retaining 99% of the variance acting at 12.67 years. This was necessary to remove long-term noise variance (e.g. age effects) from the measured series and to preserve signals acting on shorter frequencies of interest (Cook, 1985). The residual chronology has had all autocorrelation stripped from the series, making it a suitable chronology to assess climate effects on growth. Summary statistics for the 1935-2013 chronology were computed, including the autocorrelation removed, expressed population signal (EPS), and running RBAR. The red pine residual chronology was used to assess climate sensitivity prior to harvesting and was not used as a measure of disturbance impact on growth. The VRH experiment was initiated in February of 2014. Therefore, the final three years of the red pine residual chronology (2014-2016) were excluded from the analyses.

3.3.4 Climate correlations

The residual growth chronology was compared to local climate data over the 72-year period for the years 1942-2013. Climate to ring index relationships were quantified using pairwise Pearson's correlation coefficients of monthly climate variables (temperature, precipitation, PDSI) for individual months and for all possible combinations of months between January and December for both the previous and current growth years. To evaluate how growth sensitivities may have changed through time, moving interval correlation between radial growth and monthly climate variables were calculated in DENDROCLIM 2002 (Biondi and Waikul, 2004). Moving interval calculations in DENDROCLIM 2002 use 1000 bootstrapped re-samples to determine statistical significance (95%) of coefficients instead of traditional linear approaches (Biondi, 1997; Biondi and Waikul, 2004). This analysis was also used to examine if the climatic response is stable or if it has changed through time (Biondi and Waikul, 2004).

3.4 Results

3.4.1 Chronology characteristics

For this study, the minimum number of series used to construct the ring width chronology in any given year was 18 series. This minimum number was chosen to exclude index values derived from small sample pools. As a result, the

minimum sample depth used to construct the mean ring width chronology was not reached prior to 1942 (Figure 3.2).

Summary statistics for the red pine chronology are presented in Table 3.1, and the inter-annual mean ring width index (RWI) is shown in Figure 3.2. Ninety-five series were used to construct the red pine chronology. The ring width chronology covers the period from 1935 to 2013, when the VRH experiment was initiated. There are some notable trends in indexed time series values. From 1942-1946, index values are more variable (0.95 ± 0.17 SD) compared to the following period 1947-1960, when index values are lower and show reduced variability (0.90 ± 0.05 SD). During the middle part of the record 1961-1984, the chronology shows higher index values and relatively high variability (1.07 ± 0.13 SD), once again followed by four years (1981-1984) of low inter-annual variability in growth index (1.01 ± 0.02). The recent part of the record shows high inter-annual variability in index values (0.96 ± 0.15 SD). Years of low growth index include 1988 (0.74), 1993 (0.77), and 1999 (0.63), while high growth index occurred in 1968 (1.33), 1994 (1.27) and 2010 (1.23).

Chronological means of series inter-correlation, mean ring width, autocorrelation, expressed population signal (EPS) running RBAR, and mean sensitivity are shown in Table 3.1. Incremental means of running RBAR, SD, SE, and EPS were determined for ten-year windows with a five-year overlap using

ARSTAN (Table 3.2). Series inter-correlation, the average correlation of each individual series to the master chronology, is $r = 0.329$. The mean annual ring width is 1.55 mm yr^{-1} . Based on data from the International Tree ring Databank (ITRDB) annual width at the study site is similar to other red pine chronologies from sites in the lower Great Lakes region and Ohio River valley with values between 1.4 to 1.8 mm yr^{-1} , but higher than red pine growth in northern Ontario and Minnesota where annual ring width values are 0.6 to 0.7 mm yr^{-1} . Autocorrelation in the growth series was high with a value of 0.88 , which was slightly higher than other red pine chronologies from this region (0.77 to 0.84). This autocorrelation was removed to construct the site residual chronology. Expressed population signal (EPS) is very high (Table 3.2), likely due to the large sample pool and the similar age of sampled trees. Mean running RBAR, the average correlation between all possible series in any given 100-year window, is 0.38 . Mean sensitivity for the chronology is 0.26 . Ten-year means (Table 3.2.) of running RBAR show higher values for the first and last decades of the chronology with lower values centered in the 1970s. SD values remain similar to the chronological mean of 0.41 for the duration of the chronology. SE values are higher for the first two decades of the chronology, which is likely a result of fewer series represented during this portion. EPS remains high (≥ 0.92) for the duration of the chronology.

3.4.2 Climate record integrity and trends

The temperature record from Delhi station was significantly correlated with other Environment Canada station's monthly temperature data within the region ($r = 0.97$ to 0.99 ; $p < 0.01$) and to the TPFS monthly temperature record 2003 to 2017 ($r = 0.99$; $p < 0.01$). The total monthly precipitation record from Delhi station was significantly correlated to two stations that archived monthly precipitation for longer than 10-years: Foldens (1963 to 2017) ($r = 0.78$; ($p < 0.01$)), Port Dover (1935 to 1982) ($r = 0.80$; ($p < 0.01$)) and to the CA-TP4 record (2003 to 2017) ($r = 0.63$; ($p < 0.01$)). Therefore, we used temperature and precipitation data from the Delhi station for the period 1935 to 2017 and gaps in the Delhi station precipitation data were filled using data from Port Dover and Foldens stations.

To observe temporal meteorological trends, monthly climographs (Figure 3.3a-d) were constructed from climate data from Delhi Station ($42^{\circ}52'N$, $80^{\circ}33'W$) for two 30-year periods: 1941-1970, and 1981-2010; to overlap with earlier and recent decades during the period of analysis. Temperature has increased in recent years compared to the earlier decades in all months except October with the largest increases in winter and spring (November to April) (Figure 3.3a). Precipitation has increased in early summer (May-July) and during the fall and winter seasons (September-January) in recent years, but declined during late winter to spring (February-April) and during August (Figure 3.3b).

Water availability, quantified as precipitation minus potential evaporation (P-PE), has declined during spring (March-April) and increased during summer (June and July) in recent decades (Figure 3.3c). Drought, indicated by negative PDSI values, has increased from February through June in recent decades (Figure 3.3d).

3.4.3 Climate and tree ring growth relationships 1942-2013

The inter-annual variability in ring width index (RWI) was compared to monthly combinations of measured (temperature, precipitation) and calculated (PDSI) climate variables from Delhi station over the 72-year period from 1942 to 2013. Pairwise Pearson's correlation coefficients were calculated between RWI and climate variables for individual months and for all possible combinations of months between January and December for both the previous and current growth year. The area of the charts that corresponds to correlations during the growing season (April-September) is indicated by a stair-step box. Correlation coefficient values (r -values) are shown in the Supplemental Data section at the end of this chapter.

During the previous growing season, temperatures in July were significantly correlated ($r = -0.23$, $p < 0.05$) with ring width. Additionally, mean temperature during previous July-August-September were also significantly correlated with tree ring width ($r = -0.26$, $p < 0.05$). During the current growing

season, significant ($p < 0.05$ and $p < 0.01$) temperature and ring width relationships were generally negative for individual months (current year shown in Figure 3.4a; Supplemental Data). During the current growing season, mean July air temperature was significantly correlated with ring width ($r = -0.26$, $p < 0.05$). For combined monthly temperature series, correlations between mean temperature and ring widths were more negative and the significance of those relationships were higher (e.g., May-June-July, $r = -0.32$, $p < 0.01$) than for individual months. A significant positive correlation was found for the period March-April, when increased air temperature may contribute to increase RWI ($r = 0.23$; $p < 0.05$). Otherwise, significant air temperature and RWI relationships were negative.

For the previous growing season, total monthly precipitation was not correlated to ring growth for any month or combined month period. During the current growing season, correlations between total monthly precipitation and ring width were positive (Figure 3.4b; Supplemental Data). Precipitation during the month of June was significantly correlated with tree growth ($r = 0.27$; $p < 0.05$). The combination of total monthly precipitation for May-June-July, yielded the highest correlation with RWI ($r = 0.34$, $p < 0.01$). Interestingly, this is generally a period of water deficiency during mid-summer (Figure 3.3c).

For the previous growing season, mean monthly PDSI was not correlated to ring growth for any month or combined month period. During the current growing season, the RWI record shows a significant positive relationship to monthly PDSI (Figure 3.4c; Supplemental Data). Significant relationships were found for the individual months of May ($r = 0.25$; $p < 0.05$), June ($r = 0.35$; $p < 0.01$), July ($r = 0.32$; $p < 0.01$), and August ($r = 0.30$; $p < 0.05$) and for month combinations, May-June-July ($r = 0.32$, $p < 0.01$) and May-June-July-August ($r = 0.33$, $p < 0.01$).

3.4.4 Temporal climate and growth relationships 1942-2013

To assess the significance of temporal climate-growth correlations, moving interval correlation functions were computed between RWI and monthly climate values using DENDROCLIM 2002 ((Biondi, 1997; Biondi and Waikul, 2004). Moving interval correlation analysis was used to show the years in which monthly variation in climate were significant (95% confidence) for generating variability in tree growth for the 16-month period lasting from May of the previous year to August of the growth year (Figure 3.5). The length of the interval may vary between a minimum length of twice the number of predictors which in this case is 16 months $\times 2 = 32$ years, and a maximum length of $<80\%$ of the chronology which is $0.8 \times 72 = 56$ years. The minimum length of 32 years was

long enough to capture the years when monthly climate variations generated significant variability in tree growth (Figure 3.5). The sign (\pm) of the r -value correlations from the moving interval results were similar to the monthly and multi-month pairwise correlation results (section 3.4.3) (Figure 3.4). Air temperatures were negatively correlated with ring width while precipitation and PDSI had positive correlations. Monthly temperature may have generated increased variability in growth during the late 1980s (May) and late 1990s (July), although it is not stable over time. June precipitation was also found to be important to control variability on growth on growth prior to the late 1980s. A positive correlation of May-June PDSI was found during the current growth year. Drought becomes a significant control on growth variability in the late 1980s, and this signal remains consistent until the end of the record (Figure 3.5).

Visual inspection of RWI plotted with temperature, precipitation, and PDSI (Figure 3.6) verifies that lower ring widths seem to correspond with negative PDSI values. However, this relationship appears to breakdown during the interval 1962-1967, when temperature seems to be more strongly correlated with growth rather than PDSI. Closer examination of the ring width to PDSI relationships show that from 1942-1970, these relationships were non-significant ($n = 28$, $r = 0.06$). However from 1970-2013, PDSI was significantly related to tree ring growth ($n = 44$, $r = 0.47$, $p < 0.01$). Therefore, air temperature may have acted as a dominant limiting factor on growth during these years. It is also clear

that years with enhanced drought produced smaller ring widths for that year or the following year (Figure 3.6c).

3.5 Discussion

The ring width chronology developed from this red pine plantation shows that past temperature and drought conditions are important climate factors controlling the growth of red pine in this region. Variability in temperature during May-June-July was an important factor controlling the growth of red pine as indicated by the correlations computed between ring width and temperature. Increasing temperatures during the month of May may be critical to lowered RWI later in the growing season, as the temperature effect in May may propagate into later months of the growth year (Figure 3.4a - horizontal line 5). Similarly, significant ($p < 0.05$) negative correlations were found in an uncut red pine stand in Michigan for the April-July period (1948-2010) (Magruder et al., 2013). The negative relationship between tree growth and May-June-July temperature may cause an increase in tree respiration rates (Adams et al., 2009). Increased respiration consumes photosynthates that otherwise could have had the potential to be sequestered as stem biomass (Pallardy, 2007; Magruder et al., 2012). Negative correlations between temperature and growth during the growing season have been observed in the Great Lakes region for other red pine dendrochronological records (Graumlich, 1993; Flannigan and Woodward, 1993;

St. George et al., 2008; Kipfmuller et al., 2010). In upper Michigan, June temperature was most significant for red pine ($r = -0.30$; $p < 0.05$) (Graumlich, 1993). Kipfmuller et al. (2010) also found temperature in the June-July interval to be important for red pine growth in Minnesota ($r = -0.30$; $p < 0.05$). Some studies suggest that higher temperatures could further stress and weaken red pine stands in the southern part of its range and may favour other competitors over red pine (Flannigan and Woodward, 1993). In this study in southern Ontario, Canada, higher temperatures and drought severity poses a climate risk that could lead to decreased growth and tree productivity for red pine stands such as the managed plantation forests investigated here.

The significant positive relationship between growth and precipitation was particularly enhanced during the month of June (Figure 3.4b), although this relationship was more important in the 1970s and again in the 2000s (Figure 3.6). According to other studies, precipitation has been found to be a significant driver of tree ring growth in the Great Lakes region. In Michigan, correlation between 60-year old red pine growth chronologies from plantation forests, with precipitation and a climate moisture index, was positively correlated (95% confidence) during the June-July period, and were inversely related to temperature (Magruder et al., 2012; Magruder et al., 2013). Graumlich (1993) reports precipitation during July was inversely related to growth ($r = -0.25$) for pines located in upper Michigan. Additional studies of red pine growth records in

this region also report growth sensitivity to precipitation in Minnesota (July, $r = 0.45$, $p < 0.05$) (Kipfmuller et al., 2010) and Michigan (May-June-July, $r = 0.35$, $p < 0.05$) (Magruder et al., 2012). The observed correlation of growth with precipitation in this study may be the result of insufficient soil water storage capacity during the summer, which was consistently depleted in the June-July-August months for this site in southern Ontario (Figure 3.2b-c). June, in particular, is the month with the lowest precipitation over the April to August period.

The PDSI is correlated over a longer span of the growing season than precipitation, with significant and positive relationships lasting from May through August. This may seem counter-intuitive given that monthly precipitation in April through August is comparatively high relative to drier winters and springs (Figure 3.3b). It is likely summer warmth led to higher evaporative rates and moisture stress in the forest, which generated adverse effects on radial growth. The summer drought signal is widely recorded in the annual growth rings from red pine sites throughout the Great Lakes region (Kipfmuller et al., 2010; Magruder et al., 2012; Magruder et al., 2013). In Minnesota, drought acted as a significant control ($r = 0.45$, $p < 0.05$) on growth over a two month period (June-July) (Kipfmuller et al., 2010). When interpreted in combination with moving interval correlations, radial growth of red pine has become increasingly sensitive to growing season water deficits during the latter part of the 20th century. The

increased sensitivity is likely associated with warming-induced drought stress due to increasing air temperature. It is possible that increasing temperatures and drought severity could pose a climate risk to water stability in red pine plantations in this region by forcing stand structural changes through root diseases, as have been observed for other red pine stands in this region (Whitney, 1988; Gregory et al., 1991; McLaughlin, 2001). Temperature and drought may be a climatic stressor that is contributing to the increase in *Armillaria* root rot and pocket mortality observed in many plantations, particularly on sites with calcareous soil horizons where red pine root growth was inhibited (McLaughlin, 2001). Summer precipitation patterns are also different compared to the remainder of the year with most of precipitation occurring in association with convective storms rather than frontal systems. Convective storms may produce high amounts of rainfall, but the low water-holding capacity of the sandy soils near Lake Erie limits the amount of moisture available to trees when coupled with warmer temperatures.

While the external climate forcings may have partially contributed to the temporal evolution of tree ring growth responses with time, physiological changes due to aging are also important to consider. Studies that examine tree physiology within species show differing response functions across age categories (e.g. Carrer and Urbinati, 2004; Esper et al., 2008; Primicia et al., 2015). The environmental signal in tree ring growth records is a complex interaction between environmental factors and physiological response (Carrer and Urbinati, 2004).

The destination of translocated photosynthates and their storage rates has been found to change with aging (Ryan et al., 1997). In addition, reduced hydraulic resistances in younger, smaller trees (Ryan and Yoder, 1997) affects stomatal conductance which increase photosynthetic rate as compared to older members of a species (Bond, 2000). The observed differences in ring width to PDSI that take place after the mid-1980s (Figures 3.5; 3.6) may be due to aging (e.g. hydraulic conductance, photosynthetic rate). Additionally, a larger root network may limit water resources available to residual trees in TP31, which may explain the higher responsiveness due to high competition during drought, as well as the aforementioned indirect influence of increased temperature on water availability to individual trees.

Climate models suggest that growing season air temperatures in the Great Lakes region are likely to increase 1.1 to 2.6°C and precipitation is also likely to increase by approximately 10% by the end of the 21st Century (50th percentile, RCP 4.5) (IPCC, 2013 Annex 1). However, it has been suggested (Bottero et al., 2016) that increased warming may increase evapotranspiration rates to drive down water availability. Therefore any tree growth benefits that may occur from increased precipitation may in fact be reduced. The temperature and drought correlations with growth found in this study may be a useful contribution to the growing body of knowledge of the resilience of red pine plantations. Growth sensitivity to May-July drought has also been increasing in recent decades, with

enhanced pairwise correlation since the 1970s. Additionally, the development of a drought signal since the mid-1980s relative to past decades may be further sign that this forest system may be in a state of transition and decline, which parallels the results of other studies in the Great Lakes region (McLaughlin, 2001; Kipfmuller et al., 2010; Magruder et al., 2012; 2013). With increasing temperatures forecast to occur, the resilience of this and other red pine monocultures may continue to decline. In the face of future climate change silvicultural management should be aimed to manage declining red pine stands. Low correlation between radial growth and precipitation has been reported in uncut red pine stands in the Great Lakes region (Magruder et al., 2013). The low correlation may be the result of the low water holding capacity of the soil, or it may be due to high stand density and competition (Magruder et al., 2013). The examination of the effects of thinning intensity on climate resilience of forest stands is often done using retrospective analysis (Laurent et al., 2003; Cescatti and Piutti, 1998). It has been found that increased thinning intensity resulted in increased resiliency to temperature and drought stress in Norway spruce (*Picea abies*) (Laurent et al., 2003) and European beech (*Fagus sylvatica* L.) (Cescatti and Piutti, 1998). However, extremely high thinning intensity has been found to be detrimental to tree productivity due to damage from the thinning process and wind throw (Bradford and Palik, 2009; Powers et al., 2010).

3.6 Conclusions

The growth records developed from this red pine plantation in southern Ontario, Canada, are an indicator of the impacts of past temperature and drought conditions on growth and carbon sequestration in these managed forests. May-June-July air temperature was the dominant control on the growth of red pine during the growing season. However, years with enhanced drought caused smaller ring widths and when interpreted in combination with moving interval correlations, it appears that growth of red pine is becoming increasingly sensitive to growing season water deficits. These results indicate that temperature and drought play a dominant role in the tree ring growth in this red pine plantation. The results of this dendrochronological study are generally similar to those of other red pine plantations in the Great Lakes region. Therefore it is likely that forecasted increases in temperature will further reduce growth in these stands. This study shows that tree ring growth is a strong indicator of recent climate in this red pine forest, a common afforestation species in the region.

3.7 Acknowledgements

The technical assistance and support of William Parker and Ken Elliot of the Ontario Ministry of Natural Resources and Forestry (OMNRF) is gratefully acknowledged. We also thank Bing Xu, Stéfan Sauer, and Myroslava Khomik for assistance with data collection. The project was financially supported by the Natural Sciences and Engineering Research Council (NSERC), Global Water Futures Programs (GWF) and by the Ontario Ministry of Environment and Climate Change (MOECC). We also thank the in-kind support from the Ontario Ministry of Natural Resources and Forestry (OMNRF), the Environment and Climate Change Canada (ECCC), and the St. Williams Conservation Reserve Community Council (SWCRCC).

3.8 References

- Adams, H.D., Guardiola-Claramonte, M., Barron-Gafford, G.A., Villegas, J.C., Breshears, D.D., Zou, C.B., Troch, P.A., Huxman, T.E. 2009. Temperature sensitivity of drought induced tree mortality portends increased regional die-off under global-change-type drought. *Proceedings of the National Academy of Sciences USA* 106, 7063–7066.
- Allen, C. D., Macalady, A. K., Chenchouni, H., Bachelet, D., McDowell, N., Vennetier, M., ... Cobb, N. 2010. A global overview of drought and heat-induced tree mortality reveals emerging climate change risks for forests. *Forest Ecology and Management* 259:4, 660-684. DOI: 10.1016/j.foreco.2009.09.001
- Aukema, J., Carey, A. 2008. Effects of variable-density thinning on understory diversity and heterogeneity in young Douglas-fir forests. United States Department of Agriculture Intermountain Research Station, Research Paper PNW-RP-575, 28 pp.
- Aussenac, G. 2000. Interactions between forest stands and microclimate: Ecophysical aspects and consequences for silviculture. *Annals of Forest Science* 57, 287-301.
- Bebber, D. P., Thomas, S. C., Cole, W. G., Balsillie, D. 2004. Diameter increment in mature eastern white pine *Pinus strobus* L. following partial harvest of old-growth stands in Ontario, Canada. *Trees* 18:1, 29-34.
- Bevilacqua, E., Puttock, D., Blake, T. J., Burgess, D. 2005. Long-term differential stem growth responses in mature eastern white pine following release from competition. *Canadian Journal of Forest Research*, 35:3, 511-520.
- Biondi, F. 1997. Evolutionary and moving response functions in dendrochronology. *Dendrochronologia* 15, 139–150.
- Biondi, F. 1999. Comparing tree-ring chronologies and repeated timber inventories as forest monitoring tools. *Ecological Applications* 9:1, 216-227.
- Biondi, F., Waikul, K. 2004. DENDROCLIM2002: A C++ program for statistical calibration of climate signals in tree-ring chronologies. *Computers & Geosciences* 30, 303-311.
- Bond, B.J. 2000. Age-related changes in photosynthesis of woody plants. *Trends in Plant Science* 5, 349–353.

Bottero, A., D'Amato, A.W., Palik, B.J., Bradford, J.B., Fraver, S., Battaglia, M.A., Asherin, L.A. 2016. Density-dependent vulnerability of forest ecosystems to drought. *Journal of Applied Ecology* 54:6, 1605-1614. <https://doi.org/10.1111/1365-2664.12847>

Bunn, A.G., Jansma, E., Korpela, M., Westfall, R.D., Baldwin, J. 2013. Using simulations and data to evaluate mean sensitivity (ξ) as a useful statistic in dendrochronology. *Dendrochronologia* 31, 250-254.

Burns, R.M., Honkala, B.H. 1990. *Silvics of North America Trees. 1. Conifers.* U.S. Department of Agriculture Agriculture Handbook 654.

Canada Department of Militia and Defence. 1908. Long Point, Ontario. Scale 1:63,360. G.S.G.S. 2197, Sheet 29. Ottawa: Department of Militia and Defence, 1908.

Canada Department of Militia and Defence. 1922. Long Point, Ontario. Scale 1:63,360. Canada 1 Inch to a Mile, Sheet 29. Ottawa: Department of Militia and Defence, 1922.

Carrer, M., Urbinati, C. 2004. Age – dependent tree – ring growth responses to climate in *Larix decidua* and *Pinus cembra*. *Ecology* 85:3, 730-740.

Cescatti, A., Piutti, E. 1998. Silvicultural alternatives, competition regime and sensitivity to climate in a European beech forest. *Forest Ecology and Management* 102, 213–223. doi:10.1016/S0378-1127(97)00163-1.

Clawson, M. 1979. Forests in the long sweep of American history. *Science* 204, 1168–1174.

Cook, E.R. 1985. A time series analysis approach to tree-ring standardization. Ph.D. dissertation, University of Arizona, Tucson, USA.

Cutter, B.E., Lowell, K.E. Dwyer, J.P., 1991. Thinning effects on diameter growth in black and scarlet oak as shown by tree ring analyses. *Forest Ecology and Management* 43, 1-13.

Diaconu, D., Kahle, H-P, Spieker, H. 2015. Tree- and stand-level thinning effects on growth of European Beech (*Fagus sylvatica* L.) on a northeast- and a southwest-facing slope in southwest Germany. *Forests* 6, 3256-3277.

Draper, W.B., Gartshore, M.E. and Bowles, J.M. 2003. *St. Williams Crown Land Life Science Inventory.* Ontario Ministry of Natural Resources.

Environment Canada., 2017. Climate Data Online.
<http://www.climate.weatheroffice.ec.gc.ca>

Erbilgin, N. and K.F. Raffa. 2002. Association of declining red pine stands with reduced populations of bark beetle predators, seasonal increases in root colonizing insects, and incidence of root pathogens. *Forest Ecology and Management* 164, 221–236.

Esper, J., Niederer, R., Bebi, P., Frank, D. 2008. Climate signal age effects – evidence from young and old trees in the Swiss Engadin. *Forest Ecology and Management* 255:11, 3783-3789.

FAO, 2010: Global Forest Resources Assessment 2010. FAO Forestry Paper No. 163, Food and Agriculture Organization of the United Nations (FAO), Rome, Italy, 340 pp.

Fernández-de-Uña, L., Cañellas, I., Gea-Izquierdo, G. 2015. Stand competition determines how different tree species will cope with a warming climate. *PLoS ONE* 10, e0122255.

Flannigan, M.D., Woodward, F.I. 1993. Red pine abundance: climatic control and responses to future warming. *Canadian Journal of Forest Research* 24, 1166-1175.

Frelich, L.E. 1995. Old forest in the Lake States today and before European settlement. *Natural Areas Journal* 15, 157–167.

Fritts, H.C. 1976. *Tree Rings and Climate*. Academic Press Inc. London.

Graumlich, L.J. 1993. Response of tree growth to climatic variation in the mixed conifer and deciduous forests of the upper Great Lakes region. *Canadian Journal of Forest Research* 23, 133–143.

Gregory, S.C., Rishbeth, J., Shaw III, C.G. 1991. Pathogenicity and virulence. In C.G. Shaw III and G.A. Kile. (eds.) *Armillaria root disease*, pp. 76-87. U.S. Department of Agriculture, *Agricultural Handbook* 691.

Harrington, C., Roberts, S., Brodie, L. 2005. Tree and understory responses to variable-density thinning in western Washington. *Balancing Ecosystem Values Proceedings, Regional Experiments*. 10 pp.

Hambly. 1796. *Field notebook. Survey of Charlotteville*. Lloyd Reeds Map Collection, McMaster University Library.

Holmes, R.L. 1983. Computer-assisted quality control in tree-ring dating and measurement. *Tree-Ring Bulletin* 43, 69–75.

IPCC, 2013: Annex I: Atlas of Global and Regional Climate Projections [van Oldenborgh, G.J., M. Collins, J. Arblaster, J.H. Christensen, J. Marotzke, S.B. Power, M. Rummukainen and T. Zhou (eds.)]. In: *Climate Change 2013: The Physical Science Basis. Contribution of Working Group I to the Fifth Assessment Report of the Intergovernmental Panel on Climate Change* [Stocker, T.F., D. Qin, G.-K. Plattner, M. Tignor, S.K. Allen, J. Boschung, A. Nauels, Y. Xia, V. Bex and P.M. Midgley (eds.)]. Cambridge University Press, Cambridge, United Kingdom and New York, NY, USA.

Jacobi, J., Perrone, D., Duncan, L.L., and Hornberger, G. 2013. A tool for calculating the Palmer drought indices. *Water Resources Research* 49, 6086-6089.

Kelly, K. 1974. Damaged and efficient landscapes in rural and southern Ontario 1880–1900. *Ontario History* 66, 1–14.

Kilgore, J.S., Telewski, F.W. 2004. Climate-growth relationships for native and nonnative *pinaceae* in northern Michigan's pine barrens. *Tree Ring Research* 60, 3–13.

Kipfmüller, K.F., Elliot, G.P., Larson, E.R., Salzer, M.W. 2010. An assessment of the dendroclimatic potential of three conifer species in northern Minnesota. *Tree Ring Research* 2010:66, 113–126.

Laurent, M., Antoine, N., Joel, G. 2003. Effects of different thinning intensities on drought response in Norway spruce (*Picea abies* (L.) Karst.). *Forest Ecology and Management* 183, 47–60. doi:10.1016/S0378-1127(03)00098-7.

MAB (Man and the Biosphere). 2000. 16th Session of the ICC (International Coordinating Council) Bureau. SC-00/CONF.208/13. 9.

Magruder, M., Chhin, S., Monks, A., O'Brien, J. 2012. Effects of Initial Stand Density and Climate on Red Pine Productivity within Huron National Forest, Michigan, USA. *Forests* 2012:3, 1086-1103.

Magruder, M., Chhin, S., Palik, B., Bradford, J. 2013. Thinning increases climatic resilience of red pine. *Canadian Journal of Forest Research* 43, 878–889.

Mann, M. E., Rahmstorf, S., Kornhuber, K., Steinman, B.A., Miller, S., Coumou, D. 2017. Influence of Anthropogenic Climate change on planetary wave resonance and extreme weather events. *Scientific Reports* 7, 45242; doi: 10.1038/srep45242.

McLaughlin, J.A. 2001. Impact of *Armillaria* root disease on succession in red pine plantations in southern Ontario. *The Forestry Chronicle* 3:77, 519-524.

Natural Resources Canada, 2009. Land Cover, circa 2000-Vector. Feature Catalogue. <http://www.geobase.ca>

Niinemets U. 2009. Responses of forest trees to single and multiple environmental stresses from seedlings to mature plants: Past stress history, stress interactions, tolerance and acclimation. *Forest Ecology and Management* 260, 1623-1639.

Pallardy, S.G. 2007. *Physiology of Woody Plants*, 3rd ed.; Academic Press: San Diego, CA, USA.

Parker, W.C., Elliot, K.A., Dey, D.C., Boysen, E. 2008. Restoring southern Ontario forests by managing succession in conifer plantations. *The Forestry Chronicle* 84:1, 83-94.

Peichl, M., Arain, M.A. and Brodeur, J.J., 2010. Age effects on carbon fluxes in temperate pine forests. *Agricultural and Forest Meteorology* 150, 1090-1101.

Powers, M. D., Pregitzer, K. S., Palik, B. J., Webster, C. R. 2009. Wood $\delta^{13}\text{C}$, $\delta^{18}\text{O}$ and radial growth responses of residual red pine to variable retention harvesting. *Tree Physiology* 30:3, 326-334.

Primicia, I., Camarero, J., Janda, P., Čada, V., Morressey, R., Trotsiuk, V., ... Svoboda, M. 2015. Age, competition, disturbance and elevation effects on tree on tree and stand growth response of primary *Picea abies* forest to climate. *Forest Ecology and Management* 354, 77-86.

Pukkala, T., Lähde, E., Laiho, O. 2011. Variable-density thinning in uneven-aged forest management—a case for Norway spruce in Finland. *Forestry* 84. 557-565.

Ryan, M., Binkley, D., Fownes, J. 1997. Age related decline in forest productivity: pattern and process. *Advances in Ecological Research* 27, 213–262.

Ryan, M.G., Yoder, B.J., 1997. Hydraulic limits to tree height and tree growth. *BioScience* 47, 235–242.

Scott, R.W., Huff, F.A. 1996. Impacts of the Great Lakes on regional climate conditions. *J. Great Lakes Research* 22, 845–863.

Skubel, R., Khomik, M., Brodeur, J., Arain, M. 2017. Short-term selective thinning effects on hydraulic functionality of a temperate pine forest in eastern Canada. *Ecohydrology* 10:1, DOI: 10.1002/eco.1780.

Sohn, J.A., Hartig, F., Kohler, M., Huss, J., Bausch, J. 2016. Heavy and frequent thinning promotes drought adaptation in *Pinus sylvestris* forests. *Ecological Applications* 26, 1030–1046.

Spittlehouse, D.L., Stewart, R.B. 2003. Adaptation to climate change in forest management. *B.C. Journal of Ecosystem Management* 4, 1–11.

Stokes, M.A., Smiley, T.L. 1968. *An Introduction to Tree-Ring Dating*. Chicago. University of Chicago Press. USA.

St. George, S., Meko, D.M., Evans, M.N. 2008. Regional tree growth and inferred summer climatic in the Winnipeg River basin, Canada, since AD 1783. *Quaternary Research* 70, 158–172.

SWCRMP (St. Williams Conservation Reserve Management Plan) 2007. Executive Summary, Ontario Ministry of Natural Resources. Queen's Printer, Ontario. <https://www.ontario.ca/page/st-williams-conservation-reserve-management-plan>

Thompson I., B. Mackey, S. McNulty, and A. Mosseler. 2009. *Forest Resilience, Biodiversity, and Climate Change: A Synthesis of the Biodiversity / Resilience / Stability Relationship in Forest Ecosystems*. Secretariat of the Convention on Biological Diversity, Montreal, Canada, 67 pp. [http:// www.cakex.org/virtual-library/1233](http://www.cakex.org/virtual-library/1233).

Thornthwaite, C.W. 1948. An approach toward a rational classification of climate. *Geographical Review* 38:1, 55-94.

van Mantgem, P.J., Stephenson, N.L., Byrne, J.C., Daniels, L.D., Franklin, J.F., Fulé, P.Z., et al. 2009. Widespread increase of tree mortality rates in the western United States. *Science* 323, 521-524. doi: 10.1126/science.1165000 PMID: 19164752

Walsh, T. 1795. Field notebook. Survey of Charlotteville. Lloyd Reeds Map Collection, McMaster University Library.

Whitney, R.D. 1988. *Armillaria* root rot damage in softwood plantations in Ontario. *The Forestry Chronicle* 64, 345-351.

Zavitz, E.J. 1958. 1909: Report on the restoration of waste lands in southern Ontario. Published by the Ontario Department of Agriculture, Toronto. In: Zavitz, E.J. 1958. Fifty Years of Reforestation in Ontario. Ontario Department of Lands and Forests.

Zavitz, J.A. 1960. Fifty years of reforestation in Ontario. Ontario Department Lands Forestry, Toronto, ON. 30 p.

Table 3.1 Summary statistics for the tree ring chronology from the red pine (*Pinus resinosa*) stand in southern Ontario.

RWI statistic	Value
Time interval	1935-2013
Number of series	95
Series intercorrelation	0.329
Mean ring width (mm)	1.55
Autocorrelation	0.877
Expressed population signal (EPS)	0.9747
Running RBAR	0.3789

Table 3.2 Ten-year means of running RBAR (RBAR), standard deviation (SD), standard error (SE), EPS, and number of series (Ns)

Year	RBAR	SD	SE	EPS	Ns
1950	0.6556	0.3546	0.0118	0.9908	56.6
1955	0.4841	0.4038	0.0098	0.9840	65.4
1960	0.3460	0.4661	0.0101	0.9740	70.7
1965	0.2944	0.4291	0.0087	0.9697	76.8
1970	0.1209	0.4559	0.0083	0.9200	83.6
1975	0.1596	0.4274	0.0071	0.9441	89.0
1980	0.2630	0.4603	0.0074	0.9705	92.1
1985	0.3965	0.4227	0.0065	0.9841	94.1
1990	0.3999	0.3930	0.0059	0.9845	95.0
1995	0.2734	0.3794	0.0057	0.9728	95.0
2000	0.5923	0.3451	0.0052	0.9928	95.0
2005	0.3572	0.3768	0.0056	0.9814	95.0
2010	0.2864	0.4266	0.0065	0.9744	94.8

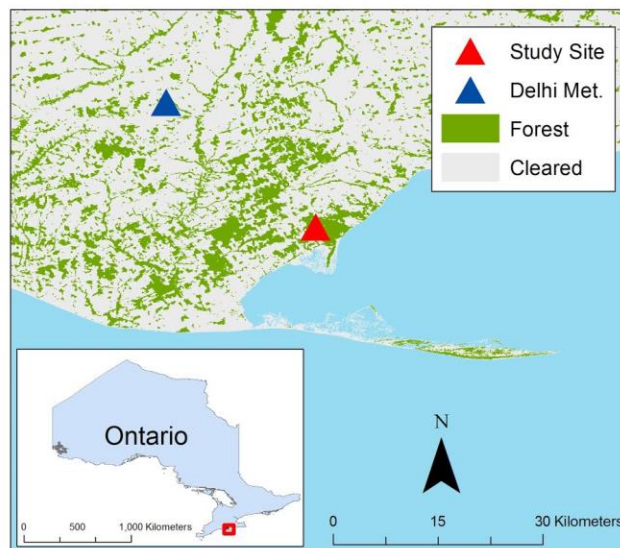


Figure 3.1 Location of the study site in southern Ontario ($42^{\circ}42'N$, $80^{\circ}21'W$) (shown as red triangle). The location of the Environment Canada Delhi meteorological station is shown as blue triangle.

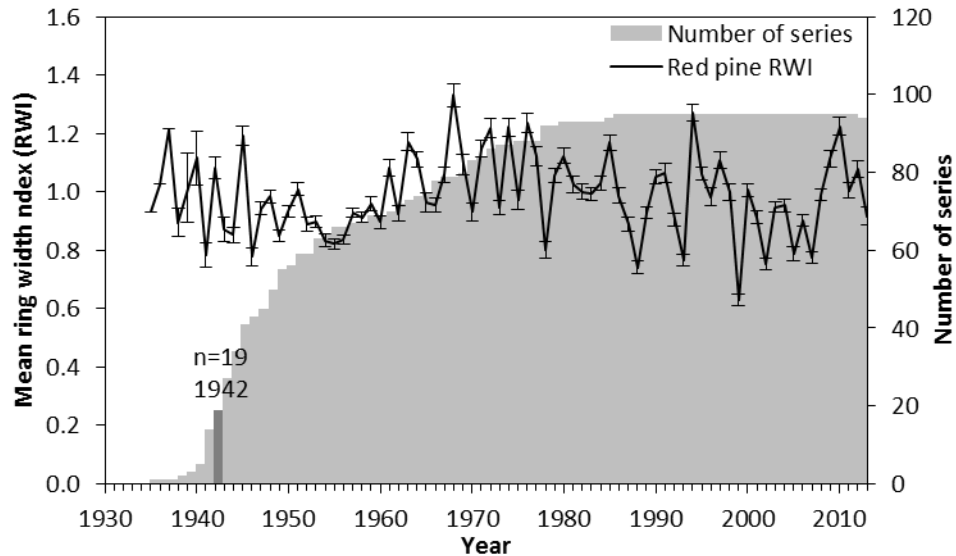


Figure 3.2 The tree ring residual chronology from the red pine plantation stand in southern Ontario. The shaded grey area corresponds to the number of individual tree ring series in the red pine chronology over time. Vertical error bars correspond to standard error. Ring widths for the 1935-1941 period were not included in the correlation analysis due to lower sample depth. The chronology is truncated in 2013 when the harvesting experiment was conducted at the site in February 2014.

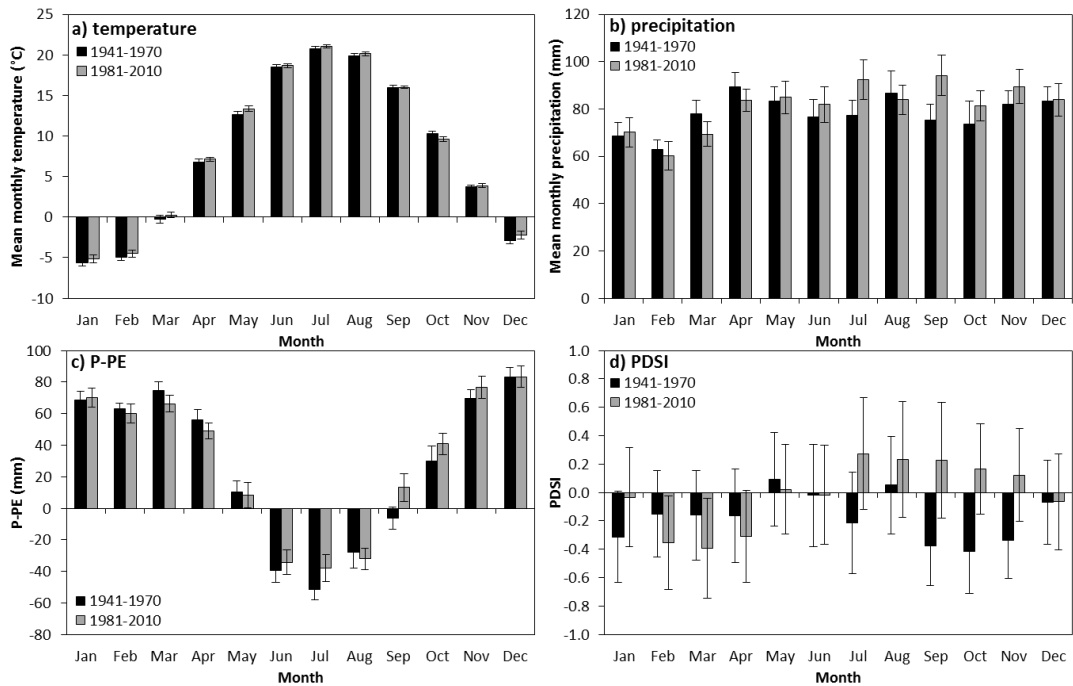


Figure 3.3 Climographs of monthly climate data for the first (1941-1970) and second (1981-2010) 30-year intervals at Environment Canada’s Delhi station (42°52’N, 80°33’W): a) mean temperature; b) mean total precipitation; c) mean total P-PE; and d) mean PDSI. The error bars correspond to standard error in monthly data.

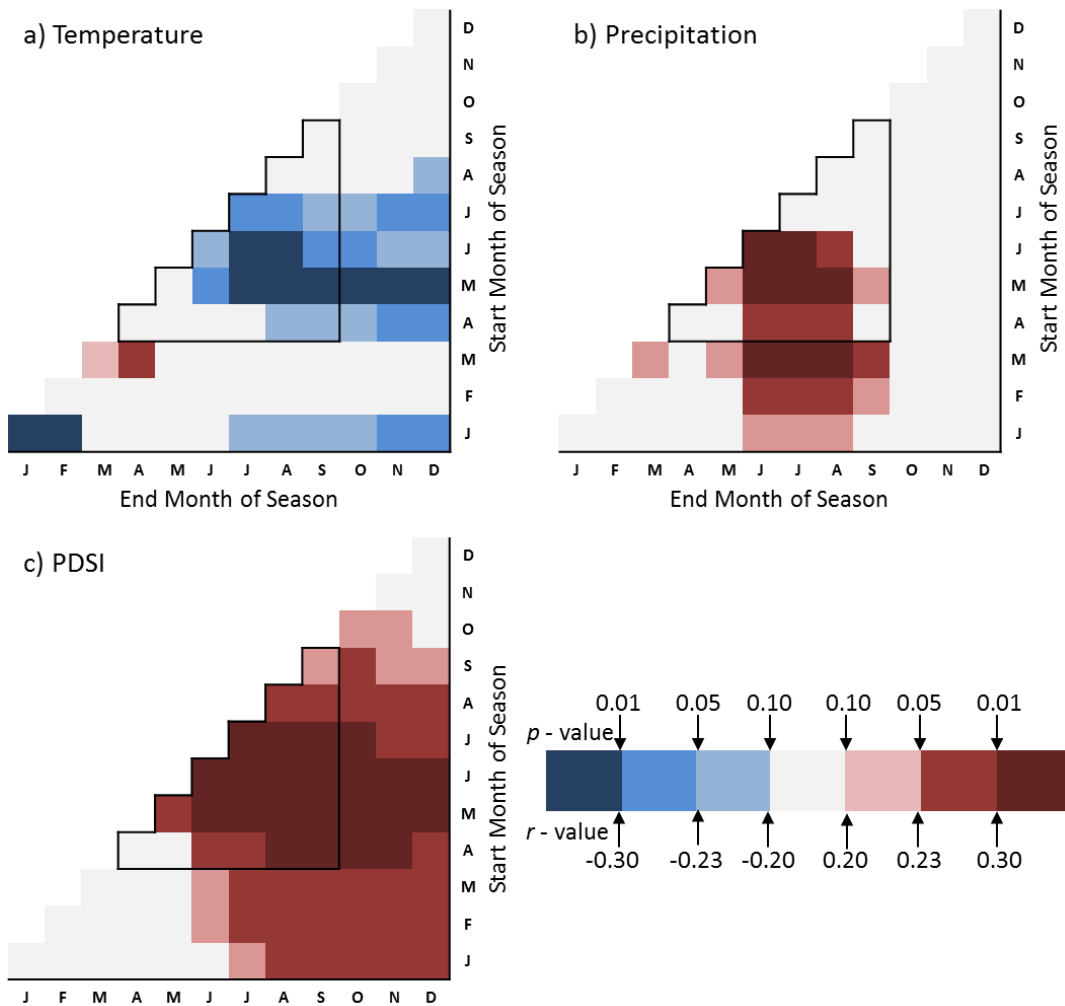


Figure 3.4 Significance of relationships between ring width index (RWI) with climate variables in a) mean temperature, b) total precipitation, and c) mean PDSI during all possible combinations of months over the January–December period for the 72-year period from 1942 – 2013. Relationship significance for individual months are shown on the corner-to-corner diagonals (e.g. 1st line January to 12th line December) whereas significance over month combinations extend to the right (e.g. 1st line, 3rd block would represent the January – March significance). The area of the charts that corresponds to correlations during the growing season (April–September) is indicated by the stair-step box. All correlation values are shown in Supplemental Data.

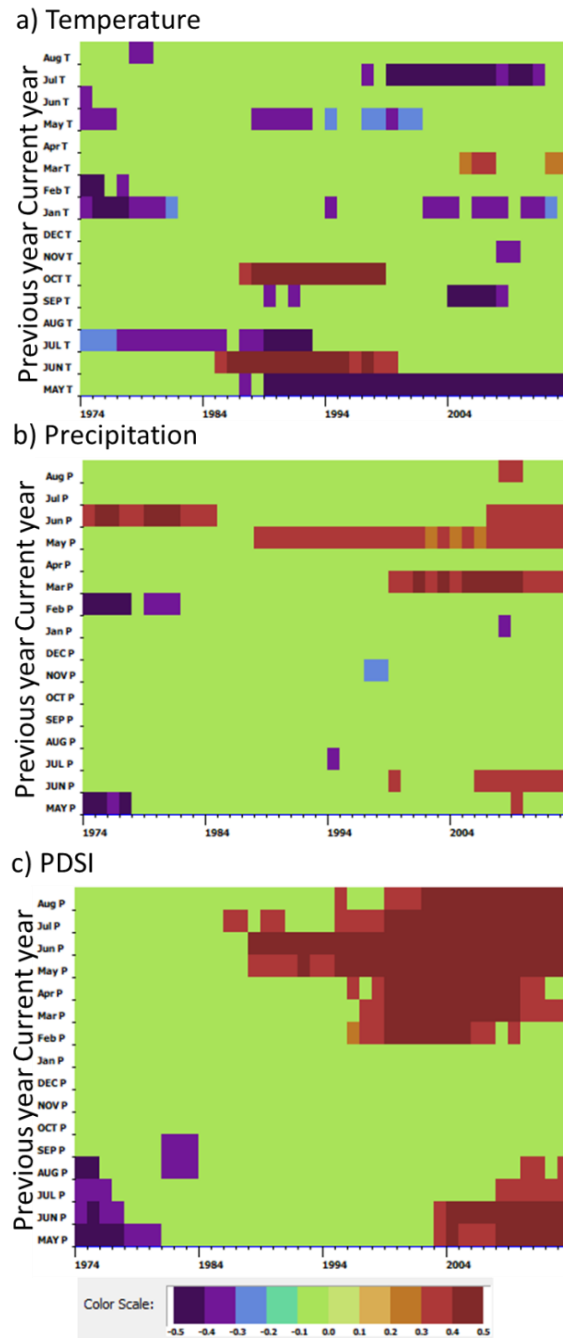


Figure 3.5 Moving interval correlations computed for red pine growth (residual chronology) and monthly climate variables of a) temperature, b) precipitation, and c) Palmer Drought Severity Index (PDSI) during the 16-month period of May of the previous year to August of the current ring year. A base length interval of 32 years was progressively moved through the total number of available years from 1942 to 2013. The positive relationship with growing season drought is the main climate signal in the tree ring chronology.

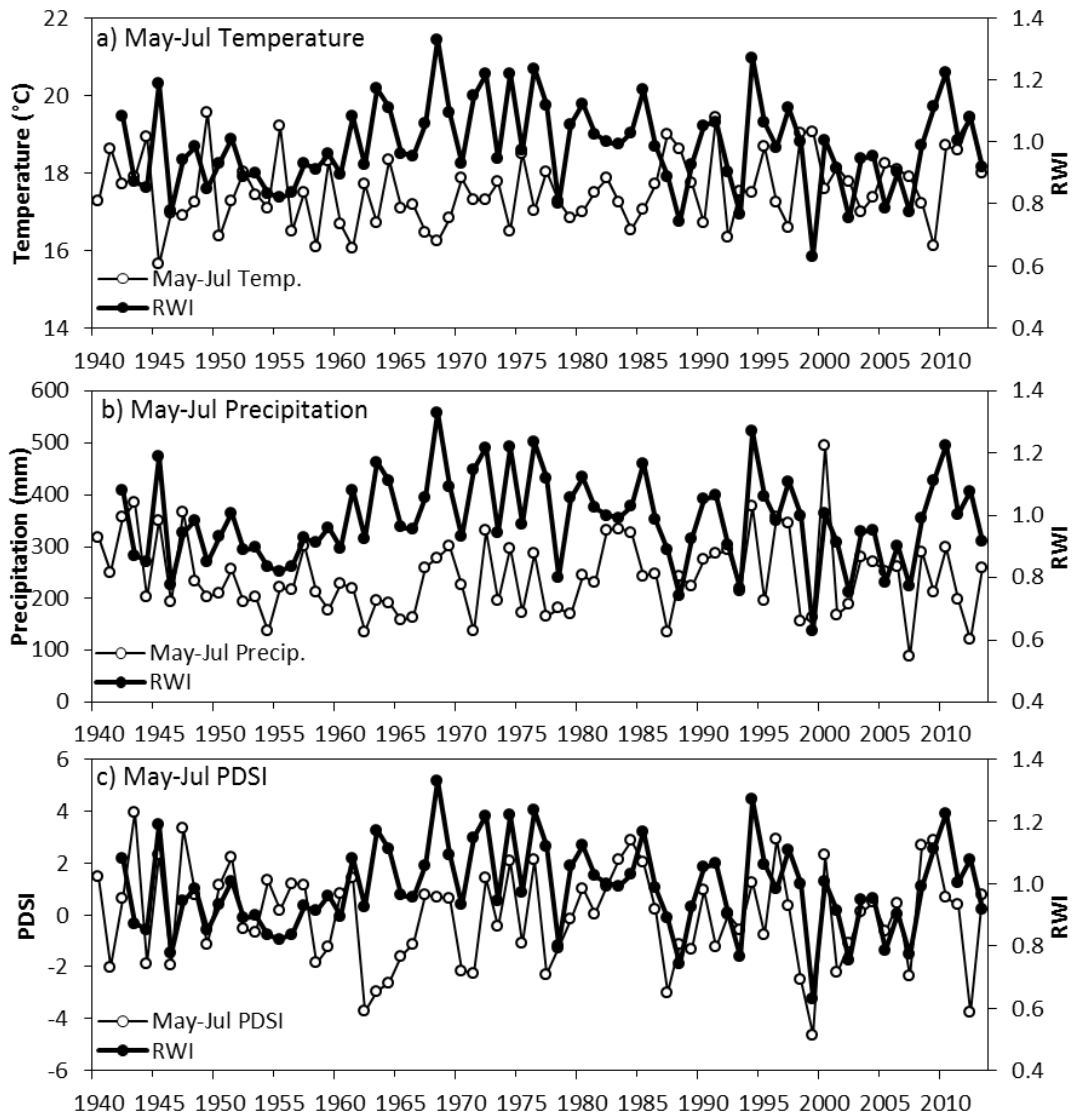


Figure 3.6 Tree ring width index and May-July a) mean temperature, total precipitation, and mean Palmer Drought Severity Index (mPDSI) versus time.

Supplemental data: Correlation coefficient values

This section contains all correlation coefficient values for the Pearson’s correlation analysis between the red pine tree ring chronology (RWI) with climate (temperature, precipitation, and PDSI) variables. As in Figure 3.4 the vertical scale corresponds to the starting month of the correlation and the horizontal month corresponds to the ending month of the correlation.

Red Pine Chronology

Temperature with RWI

J	F	M	A	M	J	J	A	S	O	N	D		
											-0.1260	D	
										-0.1118	-0.1499	N	
									-0.0890	-0.1459	-0.1793	O	
								-0.0374	-0.0908	-0.1375	-0.1749	S	
							-0.1742	-0.1375	-0.1521	-0.1885	-0.2162	A	
						-0.2291	-0.2573	-0.2594	-0.2256	-0.2312	-0.2531	-0.2655	J
					-0.2291	-0.3051	-0.3069	-0.2850	-0.2782	-0.3009	-0.3008		J
				-0.1545	-0.2742	-0.3222	-0.3279	-0.3160	-0.3130	-0.3275	-0.3241		M
			0.1430	-0.0212	-0.1281	-0.1952	-0.2213	-0.2153	-0.2307	-0.2460	-0.2617		A
		0.2237	0.2347	0.1258	0.0506	-0.0252	-0.0674	-0.0724	-0.0941	-0.1184	-0.1521		M
	-0.1120	0.0731	0.1137	0.0444	-0.0128	-0.0660	-0.0983	-0.1012	-0.1188	-0.1388	-0.1649		F
-0.3449	-0.3037	-0.1413	-0.0857	-0.1278	-0.1665	-0.1979	-0.2172	-0.2179	-0.2284	-0.2456	-0.2616		J

Precipitation with RWI

J	F	M	A	M	J	J	A	S	O	N	D	
											-0.0379	D
										0.0566	0.0136	N
									-0.0995	-0.0375	-0.0479	O
								-0.0984	-0.1410	-0.0926	-0.0909	S
							0.0122	-0.0638	-0.1128	-0.0765	-0.0767	A
						0.1127	0.0907	0.0057	-0.0466	-0.0202	-0.0288	J
					0.3269	0.3147	0.2774	0.1509	0.0946	0.1060	0.0820	J
				0.2285	0.3415	0.3419	0.3247	0.2149	0.1659	0.1711	0.1426	M
			-0.0325	0.1427	0.2731	0.2877	0.2716	0.1855	0.1409	0.1491	0.1257	A
		0.2071	0.1242	0.2159	0.3236	0.3345	0.3151	0.2375	0.1903	0.1940	0.1681	M
	-0.0748	0.1034	0.0677	0.1583	0.2724	0.2873	0.2687	0.2022	0.1598	0.1654	0.1417	F
-0.1730	-0.1747	-0.0082	-0.0208	0.0780	0.1989	0.2200	0.2082	0.1527	0.1125	0.1199	0.1012	J

PDSI with RWI

J	F	M	A	M	J	J	A	S	O	N	D	
											0.1226	D
										0.1566	0.1452	N
									0.2301	0.2050	0.1848	O
								0.2124	0.2400	0.2274	0.2090	S
							0.2959	0.2728	0.2808	0.2676	0.2482	A
						0.3205	0.3264	0.3056	0.3081	0.2966	0.2799	J
					0.3498	0.3433	0.3456	0.3300	0.3311	0.3212	0.3065	J
				0.2482	0.3083	0.3221	0.3314	0.3244	0.3271	0.3198	0.3083	M
			0.1149	0.1900	0.2574	0.2863	0.3028	0.3034	0.3086	0.3038	0.2954	A
		0.1136	0.1182	0.1702	0.2306	0.2635	0.2831	0.2881	0.2945	0.2915	0.2849	M
	0.0417	0.0809	0.0958	0.1425	0.1995	0.2354	0.2578	0.2662	0.2745	0.2734	0.2688	F
-0.0230	0.0089	0.0477	0.0680	0.1130	0.1684	0.2068	0.2321	0.2433	0.2535	0.2540	0.2512	J

Chapter 4: Influence of climate and environmental variability on tree ring $\delta^{13}\text{C}$ and water use efficiency in temperate pine plantation forests

4.1 Abstract

Growth rings from three tree specimens in two different aged (14- and 77-year old) white pine plantation forests were analyzed for stable carbon isotope ratios to identify both short- and long-term variations in physiological response to changing environmental conditions. Isotopic ($\delta^{13}\text{C}$) and intrinsic water use efficiency (iWUE) time series were constructed from whole wood samples and compared to historical climate data (temperature, precipitation) from 1939 to 2014. Additionally, these iWUE records were compared to annual gross ecosystem productivity (GEP), ecosystem respiration (RE) and evapotranspiration (ET) for 2003 to 2014 period using eddy covariance technique. iWUE record of the 72-year stand may contain a significant change point (95% conf., year 1969) in inter-annual change from nearly constant ($-0.02 \mu\text{mol mol}^{-1} \text{yr}^{-1}$) value to $0.98 \mu\text{mol mol}^{-1} \text{yr}^{-1}$. This indicated a shift in passive to active homeostasis resulting in iWUE increase. Overall, iWUE increased by approximately $50 \mu\text{mol mol}^{-1} \text{yr}^{-1}$ over a 55-year period (1969-2012). It indicates that climatic variations in temperature and consequently atmospheric evaporative demand have acted as a significant control ($p < 0.05$) on iWUE. iWUE was also positively related to April to May GEP and ET in the 14-year-old stand and June-July GEP and ET in

the TP39 stand. The $\delta^{13}\text{C}$ -inferred signal preserved in the wood may be influenced by significant (> 90% confidence) shifts in climate such as a $+0.5^\circ\text{C}$ increase in growing season temperature that occurred in the mid-1980s. Additional long records would be useful to validate the results obtained from this site. The study outcomes may be useful to improve forest management and conservation in plantation conifer forests.

4.2 Introduction

Atmospheric warming and extreme climatic events have escalated over the past 200 years due to carbon emissions caused by industrial activities, land use change and ecosystem degradation ((Masson-Delmotte et al., 2015; Strack et al., 2007). Understanding the physiological responses of trees to environmental stressors is important to evaluate and predict response of forest ecosystems to future changes in the climate. Tree ring properties such as ring-width and stable carbon isotope ratios ($^{13}\text{C}/^{12}\text{C}$) of wood cellulose have been used as reliable tools to interpret the effects of climate and environmental factors on the growth of trees (e.g. Fichtler et al., 2010; Hall et al., 2009; McCarroll and Loader, 2004; Gagen et al., 2011). Trees serve as an excellent physical archive of past climate information because of the bookmarking of inter-annual variation into annual growth rings at the end of the season as latewood. Variation of tree ring parameters such as stable

isotope ratios of wood cellulose is therefore assigned to specific years with high confidence.

Carbon isotope fractionations occurring in plants are influenced by the $\delta^{13}\text{C}$ value of the atmospheric CO_2 (Farquhar et al., 1982; Loader et al., 2003; Weiwei et al., 2018). It has been demonstrated that tree ring $\delta^{13}\text{C}$ ($\delta^{13}\text{C}_{\text{tr}}$) values are sensitive to atmospheric CO_2 concentration ($p\text{CO}_2$) and its $\delta^{13}\text{C}$ value ($\delta^{13}\text{C}_{\text{atm}}$) at both long and short time scales (e.g. Farquhar et al., 1982, McCarroll and Loader, 2004; Marshall et al., 2007; Gagen et al., 2011; Weiwei et al., 2018). Atmospheric CO_2 has significantly increased due to human activity over the past 150 years through increased fossil fuel emissions as well as land use changes (Borden et al., 2016; Le Quéré et al., 2016). This anthropogenic change has led to increased $p\text{CO}_2$ from a pre-industrial mean of approximately 260 ppm before 1850 AD (Francey et al., 1999) to an excess of 400 ppm in 2018 (Scripps CO_2 Program, 2018). Likewise, global estimates of $\delta^{13}\text{C}_{\text{atm}}$ have decreased from a pre-industrial mean of -6.41 ‰ before 1850 (Francey et al., 1999) to -8.5 ‰ in 2018 (Scripps CO_2 Program, 2018). Because both $p\text{CO}_2$ and $\delta^{13}\text{C}_{\text{atm}}$ of atmospheric CO_2 have risen at unprecedented rates when compared to the past 1000-year record of proxy and measurement data (Francey et al., 1999; Marshall et al., 2007; Elsig et al., 2009; Scripps CO_2 Program, 2017), it is necessary to correct carbon isotope concentrations of tree ring material ($\delta^{13}\text{C}_{\text{tr}}$) for modern atmospheric CO_2 change.

Carbon isotope fractionation in plants is also influenced by the ratio of intercellular (internal) concentration of CO₂ to the external concentration of CO₂ (Farquhar et al., 1982; Loader et al., 2003). Moisture stress influences stomatal closure during drought, reducing the internal CO₂ concentration which increases ¹³C fixation resulting in higher δ¹³C values (Farquhar et al., 1982; Leavitts, 1992). Stomatal regulation has the effect of reducing evapotranspiration (ET) and increasing the molar ratio of carbon fixed to water lost through the increase of intrinsic water use efficiency (iWUE) (Marshall et al., 2007). Lowered stomatal conductance reduces CO₂ equilibria rates across the stomatal aperture (Farquhar et al., 1982; Farquhar and Richards, 1984; Campbell and Norman, 1998). As photosynthetic processes preferentially consume ¹²CO₂, the remaining leaf chamber is enriched in ¹³CO₂ during periods of water stress (e.g. Marshall et al., 2007). Prolonged water stress conditions and reduction in stomatal conductance forces the fixation of progressively ¹³C-enriched carbon dioxide while decreasing the interior leaf air chamber CO₂ concentration relative to the external ambient atmospheric CO₂ concentration. Comparison of the occurrence and duration of physiological stressors to climate records over the lifetime of the trees will contribute to our understanding of forest response to climate change and extreme events.

This study presents three $\delta^{13}\text{C}$ records of the growth rings from two different aged (77- and 14-year old as of 2016) monoculture white pine (*Pinus strobus* L.) plantation stands in southern Ontario, Canada. The main objective was to examine tree ring isotope compositions and their iWUE records to determine if there are relationships between intra-annual climate variables of temperature, precipitation, and drought at monthly and over multi-monthly intervals of the growing season. Additionally, the isotope and iWUE records were compared to quantifications of stand-based gross ecosystem productivity and evapotranspiration gathered through eddy covariance methods. Relationships found between climate and iWUE in these trees will contribute to our understanding of climate effects on tree water use efficiency.

4.3 Materials and methods

4.3.1 Site description, climate data, and eddy covariance measurements

The study sites include two even-age white pine stands planted as monoculture forests. The site history of each location is well documented through land surveys beginning in the mid-1800s (Zavitz, 1926; Draper, 2003). These study sites are part of Turkey Point Observatory as well as Global Water Futures Program and global Fluxnet (identified as CA-TP1 and CA-TP4 sites). The stands have been extensively studied for carbon fluxes (e.g., Arain and Restrepo Coupe,

2005; Peichl et al., 2010a; Chan et al., 2018 Peichl et al., 2010b), water fluxes (McLaren et al., 2008; Skubel et al., 2015; Skubel et al., 2017) and harvesting impacts (Chan et al., 2018; Skubel et al., 2017).

The 77-year old stand (42°42'N, 80°21'W) was established by planting white pine trees in 1939 on cleared oak savanna land (here after known as TP39 site) (Figure 1). It is managed by the Ontario Ministry of Natural Resources and Forestry (OMNRF) and is being developed under the shelterwood silviculture system. The stand was harvested for the first time in 1983 by removing 105 m³ ha⁻¹ of wood, resulting in a stand density of 429 ± 166 stems ha⁻¹ (Peichl and Arain, 2006). The average distance between trees varied from 3 m x 3 m to 5 m x 6 m (Peichl and Arain, 2006). The stand was harvested again in early 2012 where one third of the trees were removed resulting in a stand density of 321 ± 111 stems ha⁻¹ (Skubel et al., 2015). TP39 has extensive understory consisting of black oak (*Quercus vultina*), balsam fir (*Abies balsamifera* L. Mill) and black cherry (*Prunus serotina*). The overstory tree species consists of white pine (82%) balsam fir (11%) and native Carolinian species (7%) (Thorne and Arain, 2015). Nine circular plots 24 m in diameter were established in the stand in 2004 following of National Forestry Inventory (NFI) protocol (Fluxnet Canada). In these plots, all trees with diameter at breast (1.3m) height (DBH_{1.3}) of 8 cm or larger were tagged and biometrics information, including DBH_{1.3m} and height were recorded. In 2015, the mean tree DBH_{1.3m} was 34.29 ± 12.94 cm, while mean

tree heights recorded in 2012 was 23.38 ± 2.08 m. These measurements were based on 152 individual trees located in the NFI plots.

The 14-year-old stand ($42^{\circ}39'N$, $80^{\circ}33'W$) was established in 2002 by planting white pine seedlings on a former agricultural land that was abandoned 10 years prior to plantation (here after known as TP02 site). At this site trees were planted at a density of 1683 ± 189 stems ha^{-1} and has not been disturbed since establishment. Some dieback occurred during stand evolution resulting in a stem density of 1583 ± 29 stems ha^{-1} as measured in 2012. Tree spacing at this site is approximately 2 m x 2.5 m (Peichl and Arain, 2006). Due to high shading, the understory is limited to bryophytes at this site and the stand remains homogeneous white pine. Biometric measurements for this site were gathered from 205 individuals growing in three rectangular NFI plots. After the 2016 growing season the mean tree $DBH_{1.3m}$ was 15.74 ± 2.45 cm and the mean tree height as of 2012 was 6.85 ± 0.33 m (Chan et al., 2018).

Soils at the sites consist of highly porous brunisolic grey-brown luvisol in the Canadian System of Soil Classification (Presant and Acton, 1984) dominated by wind-blown lacustrine sand-sized grains, which allows for drainage and low water-holding capacity. The sand layer is highly variable in thickness (60-80 m) and overlies the Middle Devonian Dundee Formation, which consists of limestone-chert dipping southwest (OGS, 1991). The organic humus-litter layer is

approximately 5 cm thick at the older stand and < 1 cm at the younger stand. Organic carbon content is largely derived of shed needles and moss with volumetric weight percent decreasing rapidly with depth within 10-20 cm of the surface. The permanent ground water is quite deep and separated from the overlying soil by a clay horizon at 5 – 9 m depth (Norfolk County, unpublished data).

The climate in the region is sub-humid temperate and relatively moderate as compared to the rest of Canada. The continuous climate record (Delhi climate station; 1935-2016) of temperature and precipitation available in this region, allowed for direct comparison to the isotope time series. The 80-year mean annual temperature in the region was 8.0°C, with the mean temperature of the hottest month (July) of 21.0°C based on historical climate data from the Environment Canada weather station at Delhi (42°52'N, 80°33'W, 231.6 m elevation), which is approximately 22 km north of the TP02 and 30 km northwest from the TP39 study sites (Figure 1). The mean temperature of the coldest month (January) was – 5.5°C. Mean temperature for the most recent 15 years (2001 – 2016) was comparatively elevated at 8.2°C. Mean January temperature was also elevated at – 5.3°C for these 15 years (Environment Canada). Inter-annual variation in temperature is large, with six years (1949, 1955, 1959, 1991, 1998, and 2016) with 1.5 SD (1.1°C) warmer than the mean. The 82-year (1935 – 2016) mean

annual precipitation (P) was 937 mm and evenly distributed over the months of the year (Environment Canada).

From mean monthly temperatures and the latitude, potential evaporation (PE) was calculated following Thornthwaite (1948) using a tool published in Jacobi (et al., 2013). The input variables are monthly mean temperature, precipitation, latitude of the meteorological station, and available water content (assumed to be a maximum of 35 mm for these sandy soils). The tool was prompted to calculate PE according to the Thornthwaite (1948) method and the calibration period was taken to be for the full available record 1935-1990. The PE outputs were used in further pairwise correlation analyses as a measure of drought index. The long-term (1935 – 2015) mean ratio of monthly precipitation P to PE was highly variable seasonally. In spring (April – May) and autumn (September – October) the P/PE ratios were 1.97 ± 0.79 and 1.47 ± 0.63 respectively, indicating adequate water availability to vegetation. In summer (June – August), the P/PE ratio was 0.67 ± 0.20 which suggests water stress was common at the site during these months.

4.3.2 Sample preparation and stable isotope analyses

Three trunk samples of one juvenile (TP02 site) and two of mature (TP39 site) white pine trees were analyzed at high resolution for stable carbon isotope

compositions ($\delta^{13}\text{C}_{\text{tree}}$). One trunk disc was collected from the TP39 in September of 2012 (TP39-1). This tree was felled as part of the 2012 disturbance linked to the silviculture management program performed by the OMNRF. Due to the presence of narrow rings in the recent portion of TP39-1 ring record, a core collected in September of 2015 was preferentially selected because of the presence of wide rings in the most recent 15-years of growth (TP39-2). From the TP02 site, one trunk disc was collected from a tree cut in August 2015. The trunk discs were polished with a rotary sander with 200 grit sandpaper and followed by hand sanding with 600 grit sandpaper. Growth ring boundaries were measured using a Velmex measuring system with a linear encoder to 0.001 mm precision (Figure 4.2). Due to known felling information for the three trees, ring ages were determined by counting. The counted ages of rings in TP39-1 and TP39-2 were verified with tree ring chronologies developed from the same site (TP39). For all three trees, visible rings along the longest radius from centre to bark were defined for $\delta^{13}\text{C}$ sampling to ensure that the maximum number of samples for isotopic analysis could be taken.

In total 370 whole wood samples were collected from three discs for carbon isotope analysis. Processing costs and time-labour involvement was high per sample which limited the number of discs that could be analyzed. Other published studies in literature have also used similar number of sampled trees and produced meaningful results (Fichtler et al., 2010; Hall et al., 2009; West et al.,

2001). In our study, the high-resolution of sampling allowed several samples to be obtained from a single ring and allow intra-ring variation to be identified, which was a unique aspect of this study. Between seven and nine samples could be taken from the wider rings during the first three decades of growth (1943-1965), while in narrower rings only one or two samples could be taken. Wood powder was extracted from the growth rings using a twist drill (Micromat 50E, Proxxon, Germany) equipped with a 0.8-mm-width bit in paths parallel to the rings. Growth ring samples were identified as having been extracted from either the earlywood ($\delta^{13}\text{C}_{\text{ew}}$) or latewood ($\delta^{13}\text{C}_{\text{lw}}$) portion of each growth ring. Intra-annual labelling of samples was identified based on the general span of the growing season of April to October in the region. Leaf senescence and ecosystem flux measurements also suggest the growing season begins in April and ends in October (Chan et al., 2018). The wood powder samples were not chemically treated, as it has been suggested that $\delta^{13}\text{C}$ of untreated whole wood is sufficiently reliable as a proxy indicator of temporal environmental conditions (Loader et al., 2003). The wood powder samples were homogenized for uniformity. For analysis, 400 μg of wood powder was loaded in a tin capsule for stable isotope analyses. Standards with known carbon isotope compositions were included in the analysis and comprised of USGS – 40 (glutamic acid), USGS – 24 (graphite), IAEA – 600 (caffeine), IAEA – C3 (paper), IAEA – CH7 (plastic), and in-house sucrose standardized to ANU IAEA – CH6. Weight percent of carbon was standardized using in-house glutamic acid with a known carbon weight percent composition. The carbon

isotope composition was measured on-line by loading samples and the standard suite batch-wise into an auto-sampler. The material was combusted at 1450°C in a Costech Elemental Analyzer directly coupled to a Thermo Finnigan Delta plus XP isotope ratio mass spectrometer (EA-IRMS) in the McMaster Research Group for Stable Isotopologues laboratory. The error of $\delta^{13}\text{C}$ measurement among the standard suite was ± 0.1 ‰. The mean difference between sample replicates was ± 0.2 ‰. Results were expressed using delta-notation (δ) in permil (‰) relative deviation from the Vienna Pee Dee Belemnite (VPDB) standard:

$$\delta^{13}\text{C} = (R_{\text{sample}} / R_{\text{standard}} - 1) \times 1000 \quad (1)$$

where R_{sample} and R_{standard} are the $^{13}\text{C}/^{12}\text{C}$ ratios in the sample and standard, respectively.

4.3.3 Data treatment

In this study, standardized carbon isotope data ($\delta^{13}\text{C}_{\text{tr}}$) from all three trees was corrected to distill the climate signal of modern wood from long-term trends in $\delta^{13}\text{C}_{\text{atm}}$ to generate $\delta^{13}\text{C}_{\text{corr}}$. This was done by correcting $\delta^{13}\text{C}_{\text{tr}}$ of TP39-1 to a pre-industrial atmospheric $\delta^{13}\text{C}_{\text{a}}$ base of -6.4 ‰ using the simple additive method demonstrated in McCarroll and Loader (2004):

$$\delta^{13}\text{C}_{\text{corr}} = \delta^{13}\text{C}_{\text{tr}} - (\delta^{13}\text{C}_{\text{atm}} + 6.4). \quad (2)$$

Eq. 2 was applied to all samples. Samples corresponding to the latewood portion of the ring ($\delta^{13}C_{lw}$) were taken to produce the $\delta^{13}C_{lwcorr}$ time series. No further corrections were applied to the isotope time series.

Stable carbon isotope ratios can be expressed in terms of intrinsic water use efficiency: the ratio of carbon fixed to water lost. This is because the water lost is controlled by stomatal conductance and photosynthetic rate. Intrinsic water use efficiency is related to measured plant carbon isotope ratios ($\delta^{13}C_{plant}$):

$$iWUE = c_a[(1 - c_i/c_a)]0.625 \quad (3)$$

and

$$c_i/c_a = (\delta^{13}C_{plant} - \delta^{13}C_{atm} + a)/(b - a) \quad (4)$$

where c_i and c_a are intercellular and atmospheric CO₂ concentration respectively, $\delta^{13}C_{plant}$ is the δ -value (Eq. 1) of plant material, $\delta^{13}C_{atm}$ is the δ -value of the atmospheric CO₂, a is the diffusivity discrimination of ¹³CO₂ as it crosses the stomata (−4.4‰) and b is the net discrimination of ¹³CO₂ during carboxylation (−27‰) (Farquhar et al., 1982; McCarroll and Loader, 2004). Stable carbon isotope measurements from tree rings are a proxy for the internal concentration of CO₂ within the leaf space as regulated by stomatal conductance and photosynthetic rate (Gagen et al., 2010).

4.3.4 Correlation of *iWUE* with climate and eddy-flux measurements

Tree ring $\delta^{13}\text{C}_{\text{corr}}$ and iWUE from all three samples (TP39-1, TP39-2 and TP02) were subjected to Pearson correlation analysis with archived climate data at Delhi Station (Environment Canada) in southern Ontario. The climate data consisted of temperature and precipitation, and estimated values of potential evaporation (PE), and the Palmer Drought Severity Index (PDSI). The correlation analysis was performed at monthly and multi-month seasonal indices (e.g. May-June-July). For all three trees, the annual measurement of $\delta^{13}\text{C}$ and its derived value of iWUE correspond to the latewood portion of the growth ring which was compared to monthly values of air temperature, precipitation, PE, and PDSI. Close examination of climate records (e.g. monthly temperature and precipitation values) showed that these records do not vary considerably between stations located within the Norfolk region of southern Ontario (see section 3.4.2.). The general span of the growing season was taken to last from April to October based on leaf senescence and ecosystem flux measurements (Chan et al., 2018).

Half-hourly fluxes of water vapour and carbon dioxide CO_2 were measured since 2003 using eddy covariance (EC) systems at the TP39 and TP02 sites. Further information on EC systems and site set-up have been published (Arain and Restrepo-Coupe, 2004; Peichl et al., 2010a; 2010b, Chan et al., 2018). Eddy covariance derived values of gross ecosystem productivity (GEP) and evapotranspiration (ET) were compared to tree ring $\delta^{13}\text{C}_{\text{lwc}}_{\text{corr}}$ and iWUE over the period of overlap from 2003 to 2014. Pearson's correlation coefficients of

monthly variables were conducted for individual months and for all possible combinations of months between January and December.

4.4 Results

4.4.1 Trends in tree ring isotope compositions and *iWUE*

As mentioned earlier, relatively large growth rings during early growth years 1943-1965 (Figure 2) allowed up to 10 samples to be extracted per ring. Carbon isotope values showed a distinct seasonal pattern relative to ring growth with the lowest $\delta^{13}\text{C}_{\text{tr}}$ and $\delta^{13}\text{C}_{\text{corr}}$ values occurring at the ring boundaries, with mean seasonal variance of 1.4 ‰ over these initial 22 years. The reason for this intra-annual pattern could be linked to physiological responses of the tree to conserve water use during the summer months. Reduced stomatal conductance would increase fixation of $^{13}\text{CO}_2$ during carboxylation resulting in enriched $\delta^{13}\text{C}$ values. Similar intra-annual patterns of ring growth were observed in the TP39-2 tree ring record from 2000 to 2015 (Figure 4.3B, grey line) and the juvenile tree of TP02 from 2003 to 2014 (Figure 4.3B grey line, dotted line), where the highest values occurred late in the growing season and the lowest values occurred at the ring boundary that marks the beginning and end of the year. The largest within-ring variation in $\delta^{13}\text{C}_{\text{corr}}$ occurred in 1947 (2.4 ‰), followed by 1952 and 1964, with similar values (2.1 and 2.0 ‰, respectively), while the lowest variation

occurred in 1959 (0.2 ‰) and 1958 (0.4 ‰). The varying level of year-to-year $\delta^{13}\text{C}_{\text{corr}}$ in the mid-growing season may be tied to external growth influencing patterns. However, the sampling method used in this study may have limited the observed variance of intra-annual $\delta^{13}\text{C}$ in a given ring year. As temporal growth accumulation rates were not constrained during the study, intra-seasonal correlation of earlywood $\delta^{13}\text{C}_{\text{tr}}$ and $\delta^{13}\text{C}_{\text{corr}}$ were not analyzed further for significant relationships.

The $\delta^{13}\text{C}_{\text{tr}}$ record from TP39-1 shows a downward trend over the record of the tree with maximum $\delta^{13}\text{C}$ value occur during 1947 (-24.7 ‰) and minimum value in 1998 (-28.4 ‰) (Figure 4.3A, grey line). This trend was the result of atmospheric loading of anthropogenic greenhouse gases through decreased $\delta^{13}\text{C}_{\text{atm}}$. After adjusting $\delta^{13}\text{C}_{\text{tr}}$ for $\delta^{13}\text{C}_{\text{atm}}$ to produce $\delta^{13}\text{C}_{\text{corr}}$ (Equation 2), the trend was leveled as shown by the TP39-1 record (Figure 4.3A, black line).

The number of $\delta^{13}\text{C}_{\text{lwcorr}}$ measurements that comprise each annualized value varied by year, and this was due to the inconsistency in width of the inter-annual latewood bands. Earlier in the record, wider latewood bands enabled three to four samples to be taken, and hence these values of $\delta^{13}\text{C}_{\text{lwcorr}}$ were averaged to produce one annualized value. For years when $\delta^{13}\text{C}_{\text{lwcorr}}$ was averaged from three to four measurement samples the SD was ± 0.2 to $\pm 0.3\%$ within individual years. The rationale for the use of latewood isotope compositions as annualized data

comes from previous work that suggested photosynthate material comprising the latewood portion of the tree ring is closely influenced by environmental conditions that occur within the ring-year (Switsur et al., 1996; Brugnoli et al. 1998).

Multi-decadal scale slope values of the c_i/c_a ratio time series derived from $\delta^{13}\text{C}_{\text{lwcorr}}$ (Eq. 4) from the TP39-1 tree (Figure 4.4) suggested that a change in trend may have occurred during the mid-1980s. The presence of a significant breakpoint (95% confidence) was confirmed using segmented regression analysis (SegReg software; Oosterbaan, 2014). The slope in c_i/c_a prior to (m = 0.0013) and after (m = -0.0014) 1985 were sufficiently different to warrant the existence of this trend change with 95% confidence.

Multi-year inter-annual iWUE was calculated from latewood tree ring $\delta^{13}\text{C}_{\text{lwcorr}}$ values according to Eq. 3 and 4 (Figure 4.5a). Latewood values were selected as opposed to including values from the earlywood, as carbon fixed in the prior year may be utilized to form earlywood. Carbon isotope derived iWUE for the TP39-1 sample also show a significant change in inter-annual slope during the late 1960s. The slope in iWUE for the TP39-1 tree prior to 1969 was nearly horizontal (m = 0.02) while after 1969 the slope increases to nearly 1:1 (m = 0.98) (Figure 4.5a, 4.5b). The slopes of the two shorter records TP39-2 (m = 0.58) and TP02 (m = 1.79) (Figure 4.5a) are more similar to the latter part of the TP39-1

record ($m = 0.98$) as compared to the earlier ($m = -0.02$). The resulting slope change in the TP39-1 record shows iWUE increasing nearly $50 \mu\text{mol mol}^{-1}$ over the 55-year period (1969-2012). As with the TP39-1 c_i/c_a time series, the change in slope of iWUE in TP39-1 is sufficiently different to warrant the existence of this trend change with 95% confidence.

4.4.2 Relationships of iWUE with climate and eddy-flux measurements

Directly using tree ring $\delta^{13}\text{C}_{\text{lwcorr}}$ values did not reveal significant multi-monthly correlation with any climate variable. However, inter-annual climate and EC correlations with iWUE time series revealed strong monthly and multi-monthly relationships with temperature and PE for time intervals of the growing season, but these relationships were inconsistent temporally within the three series (Figure 4.6a, 4.6b). Monthly and multi-monthly correlations of iWUE with precipitation, P-PE, and PDSI were non-significant for all three samples. For the 72-year series (TP39-1) iWUE was significantly related to temperature for month combinations April-July to April-September (95%, $p < 0.05$), May-July to May-September (90%, $p < 0.10$) and June-July to June-September ($p < 0.05$) (Figure 4.6a). For PE, the TP39-2 iWUE record was also significantly related over the seasonal period beginning in April and lasting into September ($p < 0.10$). The 15-year TP39-02 iWUE record was also strongly correlated to temperature and PE over a smaller spread of monthly combinations (Figure 4.6a). For the TP02 iWUE

time series, no significant ($p < 0.10$) relationships were found for temperature for any interval of the growing season (chart not shown). For PE, the TP02 iWUE time series exhibited significant correlation only during the combined April-June (95%, $p < 0.05$) portion of the growing season which were non-significant for individual months during this period (chart not shown).

All significant ($p < 0.10$ to $p < 0.01$) correlation values of iWUE with quantified site eddy-flux GEP and ET were positive during the growing season block (Figure 4.6b) over the years 2003 to 2014, but there was inconsistency between the three series. For the TP39-1 series GEP was related to iWUE from June to July at $p < 0.01$, with the highest r -value of 0.80 during the single month of July (Figure 4.6b). For TP39-2, no significant relationships were found for GEP within the growing season block (April-September) (chart not shown). For the TP02 sample, the highest r -values occurring during April (0.67) with $p < 0.05$ significance, and for the combined April-May period ($r = 0.62$, $p < 0.05$) (Figure 4.6b). For ET, iWUE of the TP39-1 sample displayed significant ($p < 0.05$) relationships during the July-August period ($r = 0.74$) (Figure 4.6b). The relationship of ET was non-significant to iWUE for TP39-2 (chart not shown). In the TP02 sample, ET was significantly ($p < 0.05$) related to iWUE during May (0.77) and the combined April-May period (0.62), as well as over much of the growing season April to August ($r = 0.70$, $p < 0.05$) (Figure 4.6b).

4.4.3 Relationships of *iWUE* with ring width measurements

Annualized latewood $\delta^{13}\text{C}$ -inferred *iWUE* were directly compared to the tree ring width value (Figure 4.2) from which the isotope data was collected (Figure 4.7). No standardization or autocorrelation effects were removed from the tree ring width series. This was also the case for the latewood $\delta^{13}\text{C}$ -inferred *iWUE* series. For TP39-1 (red points), *iWUE* shows a significant relationship ($r = -0.72$, $p < 0.01$, $n = 74$) with ring width. Non-significant ($p < 0.05$) relationships exist between *iWUE* and ring width in both the TP39-2 ($r = 0.24$, $n = 15$) (green points) and TP02 ($r = 0.52$, $n = 12$) (blue points) tree samples. Tree ring $\delta^{13}\text{C}_{\text{lwcorr}}$ values with ring width do not show significant relationships for all three samples.

4.5 Discussion

Correcting $\delta^{13}\text{C}_{\text{tr}}$ for $\delta^{13}\text{C}_{\text{atm}}$ to produce $\delta^{13}\text{C}_{\text{corr}}$ was conducted using an additive model published by McCarroll and Loader (2004). As $\delta^{13}\text{C}_{\text{atm}}$ measurements did not begin until the 1980s it was necessary to use constructed relationships to remove the atmospheric trend prior to that time. Evidence for the downward trend in $\delta^{13}\text{C}_{\text{atm}}$ in recent decades has been recorded in free-atmosphere measurements in the North American temperate and boreal region such as those taken from a 400m high tall tower in Wisconsin, USA (White et al., 2015). This

atmospheric record demonstrates a mean annual decline of $\delta^{13}\text{C}_{\text{atm}}$ of -0.02‰ ; and an overall decline from -8.1 to -8.5‰ from 1994 to 2014 (White et al., 2015).

Tree ring carbon isotope values do not show evidence of the ‘juvenile effect’ during the first decade of growth, which has been found in other studies as a shift in inter-annual $\delta^{13}\text{C}_{\text{tr}}$ due to a CO_2 -enriched atmospheric state (Schleser and Jayasekera, 1985; Hall et al., 2009). These studies observed a shift in the time series as lower, more negative $\delta^{13}\text{C}$ values (approx. 2‰) in the oldest rings of some isotope records from tree rings. This shift is attributed to photosynthetic recycling of respired atmospheric CO_2 from the soil, which is generally depleted in ^{13}C as compared to well mixed, atmospheric CO_2 , as the tree heights were low and canopy were close to the soil (Schleser and Jayasekera, 1985; Fichtler et al., 2010). A vertical profile of subalpine coniferous-hardwood forest air $\delta^{13}\text{C}_{\text{atm}}$ values in Taiwan show a 1.2‰ difference between 0.02 m (-9.3‰) and 1 m (-8.1‰) (Kao et al., 2000). Above 1 m , the forest air appears to be well mixed in the vertical profile with $\delta^{13}\text{C}_{\text{atm}}$ values remaining at approximately -8.1‰ (Kao et al., 2000). As trees grow, the isotopic compositions of tree ring material shift to higher, more positive $\delta^{13}\text{C}$ values as the forest structure evolves (McCarroll and Loader, 2004). Lower light availability due to close interaction of trees early in their development due to high canopy thickness has also been attributed to reduced photosynthetic rates and the ‘juvenile effect’ in isotope records (Hall et

al., 2009). The lack of any ‘juvenile effect’ in TP39-1 may be due to the low quantity of organic material present in the soil and a low carbon pool at the time of afforestation, as evidenced by land descriptions of the site (i.e. windblown sandy dunes) (Zavitz, 1926; Draper et al., 2003).

This study was limited to a small sample of trees taken from two plantation forests. Comparison of the tree records (Figure 4.3B) reveals tree-to-tree variability from 2003 to 2014. Therefore, the climate relationships found here may not be a true representative for whole tree populations in either of these forests. However some interesting trends in c_i/c_a and iWUE are present in the 73-year TP39-1 series. Long-term trends in iWUE are directly calculated from tree ring $\delta^{13}\text{C}$, which essentially records the relationship between c_i and c_a through time (Eq. 3). This relationship can be described as homeostatically passive or active: passive if c_i simply follows a similar trend as c_a through time; or active if the tree uses stomatal control to limit the change in c_i as c_a increases (changes) through time (Waterhouse et al., 2004; McCarroll et al., 2009; Gagen et al., 2011). In passive homeostasis, neither stomatal conductance nor photosynthetic rate is changed, and c_i will rise by the same amount as c_a and iWUE will not increase (Waterhouse et al., 2004). If the tree is actively controlling stomatal conductance, then c_i will also rise in the same proportion as c_a which causes the ratio c_i/c_a to remain unchanged and therefore iWUE will increase with rising c_a . This has been the case in a number of observed studies

(Saurer et al., 1997; 2004; Körner, 2003). In the TP39-1 tree, it is possible there was a significant shift in iWUE in 1969, as shown through segmented regression analysis. The near-horizontal slope of iWUE prior to 1969 suggests the tree was in passive homeostasis and there was no stomatal control limiting c_i as c_a increased. Therefore iWUE was not increasing to a significant degree inter-annually. After 1969 the slope of inter-annual iWUE increased abruptly. In theory, this response may be provoked by a shift in climate. However, climate data available for this area of southern Ontario do not suggest any significant shifts or breakpoints and do not contain an explanatory trend in the late 1960s or early 1970s (see section 3.4.2 for results on climate breakpoint analysis on station archive data in southern Ontario). Therefore the breakpoint in iWUE may be a threshold response of the tree to increasing c_a and has been identified as such in other studies (Battipaglia et al., 2012; Weiwei et al., 2018). The TP39-1 record demonstrates iWUE increased by $50 \mu\text{mol mol}^{-1} \text{yr}^{-1}$ over a 72-year period (1939-2012), with >90% of the change occurring since 1969 (Figure 4.5b). Other conifer species in Scandinavia demonstrate similar increases of $+40 \mu\text{mol mol}^{-1}$ for *Pinus sylvestris* over an 80-year period (Gagen et al., 2011). An increase in iWUE was observed for 125 *Pinus*, *Picea* and *Larix* samples from Eurasia ($+19.2 \pm 0.9 \mu\text{mol mol}^{-1}$) over the past century (Saurer et al., 2004). A meta-analysis of latewood isotope chronologies from three Free Air CO₂ Experiment plantations suggest that enhanced CO₂ lead to greater iWUE (Battipaglia et al., 2012). In northern China, iWUE of 36 90-year *Platycladus orientalis* cores was found to increase by 1.1

$\mu\text{mol mol}^{-1} \text{ yr}^{-1}$ from 1974 to 2014 (Weiwei et al., 2018). For this tree it appears that iWUE is continuing to increase as of 2012. Additional long series of $\delta^{13}\text{C}$ from wood samples in these plantation sites will need to be constructed to confirm if this trend may not be microclimate-based and exists in other trees within the sites.

Internal changes in tree physiology may also be responsible for changes in long-term iWUE and the c_i/c_a ratio. The environmental signal in tree ring growth records is a complex interaction between environmental factors and physiological response (Carrer and Urbinati, 2004). The destination of translocated photosynthates and their storage rates has been found to change with aging (Ryan et al., 1997). It has also been found that lower hydraulic resistances in younger, smaller trees (Ryan and Yoder, 1997; Primicia et al., 2015) affects stomatal conductance which increase photosynthetic rate as compared to older members of a species (Bond, 2000). Age-related variation in tree ring carbon isotope ratios has been documented in coniferous tree species, which have been linked primarily to changes in carbon isotope discrimination imparted by hydraulic function in aging trees (Fessenden and Ehleringer, 2002; McDowell et al., 2002; McDowell et al., 2005; McDowell et al., 2011). As iWUE is calculated from tree ring $\delta^{13}\text{C}$, age shifts in stomatal regulation and WUE within leaves is likely to have implication to the signal preserved in woody tissues. The literature also suggests a common pattern of an increasing iWUE signal in woody tissue with increased tree age and

size (Nabeshima and Hiura, 2004; Thomas, 2010). As mentioned previously, the small sample size of this study limits whether the iWUE signal found is impacted more greatly by tree age versus a rising c_a effect. However, the similar multi-year trend in the young 14-year old tree ($m = 1.79$) as compared to two 77-year old trees ($m = 0.98$ and $m = 0.58$) suggest that rising c_a may have an influence on rising long-term iWUE in plantation *Pinus strobus* in this region.

The breakpoint in the $\delta^{13}\text{C}$ -derived c_i/c_a time series from a positive inter-annual slope to a negative slope that took place in the year 1985 may be related to climate. Increasing temperatures since the mid-1980s likely drove the atmospheric demand for moisture and thereby increased PE and ET. This was found to be the case for PE quantifications based on archived climate data for Delhi station (Figure 3.3). Higher PE and ET infer greater evaporation, which may have induced the tree to reduce stomatal conductance in an effort to conserve water (Marshall et al., 2007; Gagen et al., 2011). The tree was already in active homeostasis since 1969 which may have been caused by increasing c_a . It is speculated that the breakpoint in the $\delta^{13}\text{C}$ -derived c_i/c_a time series may be an enhancement in the active response of the tree and provoked by climate shifts. Additional long series in $\delta^{13}\text{C}$ may confirm these observations and allow statistical analysis on the reliability of trees to record iWUE and to quantify further their responses to both long term climate and increasing c_a .

With regards to climate and near surface energy fluxes and iWUE, it has been suggested by experiment that lowered stomatal conductance does have a significant impact on the near-surface climate. In a doubled-CO₂ model situation, higher temperature and higher dryness conditions occurred as trees increased iWUE (Betts et al., 2000). The 72-year inter-annual paired linear correlation analysis of climate variables with the TP39-1 iWUE record show positive relationships of iWUE with both temperature and PE. This suggests there may be a relationship between temperature and/or PE with iWUE over decadal time scales. The 9-year period of overlap of eddy-flux quantifications of GEP with iWUE also show a positive relationship, with a greater amount of carbon fixed to water lost. The positive iWUE-ET relationship may not be entirely vegetation driven, and ET may primarily come from other sources within the ecosystem during years with high iWUE. In general, there was inconsistency in the strength and presence of linear correlations between the three tested wood samples in this study. As noted previously, the inconsistency between samples stems from a low number of samples measured. Further work will be necessary to validate the linear correlation results shown in this study.

The relationship between tree ring width and iWUE demonstrates that there may be some promise to use ring width as an indicator of iWUE within individual trees. In the multi-decadal TP39-1 series, the negative correlation ($p < 0.01$) found here suggests that as iWUE increases, ring width declines. The

inverse relationship of iWUE to ring width in TP39-1 is similar to those found for individual Norway spruce (*Picea abies*) in southeastern Germany (Sanders et al., 2016). Sanders suggest that there is a trade-off of productivity when trees increase their iWUE. Linares and Camarero (2012) also identifies increasing $\delta^{13}\text{C}$ -inferred iWUE with lowered productivity during dry events, however much of the attribution of increased iWUE was attributed to rising c_a in the Linares and Camarero study. In both of these studies, the record was temporally short and addressed relationships taking place since the mid-1990s. In both of the shorter time series in this study, relationships between iWUE and ring width were non-significant. Additional long series will be necessary to identify how faithfully annual incremental tree ring growth may relate to $\delta^{13}\text{C}$ -inferred iWUE. EC-based estimates of iWUE (e.g. Knauer et al., 2017) combined with $\delta^{13}\text{C}$ -inferred iWUE may identify possible linking mechanisms between iWUE and ring growth within individual trees.

4.6 Conclusions

The $\delta^{13}\text{C}$ results obtained from growth rings from three tree specimens in two different aged (14- and 77-year old) white pine plantation forests provide some insight into past water use efficiency. Long-term trends identify significant shifts in iWUE that may be driven from anthropogenic sourcing of carbon into the atmosphere. The increase in atmospheric CO_2 concentration may have shifted the

homeostatic response of trees from a passive state in allowing inter-cellular CO₂ concentration to increase with atmospheric concentration, to an active state in which the tree strongly regulates stomatal conductance in a higher CO₂ environment. The $\delta^{13}\text{C}$ -inferred inter-cellular to atmospheric concentration of CO₂ signal, here signified as the ratio, preserved in tree ring wood may be influenced by significant shifts in climate such as a +0.5°C abrupt shift in temperature that occurred in this area in the mid-1980s. Significant linear correlations between iWUE were also found, although inconsistently duplicated between the three samples. There is a pressing need for additional long series of $\delta^{13}\text{C}$ records from white pine plantation forests in this area to confirm and validate the results found for these wood samples and strengthen the conclusions of this work.

4.7 Acknowledgements

The project was supported by the Natural Sciences and Engineering Research Council (NSERC), Global Water Futures (GWF) Program and the Ontario Ministry of Environment and Climate Change (MOECC) grants. Funding provided by the Canadian Foundation of Innovation (CFI) through the New Opportunity and Leaders Opportunity Fund and the Ontario Research Fund of the Ministry of Research and Innovation to initiate Turkey Point Flux Station is also acknowledged. In-kind support from the Ontario Ministry of Natural Resources and Forestry (OMNRF), the Natural Resources Canada, the Environment and

Climate Change, Canada, the Long Point Region Conservation Authority (LPRCA), the Long Point Waterfowl Research and Education Centre, the Normandale Fish Culture Station, Long Point Eco-Adventures and the St. Williams Conservation Reserve Community Council are also acknowledged. The authors thank Michelle Williams-Marzucco for assistance with sample preparation. A special thanks to Martin Knyf of the McMaster Research Group for Stable Isotopologues (MRSI) and the McMaster Hydrometeorology and Climatology research group for their contributions to the isotopic analysis and biometric and flux data, respectively.

4.8 References

- Arain, M.A., Restrepo-Coupé, N., 2005. Net ecosystem production in a temperate pine plantation in southeastern Canada. *Agricultural and Forest Meteorology* 128, 223–241.
- Battipaglia, G., Saurer, M., Cherubini, P., Calfapietra, C., McCarthy, H.R., Norby, R.J., Cotrufo, M.F. 2012. Elevated CO₂ increases tree-level intrinsic water use efficiency: insights from carbon and oxygen isotope analyses in tree rings across three forest FACE sites. *New Phytologist* 197:2, 544-554.
- Betts, R.A., Cox, P.M., Woodward, F.I. 2000. Simulated responses of potential vegetation to doubled-CO₂ climate change and feedbacks on near-surface temperature. *Global Ecology and Biogeography* 9, 171–180
- Boden, T.A., Marland, G., and Andres, R.J. 2016. Global, regional, and national fossil-fuel CO₂ emissions. Carbon Dioxide Information Analysis Center, Oak Ridge National Laboratory, U.S. Department of Energy, Oak Ridge, Tenn., U.S.A. doi 10.3334/CDIAC/00001_V2016
- Bond, B.J. 2000. Age-related changes in photosynthesis of woody plants. *Trends in Plant Science* 5, 349–353.
- Brugnoli, E., Scartazza, A., Lauteri, M., Monteverdi, M.C., Maguas, C. 1998. Carbon isotope discrimination in structural and non-structural carbohydrates in relation to productivity and adaption to unfavourable conditions. In Griffiths (Ed), *Stable isotopes: integration of biological, ecological and geochemical processes*, Bios Scientific Publishers Ltd, Oxford, UK: 133-146.
- Campbell, G., Norman, J. 1998. *An Introduction to Environmental Biophysics*, Chapter 14.9 Control of Stomatal Conductance. Springer-Verlag. New York.
- Chan, F.C.C., Arain, M.A., Khomik, M., Brodeur, J., Peichl, M., Restrepo-Coupé, N., Thorne, R., Beamesderfer, E., McKenzie, S., Xu, B., Croft, H., Pejam, M., Trant, J., Kula, M., Skubel, R. 2018. Carbon, water and energy exchange dynamics of a young pine plantation forest during the initial fourteen years of growth. *Forest Ecology and Management* 410, 12-26.
- Carrer, M., Urbinati, C. 2004. Age – dependent tree – ring growth responses to climate in *Larix decidua* and *Pinus cembra*. *Ecology* 85:3, 730-740.
- Draper, W.B., Gartshore, M.E. and Bowles, J.M. 2003. *St. Williams Crown Land life science inventory*. Ontario Ministry of Natural Resources.

Elsig, J., J. Schmitt, D. Leuenberger, R. Schneider, M. Eyer, M. Leuenberger, F. Joos, H. Fischer, and T.F. Stocker. 2009. Stable isotope constraints on Holocene carbon cycle changes from an Antarctic ice core. *Nature* 461, 507-510. doi:10.1038/nature08393

Farquhar, G.D., O'Leary, M.H., Berry, J.A. 1982. On the relationship between carbon isotope discrimination and the intercellular carbon dioxide concentration in leaves. *Australian Journal of Plant Physiology* 9, 121-137.

Farquhar, G.D., Richards, R.A. 1984. Isotopic composition of plant carbon correlates with water-use efficiency of wheat genotypes. *Australian Journal of Plant Physiology* 11:6, 539 - 552

Feng, X., Epstein, S., 1995. Carbon isotopes of trees from arid environments and implications for reconstructing atmospheric CO₂ concentration. *Geochimica et Cosmochimica Acta* 59, 2599–2608.

Fessenden, J., Ehleringer, J. 2002. Age-related variations in $\delta^{13}\text{C}$ of ecosystem respiration across a coniferous forest chronosequence in the Pacific Northwest. *Tree Physiology* 22:3, 159-167.

Fichtler, E., Helle, G., Worbes, M. 2010. Stable-carbon isotope time series from tropical tree rings indicate a precipitation signal. *Tree-Ring Research* 66:1, 35-49.

Francey, R.J., Allison, C.E., Etheridge, D.M., Trudinger, C.M., Enting, I.G., Leuenberger, M., Langenfelds, R.L., Michel, E., Steele, L.P. 1999. A 1000-year high precision record of $\delta^{13}\text{C}$ in atmospheric CO₂. *Tellus* 51B, 170-193.

Gagen, M., Finsinger, W., Wagner-Cremer, F., McCarroll, D., Loader, N., Robertson, I., Jalkanen, R., Young, G., Kirchhefer, A. 2011. Evidence of changing intrinsic water-use efficiency under rising atmospheric CO₂ concentrations in Boreal Fennoscandia from subfossil leaves and tree ring $\delta^{13}\text{C}$ ratios. *Global Change Biology* 14, 1064-1072.

Hall, G., Woodborne, S., Pienaar, M. 2009. Rainfall control of the $\delta^{13}\text{C}$ ratios of *Mimusops caffra* from KwaZulu-Natal, South Africa. *The Holocene* 19:2, 251-260.

Kao, W-Y., Chiu, Y-S, Chen, A-H. 2000. Vertical profiles of CO₂ concentration and $\delta^{13}\text{C}$ values in a subalpine forest of Taiwan. *Botanical Bulletin of Academia Sinica* 41, 213-218.

Knauer, J., Zaehle, S., Medlyn, B., Reichstein, M., Williams, C., Miliavacca, M., Kauwe, M., Werner, C., Keitel, C., Kolari, P., Limousin, J-M. Linderson, M-L.

2017. Towards physiologically meaningful water-use efficiency estimates from eddy covariance data. *Global Change Biology* 24, 694-710. DOI: 10.1111/gcb.13893

Körner, C. 2003. Carbon Limitation in Trees. *Journal of Ecology* 91, 4-17.

Le Quéré, C., Andrew, R.M., Canadell, J.G., Sitch, S., Korsbakken, J.I., Peters, G.P., Manning, A. C., Boden, T.A., Tans, P.P., Houghton, R.A., Keeling, R.F., Alin, S., Andrews, O. D., Anthoni, P., Barbero, L., Bopp, L., Chevallier, F., Chini, L.P., Ciais, P., Currie, K., Delire, C., Doney, S. C., Friedlingstein, P., Gkritzalis, T., Harris, I., Hauck, J., Haverd, V., Hoppema, M., Klein Goldewijk, K., Jain, A.K., Kato, E., Körtzinger, A., Landschützer, P., Lefèvre, N., Lenton, A., Lienert, S., Lombardozzi, D., Melton, J.R., Metzl, N., Millero, F., Monteiro, P.M.S., Munro, D.R., Nabel, J.E.M.S., Nakaoka, S., O'Brien, K., Olsen, A., Omar, A.M., Ono, T., Pierrot, D., Poulter, B., Rödenbeck, C., Salisbury, J., Schuster, U., Schwinger, J., Séférian, R., Skjelvan, I., Stocker, B.D., Sutton, A. J., Takahashi, T., Tian, H., Tilbrook, B., van der Laan-Luijkx, I.T., van der Werf, G. R., Viovy, N., Walker, A.P., Wiltshire, A.J., and Zaehle, S. Global Carbon Budget. 2016. *Earth Syst. Sci. Data*, 8, 605-649, doi:10.5194/essd-8-605-2016, 2016. <http://www.earth-syst-sci-data.net/8/605/2016/>

Linares, J.C., Camarero, J.J. 2012. From pattern to process: Linking intrinsic water-use efficiency to drought-induced forest decline. *Global Change Biology* 18, 1000–1015.

Loader, N.J., Switsur, V.R., Field, E.M. 1995. High-resolution stable isotope analysis of tree rings: implications of 'microdendroclimatology' for paleoenvironmental research. *The Holocene* 5:4, 457-460.

Loader, N.J., Robertson, I., McCarroll, D., 2003. Comparison of stable carbon isotope ratios in the whole wood cellulose and lignin of oak tree-rings. *Palaeogeography, Palaeoclimatology, Palaeoecology* 196, 395–407.

Marshall, J. D., Brooks, J. R. and Lajtha, K. (2007) Sources of variation in the stable isotopic composition of plants, in *Stable Isotopes in Ecology and Environmental Science*, Chapter 2. Second Edition (eds R. Michener and K. Lajtha), Blackwell Publishing Ltd, Oxford, UK.

Masson-Delmotte V., Steen-Larsen, H.C., Ortega, P., Swingedouw, D., Popp, T., Vinther, B.M., Oerter, H., Sveinbjornsdottir, A.E., Gudlaugsdottir, H., Box, J., Falourd, S., Fettweis, X., Gallée, H., Garnier, E., Gkinis, V., Jouzel, J., Landais, A., Minster, B., Paradis, N., Orsi, A., Risi, C., Werner, M., White, J.W.C. 2015. Recent change in north-west Greenland climate documented by NEEM shallow

ice core data and simulations, and implications for past-temperature reconstructions. *Cryosphere* 9, 1481-1504

McCarroll, D., Gagen, M., Loader, N., Robertson, I., Anchukaitis, K., Los, S., Young, G., Jalkanen, R., Kirchhefer, A., Waterhouse, J. 2009. Correction of tree ring stable carbon isotope chronologies for changes in the carbon dioxide content of the atmosphere. *Geochimica et Cosmochimica Acta* 73, 1539-1547.

McCarroll, D., Loader, N. 2004. Stable isotopes in tree rings. *Quaternary Science Reviews* 23, 771-801.

McCarroll, D., Pawellek, F., 2001. Stable carbon isotope ratios of *Pinus sylvestris* from northern Finland and the potential for extracting a climate signal from long Fennoscandian chronologies. *The Holocene* 11, 517–526.

McDowell, N.G., Phillips, C., Lunch, B., Bond, B., Ryan, M. 2002. An investigation of hydraulic limitation and compensation in large, old Douglas-fir trees. *Tree Physiology* 22, 763-774.

McDowell, N.G., Licata, J., Bond, B. 2005. Environmental sensitivity of gas exchange in different-sized trees. *Oecologia* 145, 9-20.

McDowell, N.G., Bond, B., Dickman, L., Ryan, M. Whitehead, D. 2011. Relationships between tree height and carbon isotope discrimination. In *Size-and age-related changes in tree structure and function* (pp. 255-286). Springer, Dordrecht.

McLaren, J.D., Arain, M.A., Khomik, M., Peichl, M. and Brodeur, J., 2008. Water flux components and soil water –atmospheric controls in a temperate pine forest growing in a well-drained sandy soil. *Journal of Geophysical Research: Biogeosciences* 113: G04031.

Nabeshima, E., Hiura, T. 2004. Size dependency of photosynthetic water-and nitrogen-use efficiency and hydraulic limitation in *Acer mono*. *Tree Physiology* 24:7, 745-752.

OGS (Ontario Geological Survey), 1991. Bedrock geology of southern Ontario, southern sheet; Ontario Geological Survey, Map 2544, scale 1:1 000 000.

Oosterbaan, R.J. 2014. SegReg: segmented linear regression with breakpoint and confidence intervals. <https://www.waterlog.info/segreg.htm>

- Peichl M., Arain, M.A., 2006. Above- and belowground ecosystem biomass and carbon pools in an age-sequence of planted white pine forests. *Agricultural and Forest Meteorology* 140, 51-63.
- Peichl, M., Arain, M.A., Brodeur, J.J., 2010a. Age effects on carbon fluxes in temperate pine forests. *Agricultural and Forest Meteorology* 150, 1090–1101.
- Peichl, M., Arain, M.A., Ullah, S., Moore, T. 2010b. Carbon dioxide, methane, and nitrous oxide exchanges in an age-sequence of temperate pine forests. *Global Change Biology* 16, 2198-2212.
- Presant, E.W., Acton, C.J., 1984. The soils of the regional municipality of Haldimand-Norfolk. Volume 1, Report No. 57. Agriculture Canada, Ministry of Agriculture and Food, Guelph, Ontario, 100pp.
- Primicia, I., Camarero, J., Janda, P., Čada, V., Morressey, R., Trotsiuk, V., ... Svoboda, M. 2015. Age, competition, disturbance and elevation effects on tree on tree and stand growth response of primary *Picea abies* forest to climate. *Forest Ecology and Management* 354, 77-86.
- Ryan, M., Binkley, D., Fownes, J. 1997. Age related decline in forest productivity: pattern and process. *Advances in Ecological Research* 27, 213–262.
- Ryan, M.G., Yoder, B.J., 1997. Hydraulic limits to tree height and tree growth. *BioScience* 47, 235–242.
- Sanders, T., Heinrich, I., Günther, B., Beck, W. 2016. Increasing water use efficiency comes at a cost for Norway spruce. *Forests* 7, 296. 8 pp. doi:10.3390/f7120296
- Saurer, M., Borella, S., Schweingruber, F.H., Siegwolf, R. 1997. Stable carbon isotopes in tree rings of beech: climatic versus site-related influences. *Trees-Structure and Function* 11, 291-297.
- Saurer, M., Siegwolf, R., Schweingruber, F.H. 2004. Carbon isotope discrimination indicates improving water-use efficiency of trees in northern Eurasia over the last 100 years. *Global Change Biology* 10, 2109-2120.
- Schleser, G.H., Jayasekera, R., 1985. $\delta^{13}\text{C}$ variations in leaves of a forest as an indication of reassimilated CO_2 from the soil. *Oecologia* 65, 536–542.
- Scripps CO_2 Program. Carbon Dioxide Measurements, History, Research, and Data. 2017. <http://scrippsco2.ucsd.edu/>

Skubel, R., Khomik, M., Brodeur, J., Arain, M. 2017. Short-term selective thinning effects on hydraulic functionality of a temperate pine forest in eastern Canada. *Ecohydrology* DOI: 10.1002/eco.1780.

Skubel, R., Peichl, M., Brodeur, J., Khomik, M., Thorne, R., Trant, J., Kula, M. 2015. Age effects on the water-use efficiency and water-use dynamics of temperate pine plantation forests. *Hydrological Processes* 2015, DOI: 10.1002/hyp.10549.

Strack, M., Waddington, J.M., Tuittila, E.-S. 2007. Effect of water table drawdown on northern peatland methane dynamics: Implications for climate change. *Global Biogeochemical Cycles* 18, 7 p.

Switsur, V.R., Waterhouse, J.S., Field, E.M., Carter, A.H.C., 1996. Climatic signals from stable isotopes in oak tree-rings from East Anglia, Great Britain. In: Dean, J.S., Meko, D.M., Swetnam, T.W. (Eds.), *Tree Rings, Environment and Humanity Radiocarbon*, pp. 637–645. Radiocarbon, Arizona.

Thomas, S.C. 2000. Photosynthetic capacity peaks at intermediate size in temperate deciduous trees. *Tree Physiology* 30:5, 555-573.

Thorne, R. and Arain, M.A. 2015. Influence of low frequency variability on climate and carbon fluxes in a temperate pine forest in eastern Canada. *Forests* 6, 2762-2784.

Thornthwaite, C.W. 1948. An approach toward a rational classification of climate. *Geographical Review* 38:1, 55-94.

Treydte, K., Schleser, G.H., Schweingruber, F.H., Winiger, M., 2001. The climatic significance of $\delta^{13}\text{C}$ in subalpine spruces (*L. otschental*, Swiss Alps). *Tellus* 53B, 593–611.

Waterhouse, J.S., Switsur, V.R., Barker, A.C., Carter, A.H.C., Hemming, D.L., Loader, N.J., Robertson, I. 2004. Northern European trees show a progressively diminishing response to increasing atmospheric carbon dioxide concentrations. *Quaternary Science Reviews* 23, 803–810.

Weiwei, L.U., Xinxiao, Y.U., Guodong, J.I.A., Hanzhi, L.I., Ziqiang, L.I.U. 2018. Responses of intrinsic water-use efficiency and tree growth to climate change in semi-arid areas of north China. *Scientific Reports* 8:308.

West, A.G., Midgley, J.J. Bond, W.J. 2001: The evaluation of $\delta^{13}\text{C}$ isotopes of trees to determine past regeneration environments. *Forest Ecology and Management* 147, 139–49.

White, J.W.C., B.H. Vaughn, and S.E. Michel (2015), University of Colorado, Institute of Arctic and Alpine Research (INSTAAR), Stable Isotopic Composition of Atmospheric Carbon Dioxide (^{13}C and ^{18}O) from the NOAA ESRL Carbon Cycle Cooperative Global Air Sampling Network, 1990-2014, Version: 2015-10-26, Path: ftp://aftp.cmdl.noaa.gov/data/trace_gases/co2c13/flask/

Zavitz, E.J. 1926. Appendix No. 36. Report of the Forestry Branch. In: Report of the Minister of Lands, Forests and Mines of the Province of Ontario. The Legislative Assembly of Ontario. Toronto. 1926.

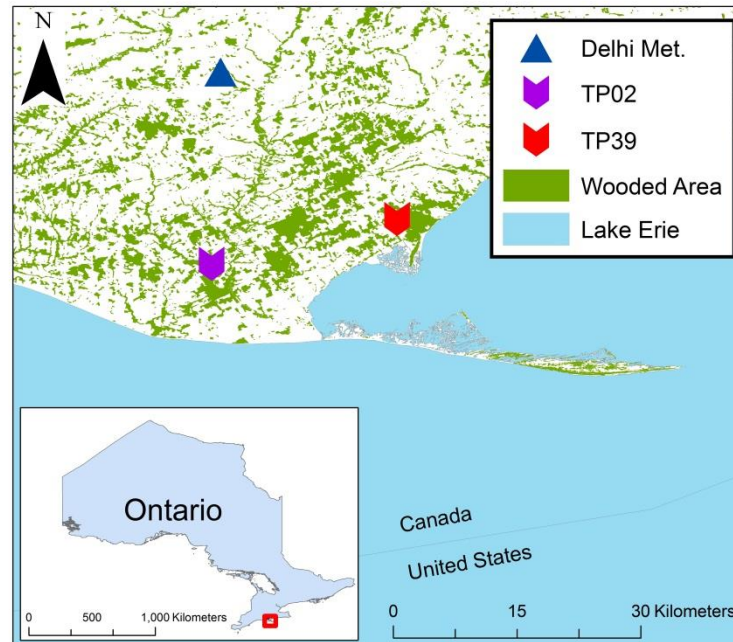


Figure 4.1: Location map of the mature (TP39) and the juvenile (TP02) forest sites and the Environment Canada Delhi Meteorological Station in southern Ontario, Canada.

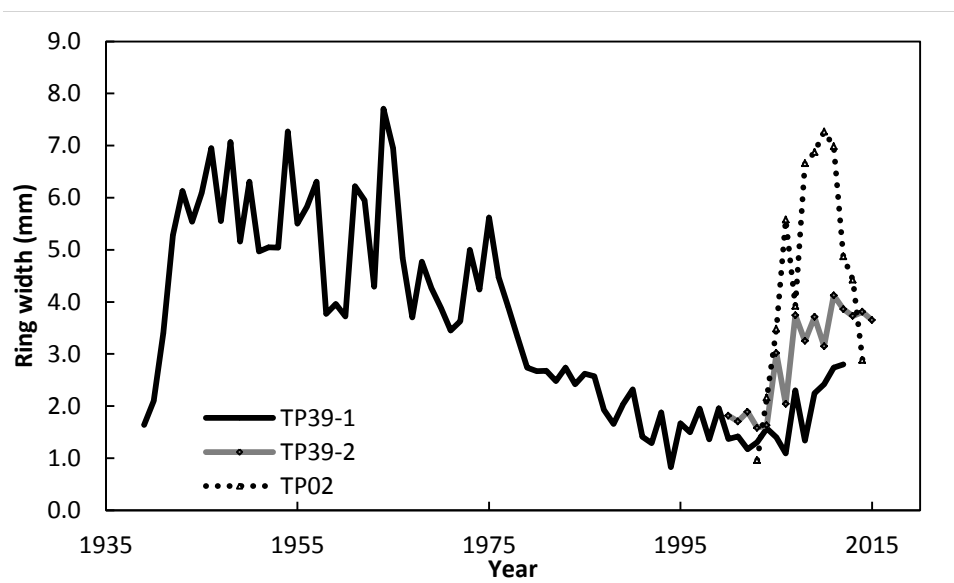


Figure 4.2: Ring widths of the three sampled trees TP39-1 (black line), TP39-2 (grey line), and TP02 (dotted line).

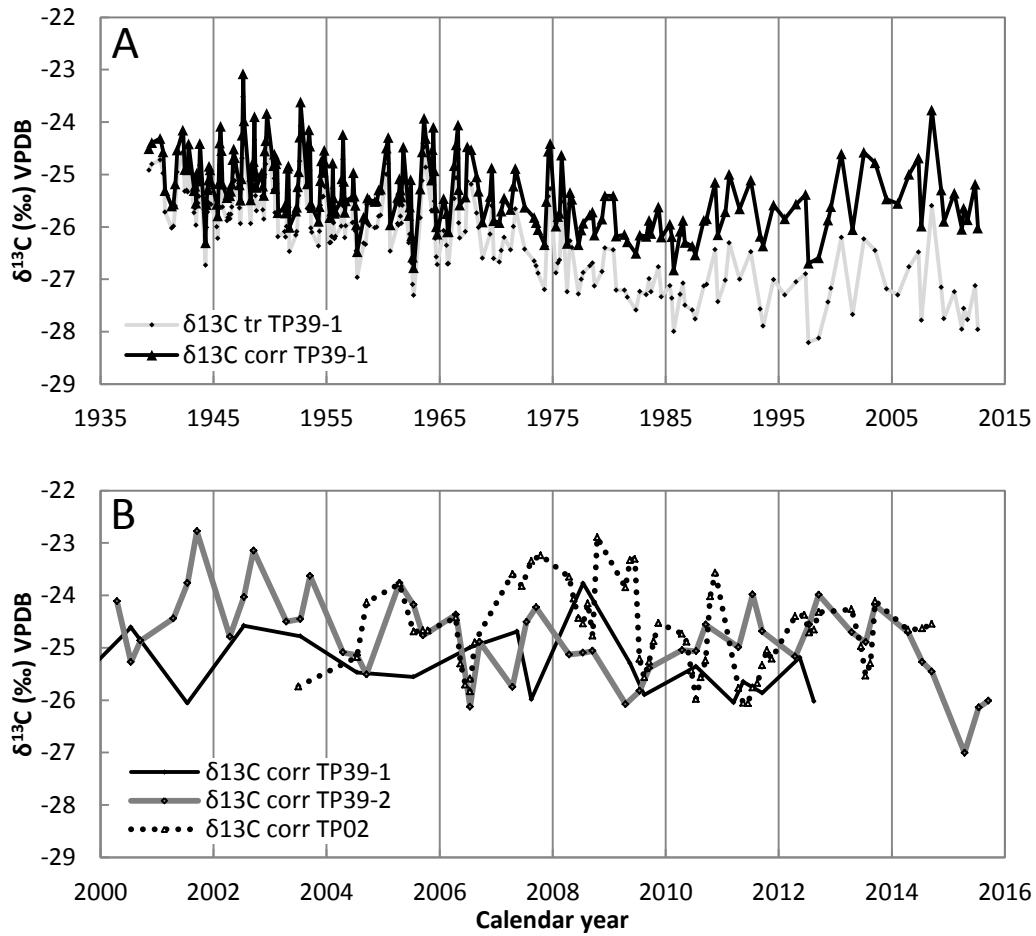


Figure 4.3: (A) The isotope record of TP39-1 uncorrected ($\delta^{13}\text{C}_{\text{tr}}$; grey line) and corrected ($\delta^{13}\text{C}_{\text{corr}}$; black line) for the atmospheric effect of decreasing $\delta^{13}\text{C}$. (B) The corrected $\delta^{13}\text{C}_{\text{corr}}$ of all three series from TP39-1 (black line), TP39-2 (grey line), and TP02 (dotted line) for 2000 – 2016.

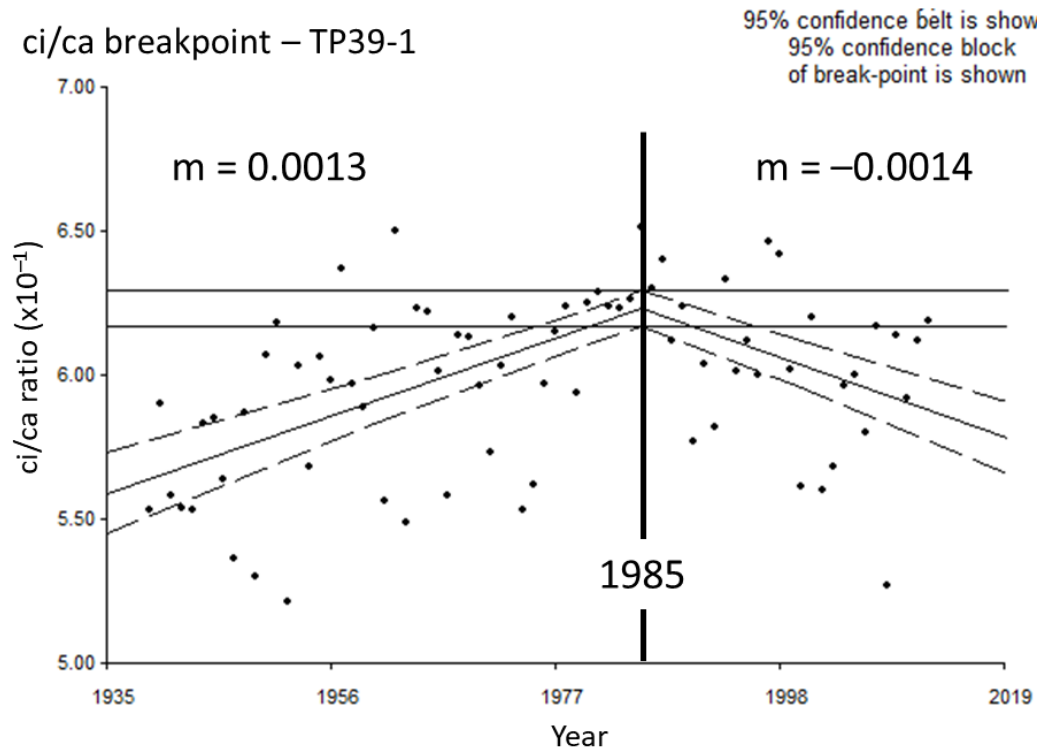


Figure 4.4. Inter-annual $\delta^{13}\text{C}$ -inferred ci/ca ratio record from the TP39-1 white pine (*Pinus strobus* L.) wood sample at Turkey Point, southern Ontario. A significant (95% confidence) breakpoint exists in the inter-annual slope in the ci/ca time series at the year 1985.

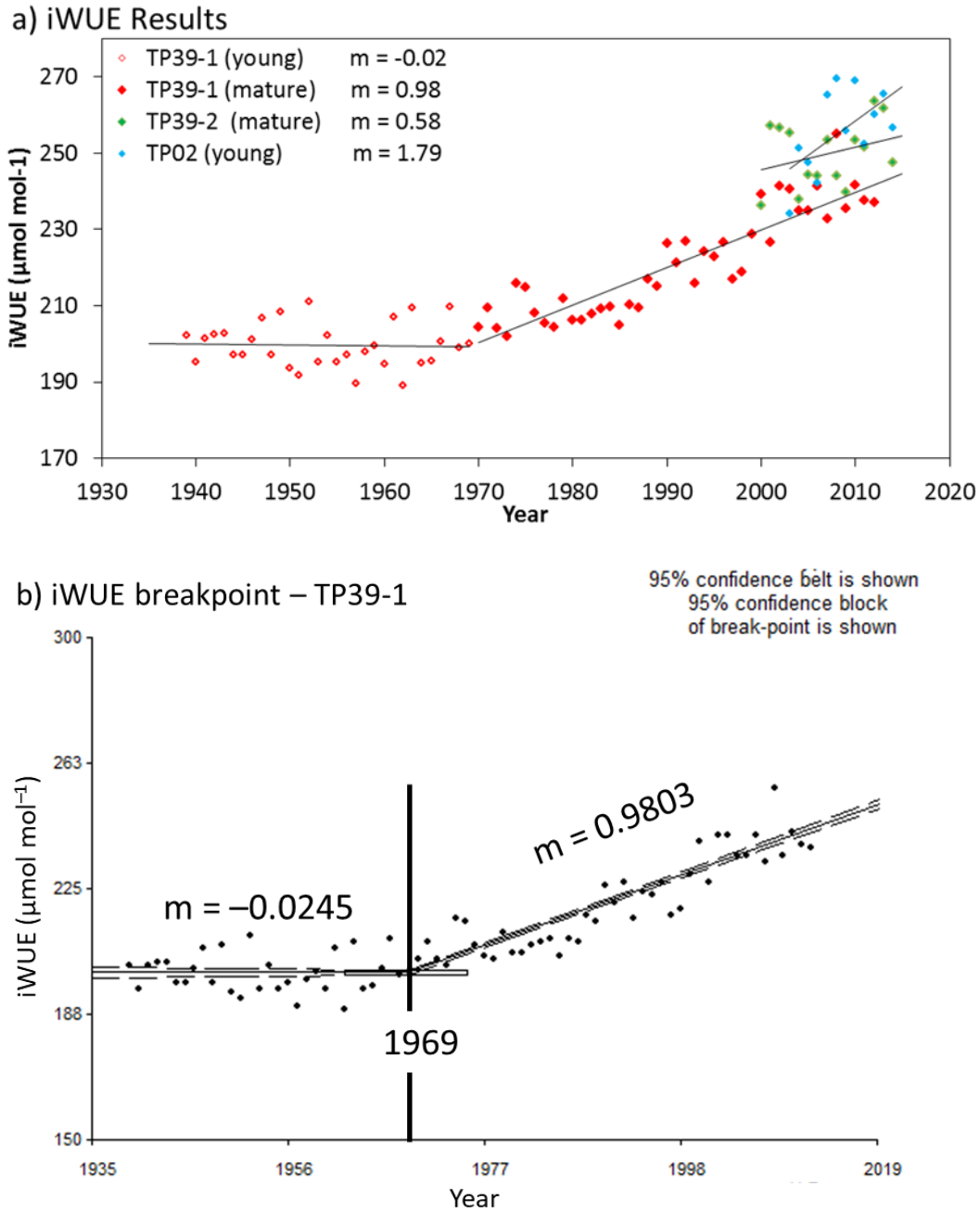


Figure 4.5. a) Inter-annual $\delta^{13}\text{C}$ -inferred a) intrinsic water use efficiency iWUE record from the three white pine (*Pinus strobus* L.) tree samples from Turkey Point, southern Ontario. b) For the TP39-1 sample, a significant (95% confidence) breakpoint exists in the inter-annual slope in the iWUE time series at the year 1969 where the slope changes from nearly horizontal ($m = -0.02$) to nearly 1:1 ($m = 0.98$).

Figure 4.6a

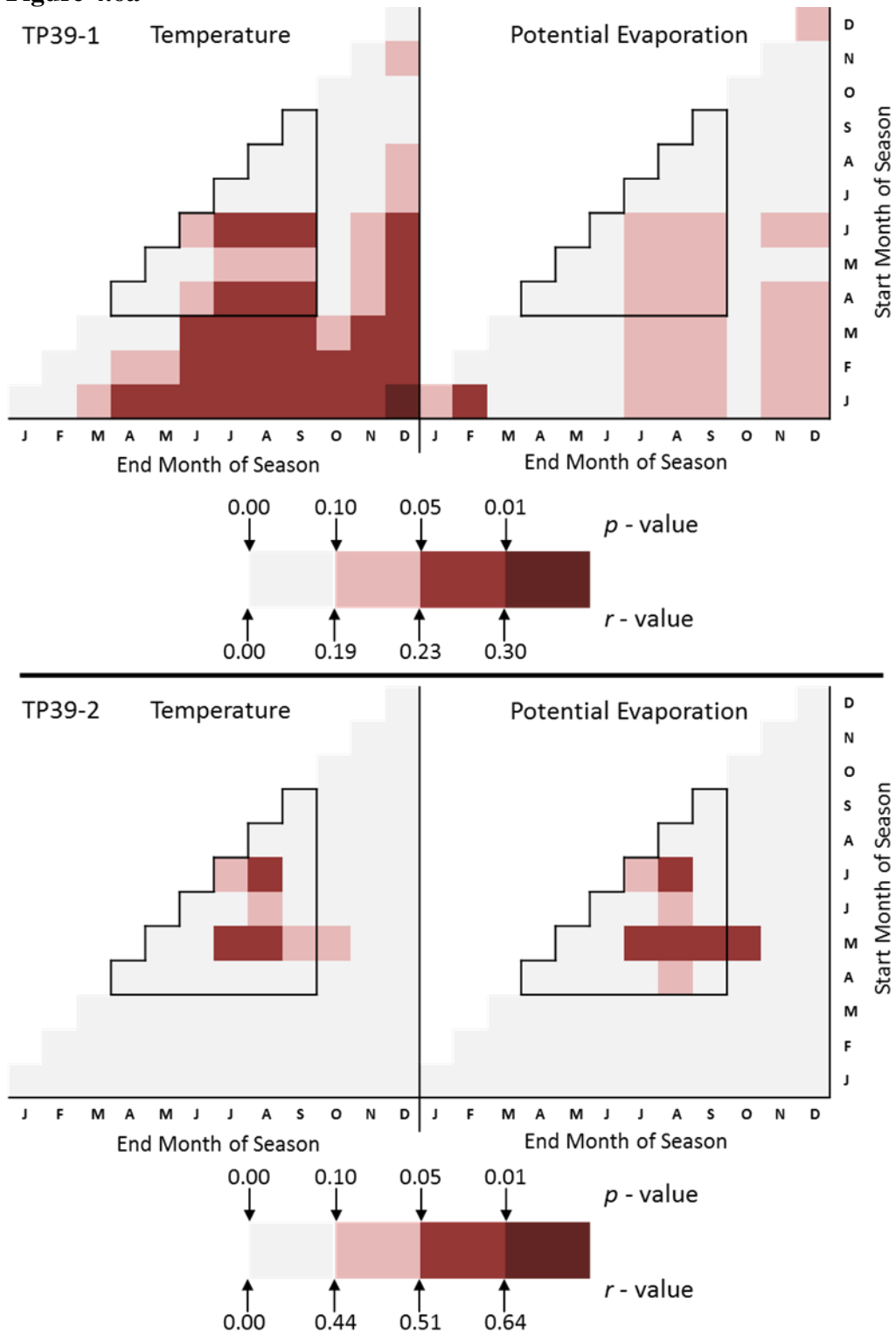


Figure 4.6b

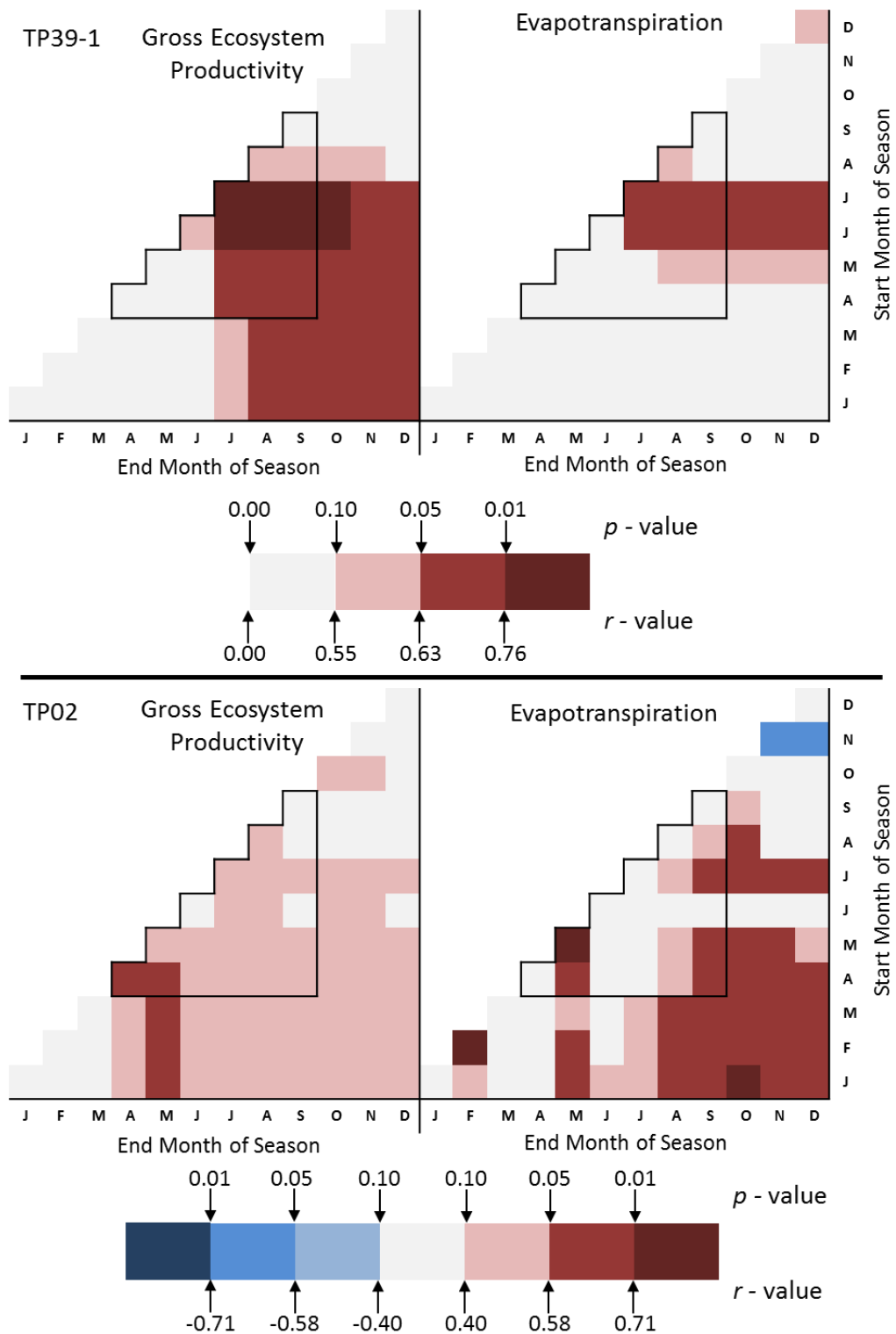


Figure 4.6. a) Significance of relationships between intrinsic water use efficiency (iWUE) with climate variables in mean monthly temperature (T) and potential evaporation (PE), and **b)** gross ecosystem productivity (GEP) and evapotranspiration (ET) during all possible combinations of months over the January–December period. The period of correlation for T and PE was 72 years (1939-2012) for TP39-1 and 15 years (2000-2014) for TP39-2. For GEP and ET, the period of correlation was 10 years (2003-2012) for TP39-1, and 12 years (2003-2014) for TP02. Relationship significance for individual months are shown on the corner-to-corner diagonals (e.g. 1st line January to 12th line December) whereas significance over month combinations extend to the right (e.g. 1st line, 3rd block would represent the January – March significance). The area of the charts that corresponds to correlations during the growing season (April-September) is indicated by the stair-step box.

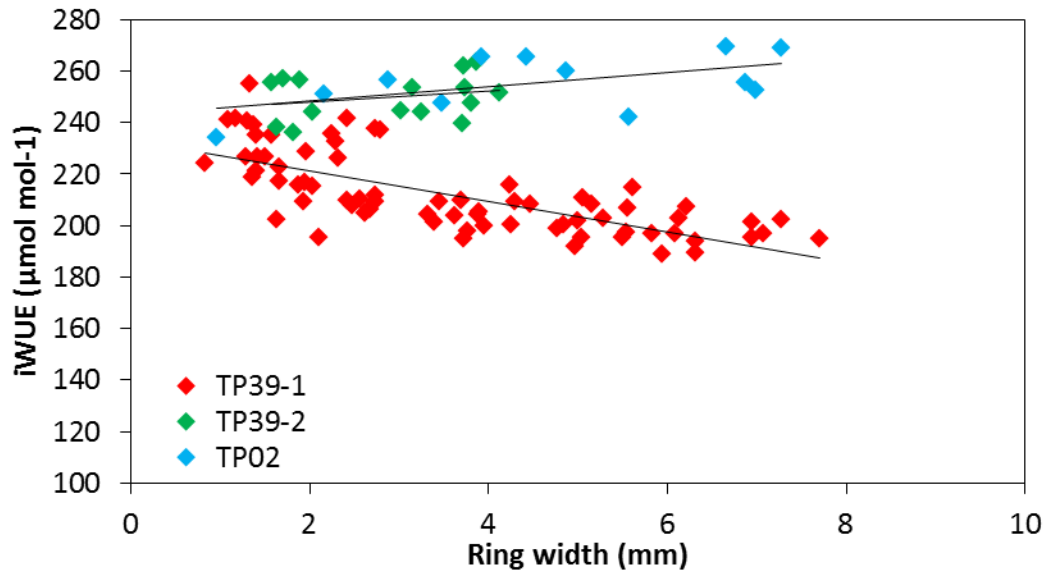


Figure 4.7. Data scatter of iWUE versus ring width for the three trees from which the isotope data was collected. For TP39-1 (red points), iWUE shows a significant relationship ($r = -0.72$, $p < 0.01$, $n = 74$) with ring width. Non-significant ($p < 0.05$) relationships exist between iWUE and ring width in both the TP39-2 ($r = 0.24$, $n = 15$) (green points) and TP02 ($r = 0.52$, $n = 12$) (blue points) tree samples.

Chapter 5: Conclusions

5.1. Major findings

This dissertation evaluated growth histories of plantation forests in southern Ontario, Canada using eddy covariance fluxes, dendrochronological records and carbon isotopic compositions. Study results revealed that overall temperature was the dominant factor on forest growth. Variations in temperature during May and June were found to be a significant controlling factor for tree ring growth in all three different-age (86-, 78- and 43-year old) and different species of pine (white and red) plantation stands. The combination of heat and water stress as indicated by the Palmer Drought Severity Index (PDSI) was found to be the most significant climate factor on growth, with large decreases in gross ecosystem productivity (GEP) and tree ring widths. The study found that the 43-year old white pine stand (TP74) was much more sensitive to drought as compared to older 78-year old (TP39) white pine stand. This implies that this middle-age stand is more vulnerable to drought events. The reason for this is likely due to stand age, structure and management history, where no thinning treatment has been applied since its plantation in 1974. In the middle-age stand, the limited root network and smaller carbohydrate reserves also contributed to its vulnerability to acute water stress. The higher stand density was also linked to greater water use and transpiration. In the 86-year old red pine stand (TP31), temperature-induced heat

stress was a significant control on growth during the latter part of the record, with years of extreme drought corresponding to reduction in tree ring growth.-

Study results showed that dendrochronological growth estimates were largely compatible with gross ecosystem productivity (GEP) quantified from eddy covariance flux measurements. For the 2003 to 2017 period, GEP was significantly ($p < 0.01$) related to tree ring records in the two white pine stands, TP39 and TP74. This relationship enabled up-scaling of biometric measurements to estimate ecosystem productivity for both sites. The relationship between RWI and GEP was further examined in an attempt to generalize what GEP values may have been over the growth history of stands. While there were some limitations to the GEP estimates calculated for the whole age of stand using tree ring records, the result of this work can be used to determine uncertainty in forest growth estimates in plantation forests alongside other techniques. Results of this tree ring study are in agreement with previous eddy covariance flux studies, where temperature has been found to be the main factor for ecosystem productivity in these plantation forests (Chan et al., 2018; Peichl et al., 2010a; 2010b). Both tree ring and GEP estimates showed notable declines during severe drought years (e.g. 2012). This implies that there is an inter-annual linkage between drivers of GEP and biomass allocation to the stem wood during extreme years.

The isotopic analysis conducted in this study evaluated tree physiological reactions to environmental change in these stands. It showed that inter-annual temperature variability was a significant control on $\delta^{13}\text{C}$ -inferred iWUE extracted from the latewood portion of tree rings. Time series of $\delta^{13}\text{C}$ -inferred data are a ratio of within-plant inter-cellular to atmospheric concentration of CO_2 which were used to identify significant shifts in past climate over the life cycle of these forests. Anthropogenic loading of CO_2 into the atmosphere since the 1930s imparted a long-term decline into the observed $\delta^{13}\text{C}$ time series from TP39. The $\delta^{13}\text{C}$ annual time series taken from latewood bands in tree samples, when converted into iWUE, were found to be significantly related ($p < 0.05$) to temperature variability. The 72-year iWUE record also contained a significant breakpoint (95% conf., year 1969) in inter-annual change from nearly constant ($-0.02 \mu\text{mol mol}^{-1} \text{yr}^{-1}$) value to $0.98 \mu\text{mol mol}^{-1} \text{yr}^{-1}$. This indicated a shift in passive to active homeostasis resulting in iWUE increase. Overall, iWUE increased by approximately $50 \mu\text{mol mol}^{-1} \text{yr}^{-1}$ over a 55-year period (1969-2012). Although such trends have been observed in long-term physiological records in the boreal region of the northern hemisphere (Waterhouse et al., 2004; Saurer et al., 1997; 2004;; Gagen et al., 2011), finding such a shift in temperate plantation stands in Great Lakes region was unexpected. Identification of this shift in temperate conifer plantation forests is an important finding that will help to advance our understanding of water use in these stands.

5.2. Future considerations

The small number of wood samples analyzed for $\delta^{13}\text{C}$ in this study may be a shortcoming of this work. Sampling of additional wood blocks may help to further reinforce these results and reduce uncertainty. It is also recommended to concentrate effort in sampling latewood bands only, rather than the entire ring (earlywood and latewood). The rate of formation of early wood material is difficult to constrain without detailed biometric measurements such as those collected from band dendrometers. In addition, photosynthate material that forms earlywood may have been mobilized from elsewhere in the tree, while it is more likely photosynthates during the current ring year were used in latewood formation (Switsur et al., 1996; Brugnoli et al. 1998).

In this study, RWI – GEP relationships used to determine ecosystem productivity through growth chronology were developed for two age ranges of white pine stands i.e. age 29 to 43 years (TP74) and age 64 to 78 years (TP39). It is recommended to improve this model using additional RWI – GEP relationships for the remaining TP89 and TP02 stands. It would constrain modelled GEP uncertainty in the younger portion of white pine's life history.

The initiation of the Variable Retention Harvesting (VRH) experiment in TP31 (section 3.3.1) provides an opportunity to investigate iWUE as tree growth

in 1 ha plots begin to diverge in reaction to structural changes. It is likely the divergence growth effect of the VRH experiment will not be detectable in tree ring chronologies for another 7 to 10 years. However, $\delta^{13}\text{C}$ -inferred iWUE extracted from phloem sap may reveal detectable responses of trees during the transition period (Pate and Arthur 1998). Anatomical divergences in the cambium cell structure and cell wall thickness may also reveal divergences within the experimental area (Gärtner et al., 2015). Lastly, shoots collected from the canopy may record seasonal variation in $\delta^{13}\text{C}$ canopy and perhaps reveal differences in water use due to stand structural variability in the experimental area.

The Turkey Point Flux Station also includes a 90-year-old naturally regenerated but managed Carolinian forest with the primary species of this stand include oak (*Quercus* spp.), maple (*Acer* spp.) beech (*Fagus grandiflora*) and birch (*Betula alleghaniensis*). This forest provides a rare opportunity to construct long isotopic and dendrochronological records as most Carolinian forests in southern Ontario are younger than 90 years of age (Suffling et al., 2003). Time series of RWI, $\delta^{13}\text{C}$ and iWUE constructed using dendrochronological and isotopic methods as well as eddy covariance flux measurements since 2012 should reveal unique growth responses and opportunities to compare these responses with those found for monoculture conifer plantations in response to changes in climate in the region. It may also be interesting to examine trends in

tree ring sulfur isotopic compositions to investigate the effects of industry in this highly industrialized region of North America.

5.3. References

Brugnoli, E., Scartazza, A., Lauteri, M., Monteverdi, M.C., Maguas, C. 1998. Carbon isotope discrimination in structural and non-structural carbohydrates in relation to productivity and adaption to unfavourable conditions. In Griffiths (Ed), *Stable isotopes: integration of biological, ecological and geochemical processes*, Bios Scientific Publishers Ltd, Oxford, UK: 133-146.

Chan, F.C.C., Arain, M.A., Khomik, M., Brodeur, J., Peichl, M., Restrepo-Coupé, N., Thorne, R., Beamesderfer, E., McKenzie, S., Xu, B., Croft, H., Pejam, M., Trant, J., Kula, M., Skubel, R. 2018. Carbon, water and energy exchange dynamics of a young pine plantation forest during the initial fourteen years of growth. *Forest Ecology and Management* 410, 12-26.

Gagen, M., Finsinger, W., Wagner-Cremer, F., McCarroll, D., Loader, N., Robertson, I., Jalkanen, R., Young, G., Kirchhefer, A. 2011 Evidence of changing intrinsic water-use efficiency under rising atmospheric CO₂ concentrations in Boreal Fennoscandia from subfossil leaves and tree ring $\delta^{13}\text{C}$ ratios. *Global Change Biology* 14, 1064-1072.

Gärtner, H., Cherubini, P., Fonti, P., von Arx, G., Schneider, L., Nievergelt, D., Verstege, A., Bast, A., Schweingruber, F.H., Büntgen, U. A. 2015. Technical perspective in modern tree-ring research - How to overcome dendroecological and wood anatomical challenges. *Journal of Visualized Experiments* 97, e52337, doi:10.3791/52337.

Pate, J., Arthur, D. 1998. $\delta^{13}\text{C}$ analysis of phloem sap carbon: novel means of evaluating seasonal water stress and interpreting carbon isotope signatures of foliage. *Oecologia* 117, 301-311.

Peichl, M., Arain, M.A., Brodeur, J.J., 2010a. Age effects on carbon fluxes in temperate pine forests. *Agricultural and Forest Meteorology* 150, 1090–1101.

Peichl, M., Arain, M.A., Ullah, S., Moore, T. 2010b. Carbon dioxide, methane, and nitrous oxide exchanges in an age-sequence of temperate pine forests. *Global Change Biology* 16, 2198-2212.

Saurer, M., Borella, S., Schweingruber, F.H., Siegwolf, R. 1997. Stable carbon isotopes in tree rings of beech: climatic versus site-related influences. *Trees-Structure and Function* 11, 291-297.

Saurer, M., Siegwolf, R., Schweingruber, F.H. 2004. Carbon isotope discrimination indicates improving water-use efficiency of trees in northern Eurasia over the last 100 years. *Global Change Biology* 10, 2109-2120.

Suffling, R., Evans, M., Perera, A. 2003. Presettlement forest in southern Ontario: Ecosystems measured through a cultural prism. *The Forestry Chronicle* 79:3, 485-501.

Switsur, V.R., Waterhouse, J.S., Field, E.M., Carter, A.H.C., 1996. Climatic signals from stable isotopes in oak tree-rings from East Anglia, Great Britain. In: Dean, J.S., Meko, D.M., Swetnam, T.W. (Eds.), *Tree Rings, Environment and Humanity Radiocarbon*, pp. 637–645. Radiocarbon, Arizona.

Waterhouse, J.S., Switsur, V.R., Barker, A.C., Carter, A.H.C., Hemming, D.L., Loader, N.J., Robertson, I. 2004. Northern European trees show a progressively diminishing response to increasing atmospheric carbon dioxide concentrations. *Quaternary Science Reviews* 23, 803–810.